POLITECNICO DI MILANO

Facoltà di Ingegneria dei Processi Industriali

Milano – Campus Leonardo

INVESTIGATIONS OF PASSIVITY AND REACTIVITY OF ALLOY PARTICLES, EFFECTS OF SONICATION AND PARTICLE SIZE

Supervisors: Klara Midander and Marco Ormellese

Co-supervisors: Yolanda Hedberg and Enrica Vernè

Master Thesis Project of:

Claudio Baldizzone 734319

Academic year: 2009-2010

Index

Scopo della ricerca

Per lo studio della corrosione e, quindi, per tutti gli usi dei metalli e delle loro leghe la passività è un elemento di cruciale importanza essendo essa che blocca o rallenta i processi corrosivi di un componente metallico nell'ambiente in cui opera. Pertanto in letteratura si trovano numerosi studi riguardo le proprietà passivanti di vari materiali; tuttavia il meccanismo di formazione dello strato passivo non è tuttora ben definito. In fatti esso dipende da molti fattori quali il materiale, il pH, la composizione della soluzione impiegata, la temperatura, il tempo di esposizione l'ambiente in cui si opera e anche le dimensione del campione.

Questo studio è focalizzato sul ruolo che gioca quest'ultimo parametro e contempla un'esplorazione dell'influenza delle dimensioni sulle proprietà di passività delle micro particelle di acciaio inossidabile AISI 316 L. Considerare un materiale in forma particolata introduce differenti parametri di cui tenere conto quali, dimensione delle particelle, la loro forma e morfologia, area della superficie, grado di agglomerazione, differenze di ossidazione superficiale, impurità, differenze microstrutturali ecc.

Negli ultimi decenni l'attenzione del pubblico e dei governi sulle conseguenze dell'esposizione ai particolati ed ai loro possibili effetti negativi sulla salute è di molto cresciuta. Ad esempio in Europa è stato creato un nuovo insieme di norme che va sotto il nome di REACH (Registration, Evaluation, Authorisation and restriction of Chemical substances). Pertanto sono stati pubblicati svariati studi riguardanti il processo di release da particelle metalliche ed il loro impatto sul corpo umano, sulla salute e sull'ambiente.

La forma particolata di metalli o materiali contenti metalli è estremamente rilevante per il corpo umano che ne viene a contatto per inalazione o per ingestione con particolare riferimento ai polmoni ed al primo tratto gastrointestinale. Quindi diviene essenziale allargare la conoscenza delle proprietà passivanti di particelle contenenti metalli, nello specifico questo lavoro rappresenta una parte di un più esteso progetto di ricerca in fieri presso la Divisione di Scienza delle Superfici e della Corrosione presso la KTH.

Purtroppo la passività di leghe in forma particolata, ad esempio l'acciaio inossidabile, non è un campo di studio molto comune e la letteratura che tratta l'influenza della riduzione delle dimensione delle particelle sulla loro passività e reattività è molto scarsa. Lo scopo principale di questo progetto di tesi è cercare di colmare questi vuoti di conoscenza e provvedere ad

una migliore comprensione della passività e della reattività delle micro particelle di acciaio inossidabile 316L.

Questo studio comprende la generazione di dati attraverso test elettrochimici utilizzando varie tecniche, ad esempio misure potenzio statiche e di Linear Sweep Voltammetry. Il definire una efficiente procedura analitica è il primo traguardo che questo progetto si prefigge di raggiungere in quanto l'elettrodo impiegato deve garantire la riproducibilità dei risultati delle prove e minimizzare la corrente di background. Successivamente in questo lavoro di tesi è stata studiata l'influenza sulla passività e sulla reattività delle dimensioni e della microstruttura delle particelle, del pH e della composizione della soluzione. L'effetto della riduzione di dimensione è stato ricavato utilizzando due differenti tipologie di particelle caratterizzate l'una da un diametro medio di 45 μm (coarse particles), l'altra da un diametro di 5 μm (UltraFine particles). Inoltre è stata dedicata una particolare attenzione agli elettroliti usati nello studio siccome devono simulare in tutto e per tutto i fluidi presenti nel corpo umano in modo da simulare quanto avviene in seguito ad inalazione. Il progetto prevede anche una dettagliate investigazione e caratterizzazione delle particelle di acciaio inossidabile 316L prese in esame per correlare i risultati dei test alle caratteristiche del materiale.

Eventuali variazioni nelle proprietà passivanti del materiale sono state rilevate tramite prove di Linear Sweep Voltammetry, nello specifico sono stati considerati parametri quali Open Circuit Potential (OCP), forma delle curve di polarizzazione, corrente media e corrente massima. In seguito sono stati testati gli elettroliti delle differenti prove tramite Graphite Furnace Atomic Adsorption Spectroscopy (GF-AAS), in modo tale da correlare i risultati della tecnica LSV con le quantità di elementi metallici (Fe, Cr e Ni) rilasciati dalle particelle e da permettere di connettere tra loro i processi di corrosione e dissoluzione.

In generale è stato rilevato un comportamento molto più passivo delle particelle, a prescindere dalle dimensioni, rispetto al campioni macroscopici dello stesso materiale. Inoltre si è osservato un indebolimento di queste proprietà passivanti riducendo le dimensioni, tuttavia è stato notato che passando a soluzioni più aggressive questa tendenza va a ridursi fino a invertirsi nel caso dell'ultima soluzione (0.7% HCl). Considerando invece il processo di dissoluzione è stato rilevato che il processo di rilascio aumenta d'intensità con il diametro delle particelle.

A seguito delle prove di LSV si è passati alle prove potenzio statiche, il cui obbiettivo era verificare l'influenza delle dimensioni delle particelle e del potenziale a cui erano mantenute sul processo di rilascio di ferro, cromo e nickel. Riguardo il processo di rilascio si è confermata la tendenza osservata in precedenza, mentre l'influenza del potenziale è risultata complessa e dipendente dalle dimensioni delle particelle considerate.

Nella parte finale di questo lavoro di tesi è stata quindi testata l'influenza di un eventuale trattamento ad ultrasuoni sulle proprietà passivanti delle particelle, tuttavia tramite la tecnica LSV non è stata riscontrata nessuna differenza di comportamento tra le particelle trattate e non.

Abstract

The particulate form of metallic or metal- containing materials is extremely relevant for human exposure through inhalation in the lungs or ingestion in the gastrointestinal tract. Therefore an improved knowledge of the passivity properties of metal-containing particles is essential, since this project represents one part of a large on-going industrial research project at the Division of Surface and Corrosion Science at KTH. However investigating the electrochemical properties of a metal in particulate form is not a trivial task. during this Master Thesis work it has been necessary to screen and select the most suitable testing technique (Paraffin Impregnated Graphite Electrode). Hence using the electrochemical techniques, Linear Sweep Voltammetry and Potentiostatic Test, it has been carried out a study concerning the influence of size, test media and sonication on the passivity and reactivity of the particles. Moreover by means of Graphite Furnace Atomic Adsorption Spettroscopy it has been possible investigate the effects of the same parameters on the dissolution process.

1 Introduction

Since the beginning the Materials Science always focused its attention on bulk materials, studying their mechanical and chemical properties in order to establish their application and performances. For this reasons the micrometric and nanometric dimension has been neglected, thou lately with the improvement of the characterization technology this branch of study has attract growing interested from scientist of different fields.

Nowadays the field of the micro- and nano- are widespread and many studies related to this topic has shown how going down with the dimensions changes radically the behavior and how in some case the bulk properties are literally turned upside down. Therefore many new branches of science have appeared concerning a growing number of different fields from surface treatment and biomedical devices to nanoelectronics and nanocomposite materials. All of these new branches share the same leit motif, that is to exploit the changes of properties that follows when we reduce the dimensional scale.

This particular study follows this line of thoughts and attempts to carry on an investigation regarding the corrosion properties of a wide known material such as Stainless Steel 316 L. The originality of this work lies in the microscopic dimensions of the samples considered, in

fact, despite the extensive studies of which the stainless steel has been object, no one yet focused his attention on the corrosion of micro particles of this common material.

This work put the stress on how the corrosion properties change reducing the scale of the sample and provides electrochemical tests concerning bulk systems and two different batches of micro particles of different sizes. Furthermore different characterization techniques, such as SEM and EBSD, have been employed in order to assess the nature and the properties of the particles before and after the tests.

The reasons behind the choice of SS 316 L as object for the research lies with the fact this materials is one of the most common biomedical materials for a wide range of applications, from screws and nails for temporary implants to scalpel and other surgical tools.

Furthermore the exposure to metal containing particles is becoming more frequent especially in urban and suburban contexts . Hence defining the corrosion process of these particles and assessing the released compounds becomes a key-issue in order to assess the potential risks for the human health.

This study comprises electrochemical and release tests carried out in solutions that simulate the human fluids present in areas such the lungs and stomach. In addition the influence of parameters such as solution pH, particle size, set up and solution composition have been investigated.

1.1 Stainless Steel AISI 316 L

The term stainless steel was mentioned for the first time in the article “A non-rusting steel” appeared on the New York Times in the 1915 and it was defined as:

> *“a stainless steel, which is claimed to be non-rusting, unstainable and untarishable”* (1)

Obviously the stainless steels are not really immune to the corrosion, they are just very resistant in a particular range of situations. And thanks to this characteristic they are widely used in many outdoor and indoor applications such as:

- Transport applications (automotive, railways, shipbuilding, aircraft)
- House furniture
- Biomedical devices
- Structural elements
- Pipes and fittings

Nowadays the term Stainless Steels is used to describe an extremely versatile range of engineering materials selected for their high resistance to corrosion and heat. These characteristics are due to the presence of chromium in the alloy, that reacting with the oxygen in the atmosphere forms a thin passive layer of 2-3 nanometers able to shield the metal from the external environment [(2)].

There are various kind of stainless steels that differ from each other for composition, microstructure and properties. The main branches of the family of the stainless steels are differentiated by the microstructure:

- Ferritic
- Duplex
- Martensitic
- Austenitic

The SS 316 L belongs to the latter one, that, as the name suggests, presents an austenitic microstructure. This branch is called also the 300 series and represent the largest category of stainless steel produced in United States. Basically the steels belonging to this branch are compositional modification of the classic 18/8 (18% Cr–8% Ni) stainless steel, such as a)addition of molybdenum, to enhance pitting resistance, b)reduction of carbon or addition of niobium or titanium to avoid intergranular corrosion, c)addition of nickel and chromium to enhance high temperature oxidation resistance and stress corrosion resistance.

The 316 L stainless steel is used in many different applications, thou is fairly common in the biomedical field. Its composition ranges of a common is reported in the table below (tab. 1).

Tab. 1.1: Composition ranges for 316 L grade stainless steel [(3)].

Grade		C	Mn	Si	P	S	Cr	Mo	Ni	N
316	Min	-	-	-	0	-	16.0	2.00	10.0	-
	Max	0.08	2.0	0.75	0.045	0.03	18.0	3.00	14.0	0.10
316L	Min	-	-	-	-	-	16.0	2.00	10.0	-
	Max	0.03	2.0	0.75	0.045	0.03	18.0	3.00	14.0	0.10
316H	Min	0.04	0.04	0	-	-	16.0	2.00	10.0	-
	max	0.10	0.10	0.75	0.045	0.03	18.0	3.00	14.0	-

The composition is correlated with the microstructure by the so called Schaeffler's diagram. This diagram is use as variables the Chromium equivalent and the Nickel equivalent, that are specific parameters depending from the given composition.

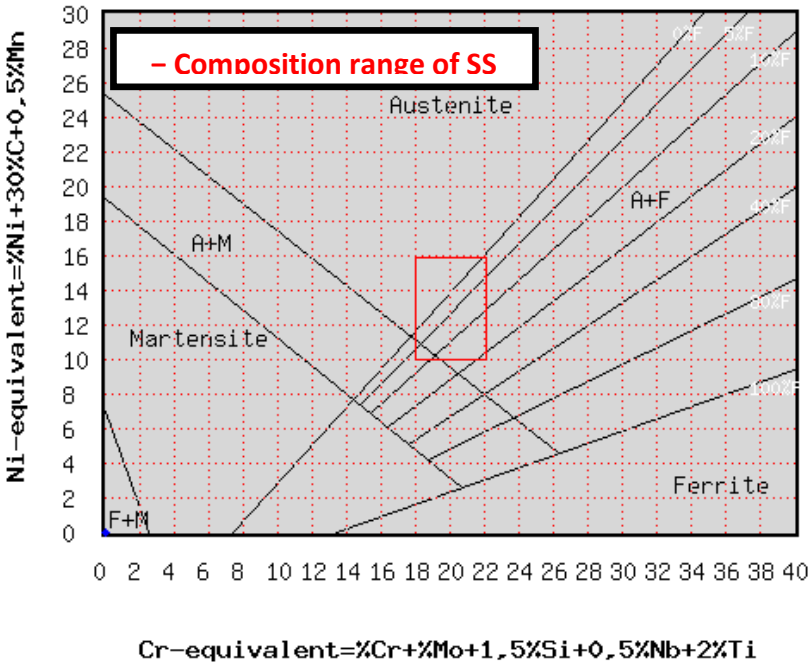

Fig. 1.1: Schaeffer's diagram with composition range for a general SS 316 L [4].

As we can see from the diagram the composition range for this alloy intersects the austenite-ferrite field meaning that beside the desiderated austenitic structure is it possible to observed the parallel formation of delta ferrite. In the modern alloy the composition is designed to minimize this phenomenon, since the delta ferrite is known to decrease the pitting resistance.

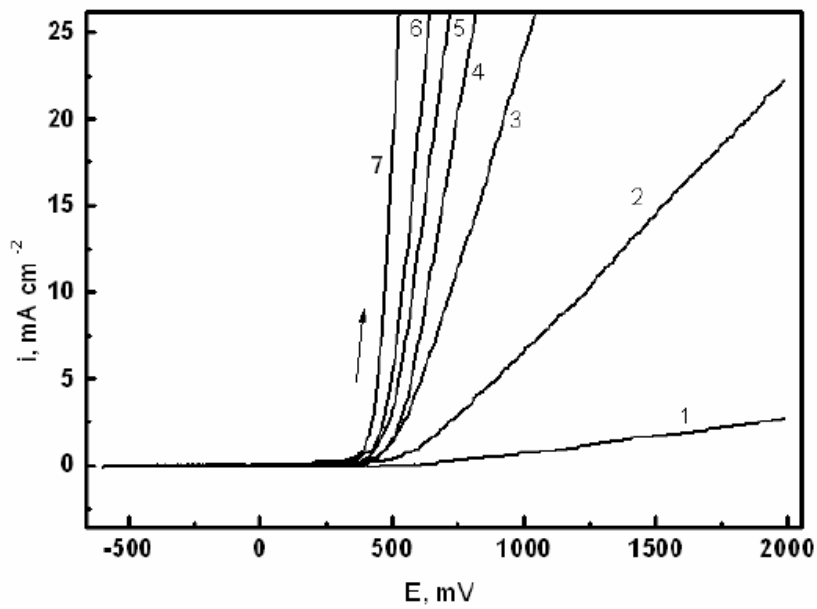

Fig.: 1.2: Anodic potentiodynamic curves for 316 L SS anode in the presence of NaCl solutions with different concentrations:1)0.01, 2)0.1, 3)0.3, 4)0.5, 6)1.0 and 7)2.0 M NaCl [5].

The pitting corrosion is of great practical interest since it represents one of the most common cause of failure for stainless steel based devices or structures. This mechanism of corrosion is an extremely localized and rapid form of corrosion and it is caused by the presence of chloride ions, which are . S.A.M. Rafaey et al. published an article concerning the corrosion properties of 316 L stainless steel in a NaCl solution [5]. The author tested the material using linear sweep voltammetry with a scan rate of 20 mV/s with a potential range from -700 mV to 2000 mV, below it is possible to observe the potential vs. current curves obtained by Rafaey.

The point in which the current increases suddenly represents the breakdown of the passive layer and the subsequent transpassive dissolution. These curves show how increasing the ions chloride content shifts the potential at which the passive layer breakdown.

1.2 Passivity of Austenitic Stainless Steel

Today is generally believed that the passivation of metals corresponds to the dissolution of the metal followed by the formation of an three dimensional oxide film. This thin film allows the metal to resist to a further dissolution, in other words the oxide protects the metal surface. Therefore the eventual breakdown of this film would mean the end of the passivity and then the dissolution would restart [6]. The figure 1.3 represents a generic curve potential vs. current usually shown by a passive metal. As we can see for potentials below $E_{passive}$ the dissolution takes place, then when the $E_{passive}$ is reached the dissolution is stopped and the current decreases, finally if the potential increases until $E_{transpassive}$ the oxide film breaks down and the corrosion of the metal takes place again.

Despite the generic process of passivation is well known, the steps of the formation, the composition and the nature of the oxide film is still object of an ongoing debate. It is known that the nature of the passive film depends from the metal on which it grows, the electrochemical treatment and the nature of the solution (pH, temperature, composition, etc.), therefore the composition of the oxide varies completely from case to case and especially for alloys can be extremely complex.

The passive film of austenitic stainless steels is general observed to be of a duplex nature, an inner oxide barrier layer and an outer hydroxide deposit or salt film [7]. The oxide is formed from starting from the rapid absorption of hydrates complexes on the surface, then the reaction with the water present in the solution gives a hydroxide layer, which further reacts to form the final oxide film.

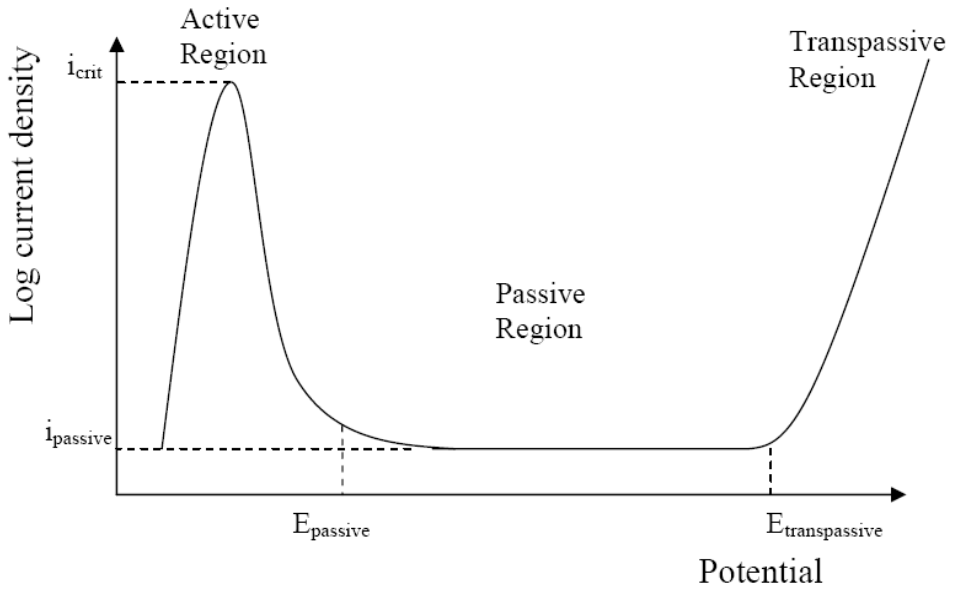

Fig.: 1.3: Anodic polarization curve for passive metals; I_{crit} = critical current density; $i_{passive}$ = passive current density; $E_{passive}$ = passive potential; $E_{transpassive}$ = transpassive potential [6].

Might be interesting observing that often the oxide film doesn't contain all the alloy elements added to the stainless steels to improve their resistance to corrosion. Therefore the latest studies combining electrochemical and surface analysis, such as XPS, included in the passivation process three different layers: barrier oxide layer, salt deposit layer and alloy surface layer.

The following discussion will concern the passivation process in two of the more important media for stainless steel, sodium chloride and hydrochloride acid. B. Brox et al. [7] carried out a study concerning stainless steel passivation using XPS analysis, they showed that the surface during the dissolution is enriched of Ni and Mo since the corrosion potential is much closer to the value shown by these two elements.

They found that oddly the Ni doesn't participate to the oxide formation, even if it known for increasing the pitting resistance. On the other hand they observed that instead the Mo contributes directly to the oxide growth even at potentials beyond its transpassive potential. The presence of the Mo^{6+} and Mo^{4+} has been observed in both layers, inner and outer, together with Cr^{3+}, that it has been found in much higher concentration than Fe. This finding assess the Cr as main passivating elements in stainless steels.

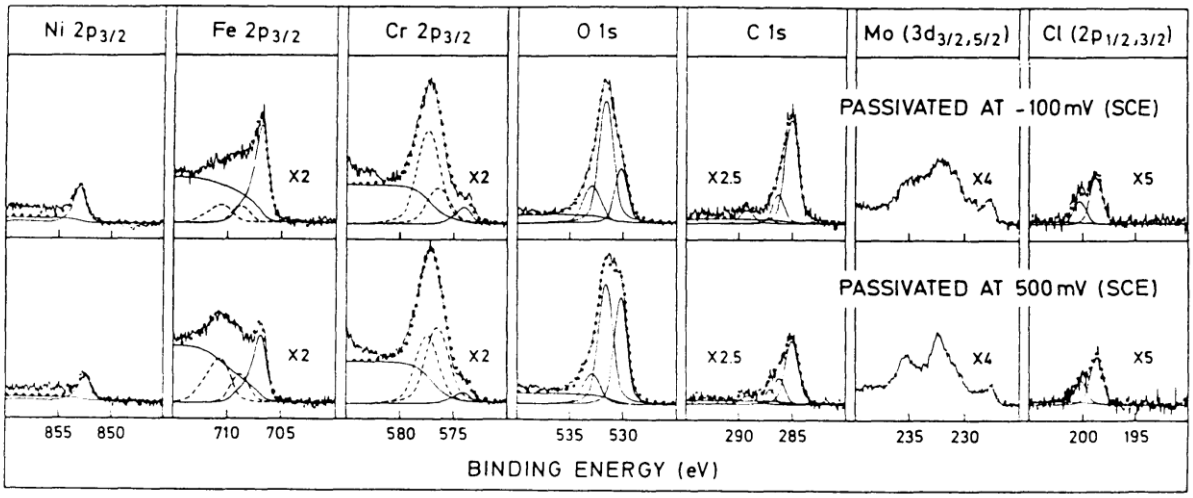

Fig.: 1.5: XPS spectra recorded from Fe18Cr14.3Ni2.5Mo after passivation at -100 mV (SCE) and 500 mV (SCE) [7].

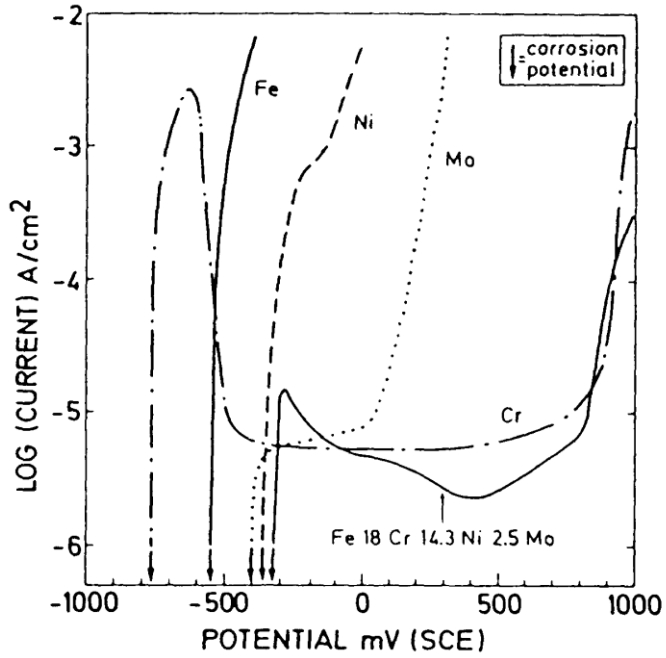

Fig.: 1.4: Anodic polarization curves of the pure metals Fe, Cr, Mo and Ni and of an austenitic stainless steel, Fe18Cr14.3Ni2.5Mo exposed to 0.1 M HCl+0.4 M NaCl at 25°C. Sweep rate 3 mV/s [7].

G. Okamoto and H. Saito [8] in a series of studies provided some insights regarding the role of bound water in the passivation process. They observed two different classes of bound water: M-OH and M-H_2O; M-O and M-OOH. The water is generally associated with Cr, still its nature varies with parameters such as applied potential, time and temperature. These studies assessed that the changes in the bound water were associated with variations in the structure of the oxide.

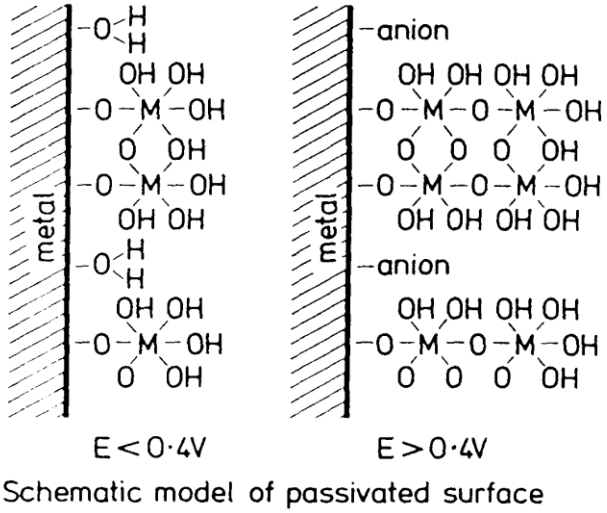

Fig.: 1.6: The Okamoto model of the structure of the passive film [8].

As we discuss above for the work of Brox et al. the Mo seems to have a crucial role in the passivation process, furthermore many studies focused on this elements and many hypothesis were made. For instance it has been proposed that the Mo^{6+} bonds in a solid solution with CrOOH avoiding the transpassive dissolution. Others assumed that, since the Mo could exist in a six- and four- valent form, it could cancelled the point defects associated with the oxide lattice of the three- valent Fe and Cr. Therefore the flux of cations and anions will be hindered preventing the oxide breakdown. A recent study postulates that the Mo plays an important role in the repassivation process. It has been proved that in presence of chloride ions the Mo bond with them to form insoluble chloride complexes. Therefore the Mo precipitating with the chlorides will lower the pH of the pitting solution and deposit a salt film at the bottom of the pit helping the repassivation process [7].

Many works have given some insights also concerning the role of the nitrogen in the passivation mechanism. The influence of nitrogen mainly concerns the repassivation process, in fact the N seems to lower down the pH of the pitting solution forming ammonium ions and enhancing the precipitation of oxyanions.

As we aid before three layers have to be attributed to the passivation process: barrier oxide, salt deposit and alloy surface. The latter one is assumed to be a some kind of intermetallic layer beneath the oxide barrier that unsure a further protection of the metal surface. The composition of this third layer has been object of many studies.

For instance Olefjord and B. Brox [7] using the XPS technique try to record the concentration of alloy elements in the superficial layer of the samples and in the electrolyte, they observed that if on one hand the Fe is selectively dissolved, on the other hand the Ni and the Mo are

found to be in higher concentration than in the bulk alloy, explaining the lacking of Ni in the oxide film.

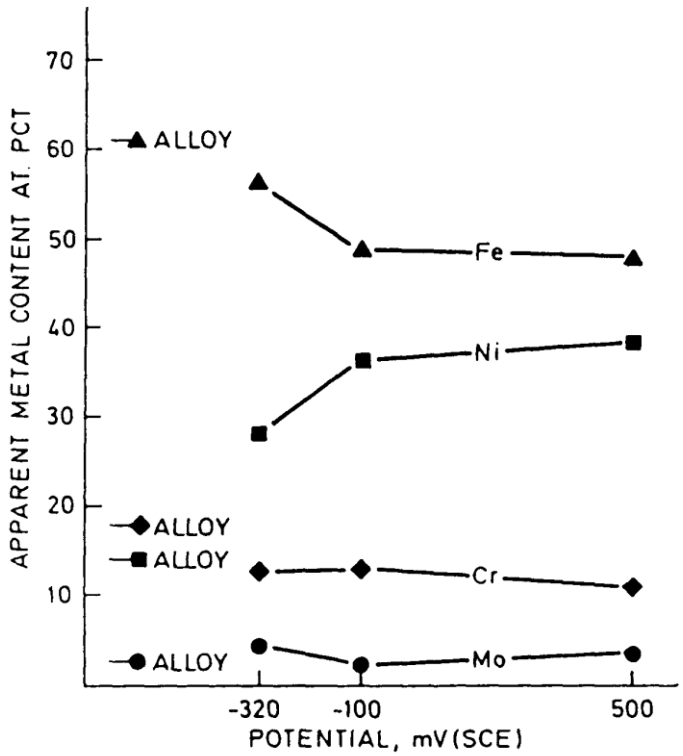

Fig.: 1.7: Apparent metal content of the alloy vs. the potentials (SCE) [7].

It has been proposed that the Mo, beside strengthening the oxide barrier, increase the segregation of Ni in the intermetallic layer. F. A. Cotton et al. suggested that the Ni bonded with Cr and Mo is able to lower down the metal dissolution and hinder the pitting process.

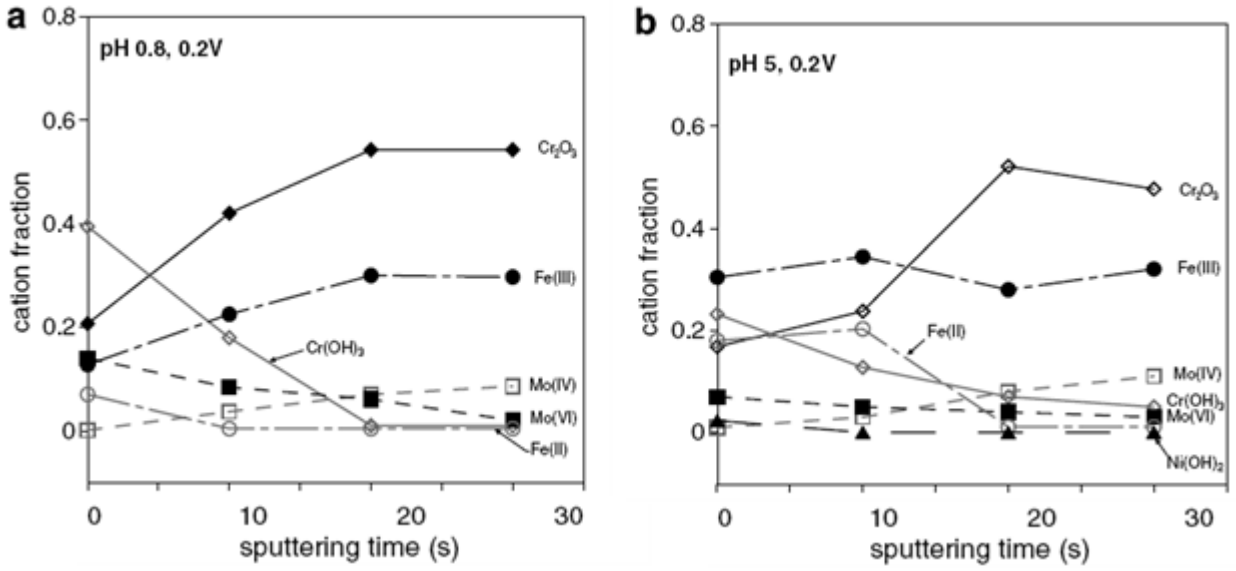

Fig.: 1.8: XPS sputtering depth profiles of the oxides in the passive film of 254SMO stainless steel after passivation for 90 min at 0.2 v (SCE) in the 3.5% NaCl solutions with (a) pH 0.8 and (b) pH 5 [8].

Moreover C.T. Liu et al. [8] published an interesting article concerning the influence of pH on austenitic steel in a 3.5% NaCl solution. This work confirms the double layer structure of the oxide theorized previously, further it reports from quantitative and qualitative analysis by means of XPS that the outermost layer is constituted by iron oxide and $Cr(OH)_3$, while the inner layer shows Cr2=3 as primary constituent. These results were found to be independent from the pH of the electrolyte.

During the passivation by means of ICP-MS it has been detected the selective dissolution of iron, beside low release rate for Ni and Mo. After passivation no Ni oxide were observed in the surface layer, indicating that the nickel partially dissolves and accumulates in the alloy layer. Instead the Mo was detected in both outer and inner layer as Mo6+ and Mo4+, respectively. Below are reported the sputtering depth profiles of the oxides in the passive layer.

1.3 Human exposure to stainless steel

In urban environment there is a high probability for humans to be exposed to airborne metal containing particles. Some professional fields are more exposed to metal containing particles than other, for instance for the workers in the metallurgic field the exposure to metal particles due to the fabrication and use of metallic materials is much high than for professionals in other fields. However the sources of these particles are many, for example they could be originated by traffic sources from tailpipe emissions, brake and tire friction and roadway dust. Other possible origins for the metal containing particles are construction sites or exhaust products from heating system. Therefore it is safe to assume that the entire urban population is exposed in different amounts to alloy materials in particulate form. M. I. Romàn [9] carried out an investigation concerning the characteristics of airborne particulates in the industrial belt of Madrid. They found a wide range of particles with different compositions dispersed in the atmosphere and they were also able to correlate the various elements to the different sources, for instance lead was found to be linked to re-suspended ground dust, while nickel, chromium and copper derive from industrial activities and fuel combustion. And finally iron and zinc were related to the metal industry.

It is also worth mentioning that not all the particulate matter is originated from sources related to human activities, for instance Obenholzner et al. [10] wrote an articles on the metal containing particles detected in the plume of Popocatèpetl volcano in Mexico.

The emissions of air pollutants is characterized by extremely strong spatial and temporal variation that make the analysis of urban pollution quite complicated. Moreover also the meteorological conditions, such as rainfalls and wind, have to be taken into account for an accurate analysis. For instance Yuh-Shen Wu et al. in a study correlated the concentration of metallic particulate matter in Taiwan with the wind speed, their findings indicate a strong influence of this factor on the suspended particulate matter. Moreover other studies proved that moving from industrial to traffic areas the composition of the air pollutants changes radically. B. Vijay Bhaskar et al. [(11)] analyzed the chemical composition of the particulate matter suspended in the area of Madurai City, India. They detected that the industrial areas had the highest concentration of heavy metals such as iron, zinc, chromium and sulphate ions, while the traffic area the most common elements were cadmium and nitrate ions. These results indicate that each area is characterized by different sources of metallic particles and therefore different compositions of the airborne matter.

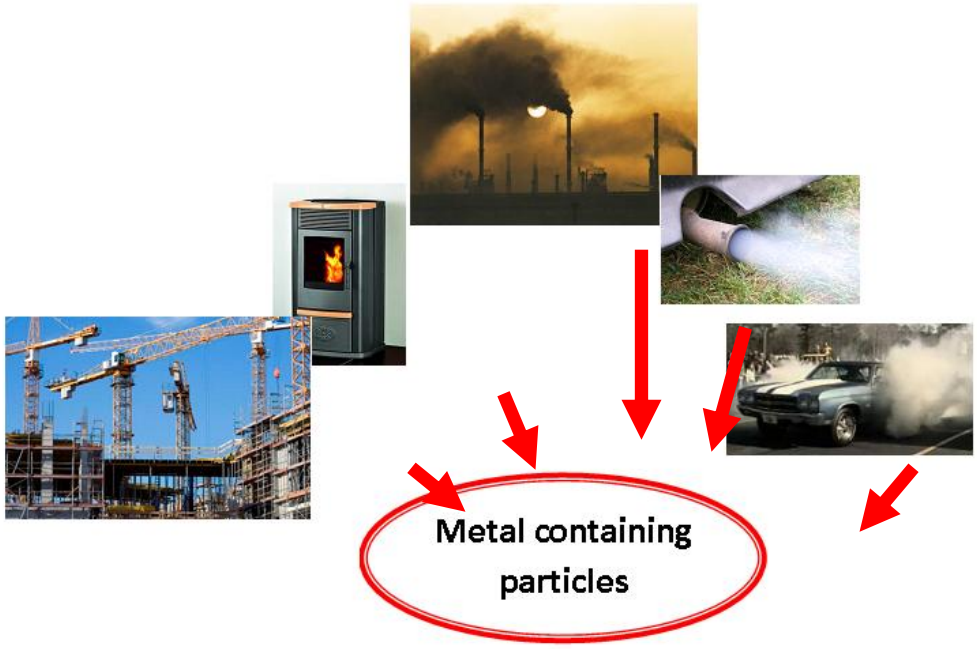

Fig.: 1.9: The main different sources for metals in particulate form.

Airborne particles are associated to a wide range of adverse effects to human health. Many studies focused on the consequences of the inhalation or ingestion of metal containing particles. The more common effects could be divided in two branches: short-terms and long-terms. The short-time effects include eye, nose, throat and lung irritation, coughing, sneezing, runny nose and shortness of breath. While for a long-term exposure the possible

consequences are exacerbation of asthma, temporary and chronic respiratory diseases, lung cancer and cardiovascular diseases. Furthermore the inhalation of metal particles could worsen preexisting health conditions such as allergic diseases.

Particles with a diameter of less of 100 μm are considered to be inhalable, while for diameters less of 5 μm the particles are thought to be even breathable. The latter particles might be able to penetrate deeply in the lung causing inflammatory responses. Moreover many studies reported the ability of soluble transition elements to induce oxidative stress and even to damage the DNA. M. Somers et al. [(12)] carried out a study concerning the possible heritable genetic mutation in sentinel mice due to metallic airborne particles, their findings indicate exposure to particulate matter as a factor affecting the mutation rate.

Metallic particles in contact with human tissue involves the release of ions that could endanger the human health. Many studies considered the different area that could be affected by metal exposure, such as skin, eyes, lungs, gastrointestinal tract. the release of the metals contained by the particles in such sensitive part of the human body could cause strong adverse effect of the health of an human being. Furthermore nowadays many alloys contain noteworthy amounts of chromium and nickel. The first if released in its hexa valent form is often cause of a quite large variety of cancer, while the second one is well known for causing skin dermatitis. Needless to say that if these elements were present in elevated concentration in a human body, this would mean serious consequences, even life threatening , for human health.

J. Zhao et al. [(13)] published an article related to nickel compounds and their possible adverse effects on human health. Due to the wide use of nickel in occupational settings nowadays the exposure to this element has become inevitable. The most common airborne exposure to nickel in the workplace are to insoluble species and they occur mainly during the refining and welding process. The chemical and physical properties of the nickel compounds strongly affect the bioavailability and toxicity. The primary route for airborne exposure is through inhalation, hence the most common target organ are skin and lungs. Usually the nickel could cause skin allergies, lung fibrosis and cancer, even thou the mechanisms for the nickel-induced canrcinogenesis is not clear.

1.3 Dissolution/Release process in Stainless Steel

The metal release process is governed by a combination of corrosion (electrochemical) and dissolution (chemical) process, and its entity relies on a large number of factors such as, barrier properties and composition of the passive oxide, environmental and exposure conditions.

Since even from metals in their passive state small amounts of ions can be released, it is necessary to define their extent in order to assess their eventual danger to human health. For instance the release even of small quantity of Ni could cause allergic reactions in a noteworthy percentage of the human population. Furthermore the eventual release of Cr in is hexavalent state could pose a serious danger since it is well known for its cancerogenity.

The surface oxide composition and properties govern the extent of released metals, although no correlation exist between the surface and the bulk composition. Therefore is impossible to assess the amount of released alloy elements only from the bulk composition. In fact usually the dissolution of the alloy elements is often selective, Fe and Ni are usually dissolved preferably when instead Cr tends to remain in the oxide layer.

Chiba et al. (14) found exposing SS 316 L to a 0.9% saline solution after 30, 60 and 90 days the extent of Ni release was much larger of Cr compared to the bulk composition. Instead for ferritic stainless steels in artificial saliva the Cr and Mo were enriched to the surface oxide due to an selective dissolution of Fe. Similar findings were reported by Leygraf et al. [15] for Fe18Cr and Fe18Cr3Mo alloy in 1 N H_2SO_4.

Many studies have focused their attention on the release in media that simulate the body fluids. For instance Y. Hedberg [16] in hers study used artificial sweat (ASW) and artificial tear fluid (ATF) for testing particles of stainless steel 316 L. The released amount of Cr and Fe was found to be slightly higher for ASW (pH 6.5) than for ATF (pH 8.0), thou the extent of the release was quite low. Furthermore it has been observed that the Cr released was in its tetravalent state and it was complexed by every media considered in the study. The Ni dissolved in the solution was below the limit of detection (0.5 μg/L) for coarse 316 L particles (45 μm), while for the Ultra fine particles (5 μm) it has been detected a release of <10 μg/L.

K. Midander et al. [17] tested a wide range of particles with different composition, including SS 316 L, in artificial lysonomial fluid (ALF). They found that the extent of the release amount increases reducing the particles size in the case of alloy particles. The amount of Cr released

was low especially for pure Cr particles and it was released in is trivalent state, the non cancerogenous one, and it was reacting rapidly with the ALF solution forming organic complexes, a tendency that is believed to be even more pronounced in a realistic cell medium. Furthermore the Ni was found to be in very low concentration in the solution and in the surface oxide, in according to literature findings that state the presence of Ni mainly in the alloy surface underneath the oxide.

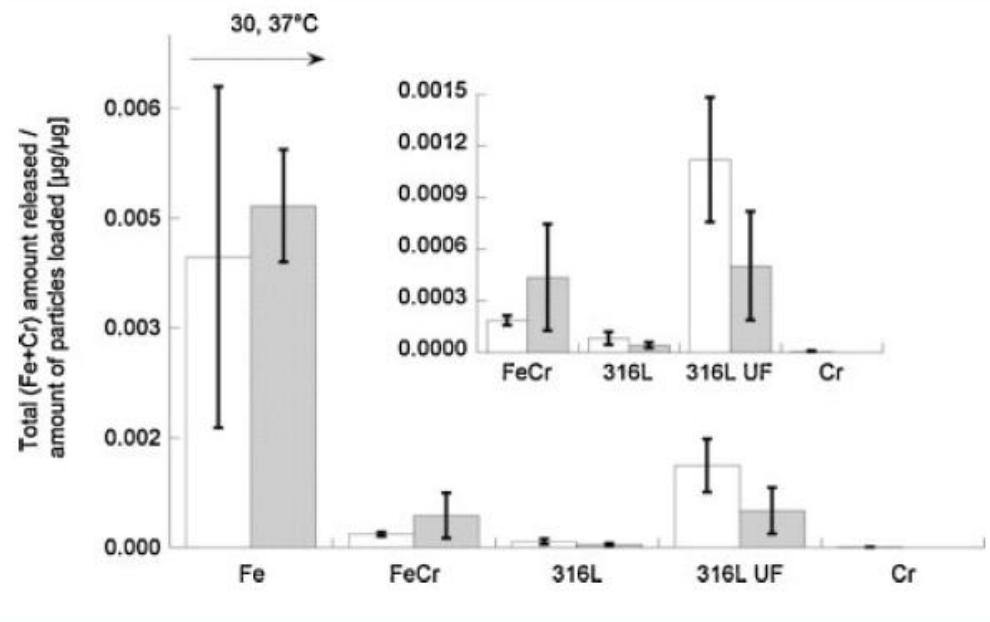

Fig.: 1.10: Amount of total metals (Fe+Cr) released per total amount of particles loaded (µg/µg) from particles of alloy (FeCr, 316 L, 316 L UF) and pure metals (Fe, Cr) immersed in artificial sweat for 24 h at 30°C (open bars) and 37°C (shaded bars)[16].

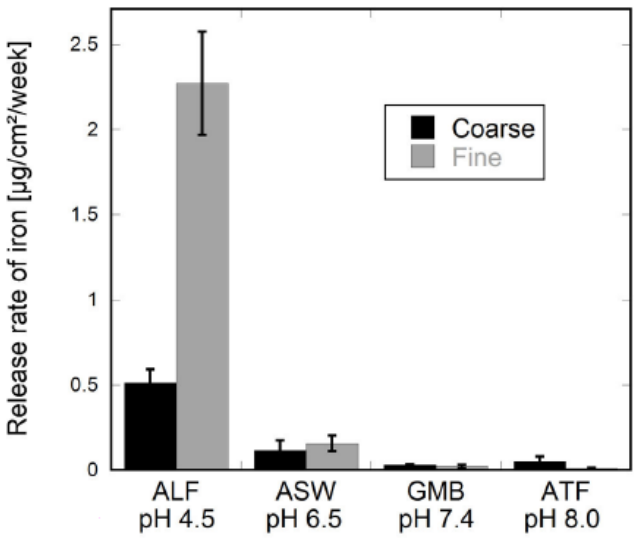

Fig. 1.11: Influence of biological media and pH on the release of iron from stainless particles[18].

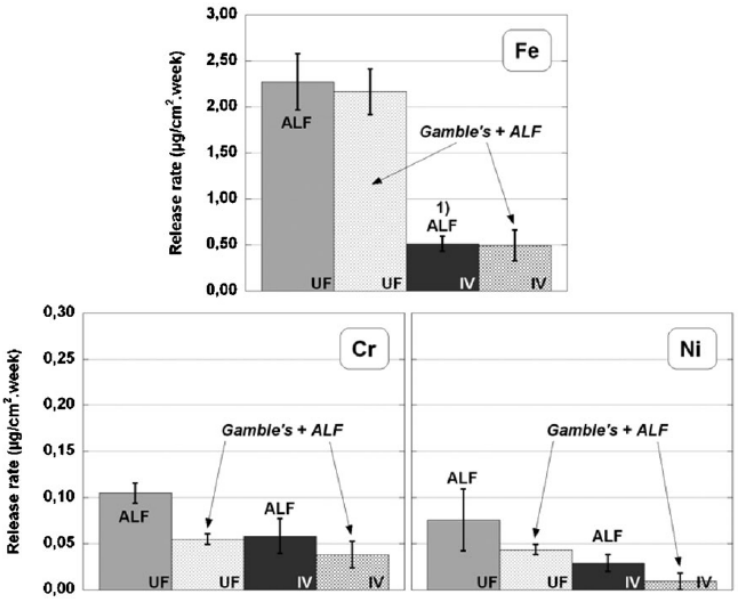

Fig. 1.12: Metal release rate of Fe, Cr and Ni per unit surface area for Ultra Fine powder and coarse powder exposed to GMB and ALF [17].

These results are also in according with a previous work by K. Midander et al. [19] concerning the influence of particles size for biological media, such as ALF and GMB solution.

The results show clearly that the release process is strongly affected by the particles sizes and the test media. The release of iron for UF particles is much higher than for both coarse particles and for Gamble's solution. Thou in the latter solution no trend related the particle size was observed. The finer particles show a more intense activity and adsorption of inhibiting species. The effect of the inhibiting species is evident for the particles tested first in the Gamble's solution and then in ALF, especially for Cr and Ni. Moreover the decrease of the release rate to a steady-state is much slower in the case of the UF particles than for the coarse particles.

In another work K. Midander [17] compared Fe-Cr alloys with pure metal in different media ALF, Gamble's solution (GMB), phosphate buffered saline solution (PBS), artificial gastric fluid (GST). The release amount for most of the alloy elements (Al, Cu, Mo, Ni, Ti and V) was below the detection limit, while it was possible to detect both Fe and Cr. The extent of the release of these elements was generally low, the highest value was observed for the GST media (pH 1.5), as it is reported in the graph below.

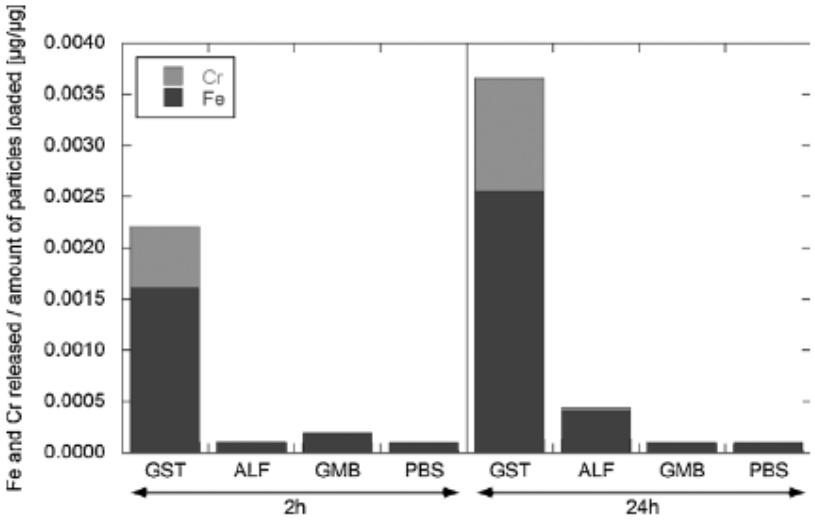

Fig.: 1.13: Total average amount of released iron and chromium from FeCr alloy particles per amount of particles loaded, in GST, ALF,GNB and PBS after 2 and 24 h of exposure [17].

The kinetic of the release was for all media except ALF showed at the beginning high rates the decline with time. Instead the ALF showed the release rate increasing until a maximum at one hour of exposure, after which the rate start declining.

1.4 Transpassivity of austenitic Stainless Steel

As we could see in the figure 1.14 if after the passivity region we keep increasing the potential, we reach the so called transpassivity region. In which the oxide layer starts breaking down and the current raises again meaning the corrosion process is taking place. Is important to mention that the presence of chloride ions decreases the transpassivity potential changing the shape of the curve and consequently reducing the extension of the passivity region, which for high concentration of chloride ions could even disappear.

A.Fattah-alhosseini (20) wrote an interesting study concerning the transpassive dissolution for SS 316 L using electrochemical impedance spectroscopy (EIS). He proposed to model the transpassive film as a highly doped n-type semiconductor-insulator-p-type semiconductor (n-i-p) structure. He proved that injecting negative defects at the solution/film interface would interfere with the growth of the transpassive oxide. This would result in dissolution and release of Cr^{+6} and Fe^{+3} respectively from Cr and Fe.

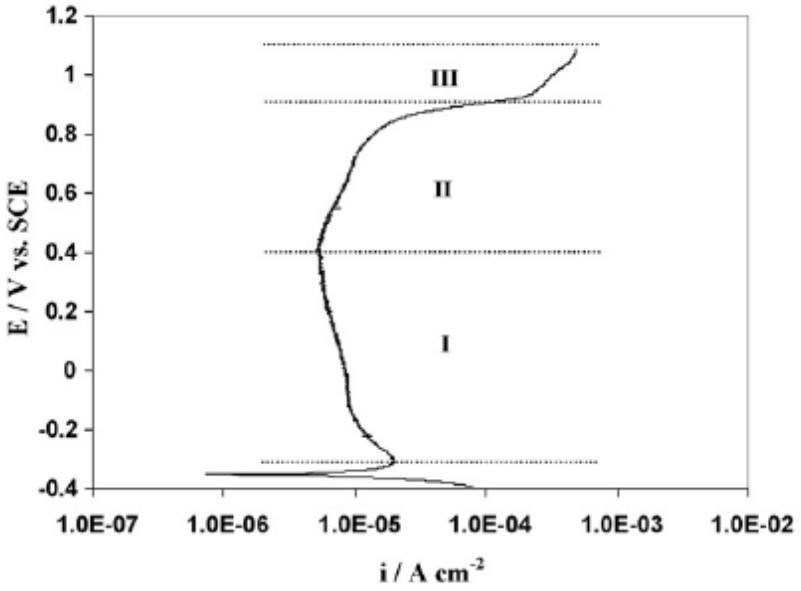

Fig.: 1.14: Potentiodynamic polarization curve (scan rate 1 mV/s) for 316L in 0.05 M H2SO4. Potential regions: I, low potential passive; II, high potential passive; III, transpassive dissolution [20].

I. Betova et al. [21] studied also the transpassive dissolution mechanism, although they focused on highly alloyed stainless steels in 0.5 sulphate and chloride solutions. the transpassive dissolution was found to start at higher potentials in solutions with higher pH and with a rate that also increasing with the pH. The retardation of the dissolution is believed to depend from the fact that lower pH leads to a lower content of Cr and a lower level of hydration in the oxide. Therefore in the outer part of the oxide the $CrOH_3$ will convert in Cr^{+6}.

In another article the same author [22] studied the transpassive dissolution mechanism for highly alloyed austenitic stainless steels (AISI 316 L, AISI 904 L, 254SMO and 654SMO) in 0.5 M sulphate solution with pH 0.2. In the transpassive the primarily released element was found to be Cr^{6+}, even thou also low amount of lower-valency Cr and Mo were detected as well.

The AISI 316 L was the only stainless steel reported to undergo secondary passivation, whereas the remaining steels dissolved at high current densities in the whole potential range. The Cr release increases in the order AISI 316 L<<AISI 904 L<254SMO<654SMO, this is probably connected to the parallel increase in chromium and molybdenum content in the alloy.

Further according to the model proposed the secondary passivation start to be effective whenever the Fe content in the outer layer exceeds the Cr. Since the dissolution of iron was

reported to increase with the alloying elements content (Cr and Mo), therefore it is safe to assume that the efficiency of the secondary passivation decrease as the Cr and Mo percentage raises.

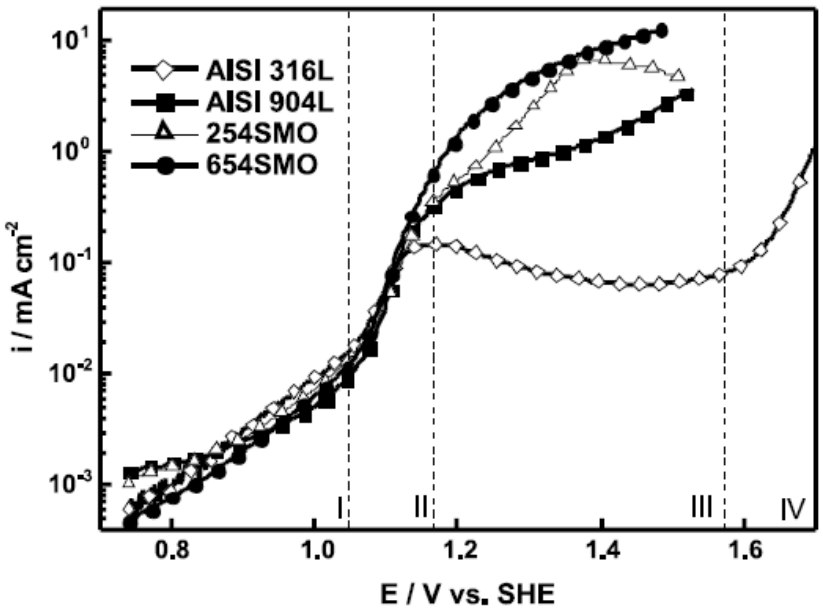

Fig.: 1.15: Current vs. potential curves (sweep rate 1 mV/s) for motionless electrodes of AISI 316L, AISI 904L, 254SMO and 654SMO in 0.5 M sulphate, pH 2 after 30 min of polarization at 0.74 V. Potential regions: I : high potential passive curves, II : Transpassivity, III : secondary passivation, IV : oxygen evolution [22].

1.5 Complexation

This section is meant to summarize very briefly some concepts regarding the complexation, thou it does not pretend to explain completely this phenomena. In chemistry a coordination complex or metal complex is a chemical entity composed by a central atom or ion connected with a various number of external compounds (molecules or anions). This chemical compounds are the result of a large number reactions, generally the process leading to a metal complex is indicated as complexation. Thou the possible reaction that have as product a metal complex are many and in this section only some of the most important will be listed.

Usually after exposure to liquid water or aqueous solutions the oxide surface have to deal to a wide number of reactions, which nature is dictated by the chemistry of the oxide itself. These reactions includes surface hydroxylation and hydration (dissociative and not dissociative water chemisorptions), chemisorptions of solutes and charge transfer reactions.

The hydroxylation can be considered as the first stage for the surface complexation in aqueous media, since it leads to the formation of hydroxocomplexes. Some of the possible products of this process are reported in the figure above. Further the chemisorptions of anions onto the oxide surface is described as a substitution process where the anions take the place of the water molecules (or their protolysis products) in the first coordination sphere of the surface metal ions.

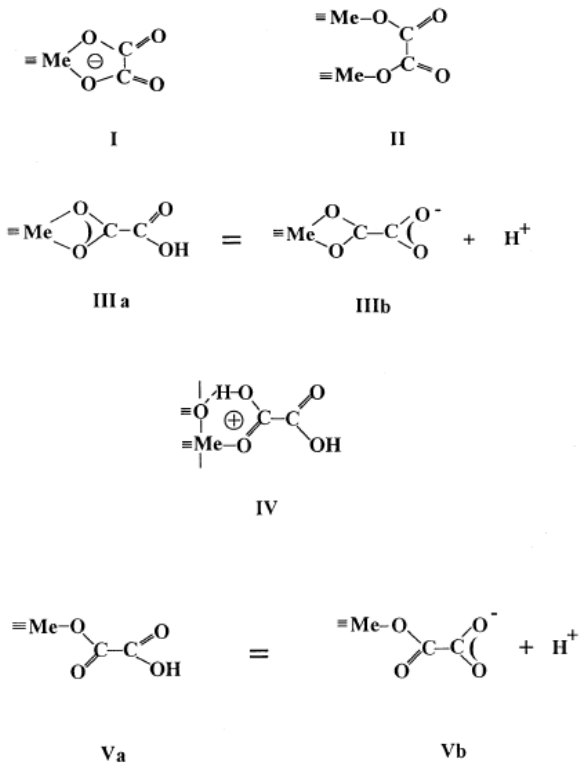

Fig.: 1.16: Some possible oxalate- surface complexes. Species linked by protolytic equilibria are indicated as a and b [23].

1.6 Sonochemistry

Chemical reactions require energy to proceed because they are matter – energy interaction. Considering energy due to ultrasonic irradiation we have to point out that it differs from the other traditional energy sources as light, heat etc, in duration, pressure and energy per molecule making ultrasounds an unique means of interacting energy and matter. In fact chemical effects of ultrasound are not due to a direct interaction with molecules involved but derives from acoustic cavitation i.e. formation, growth and collapse of bubbles in a liquid. The collapse of bubbles produces hot spots with temperature up to 5000 °C and pressure of about 500 HPa with heating and cooling rates around 10^9 K/s. Moreover Shock

waves from cavitation in liquid-solid slurries produce high-velocity interparticle collisions, the impact of which is sufficient to melt most metals. Applications to chemical reactions exist in both homogeneous liquids and in liquid-solid systems. Of special synthetic use is the ability of ultrasound to create clean, highly reactive surfaces on metals. Ultra- sound has also found important uses for initiation or enhancement of catalytic reactions, in both homogeneous and heterogeneous cases.

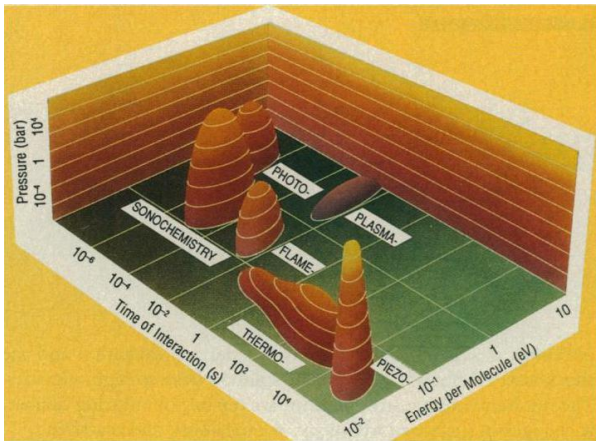

Fig.: 1.17: Chemistry: interaction energy and matter. The three axes represent duration of the interaction, pressure and energy per molecule [24].

Ultrasound span frequencies from 15 kHz to 10 MHz with associated wavelengths of 10 to 0,01 cm. Given to the fact that wavelength are highly greater than molecular dimensions direct interaction between matter and sound is impossible, so that the chemical effects of ultrasound depends on several different mechanisms influenced by the nature of the system. The most important acoustic process for sonochemistry is cavitation involving three main discrete stages : nucleation, bubble growth and implosive collapse. Cavities formation in a liquid is a nucleated process because its tensile strength is so great to preclude cavity formation simply for the action of acoustic expansion, but in the liquid are present weak points like gas filled crevices in a suspended matter or transient microbubbles due, for example, to previous cavitation the only negative pressure effect connected with ultrasound can start the bubble formation. The bubble growth can occur in different mechanisms depending on ultrasound intensity. In presence of high intensity the growth is so rapid to avoid, for inertial effects, recompression during the positive half of the acoustic cycle. On the other hand when the ultra sound intensity is lower growth can occur in case that the cavity surface area is slightly greater during expansion than in compression for the so called rectified diffusion. At some point the bubble reaches a size at which be resonant and so absorb energy from the sound field. This size depend from the ultrasound field frequency,

for instance at 20 kHz the critical diameter is about 170 μm. The cavity, if in phase with sound field, growths rapidly in a single expansion cycle, but, when overgrown. it cannot absorb energy and no longer sustain itself so will implode by liquid rushing in.

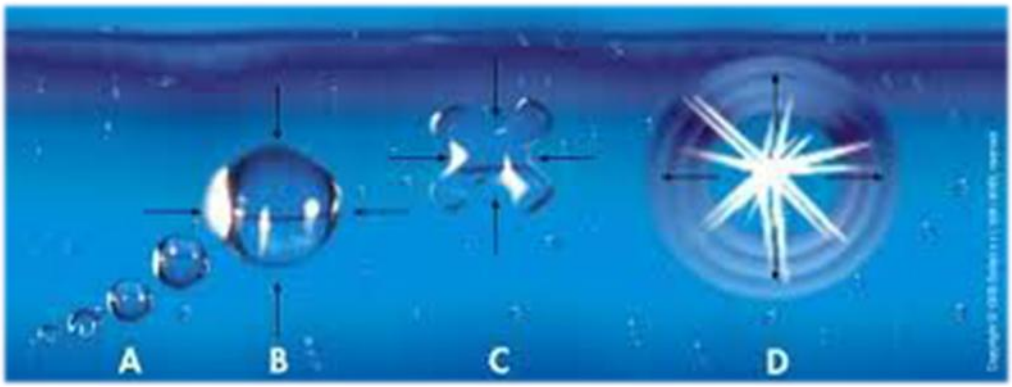

Fig. 1,18: Acoustic cavitation process: (A-B) Creation and growth of the cavitation bubbles in negative pressure, (C-D) The bubbles after reached the maximum size start collapsing in compression and finally implode [24].

The gas into the bubble is rapidly compressed and generates heat and in irradiated liquid the collapse is more rapid then thermal transport generating in this way shot life hot spots in a otherwise cold liquid and this hot spot is the source of sonochemistry. Cavitation collapse generates extraordinary local temperature and pressure and related very high heat transfer rates indicating that ultrasound an unusual mechanism for generating high energy chemistry. Control of sonochemical reactions has the same limitation that any thermal process has because the Boltzmann energy distribution means that the energy per molecule can vary widely. However it is possible to have control on the intensity of heating generated using different parameters such as thermal conductivity of dissolved gases solvent vapour pressure inside the bubble and ambient pressure. An important phenomenon observed during homogeneous sonochemistry is an emission of light called sonoluminescence, which happens both in water and organic liquid studies. Many researches focused their studies on the sonoluninescence, nowadays it is believed that this phenomenon is caused by chemical reaction of high energy species forming during cavitational collapse. For this reason sonoluminescence is a form of chemioluminescence not involved in blackbody radiation or electrical discharge. Obviously the cavitation process near extended liquid solid interfaces is, obviously, very different from cavitation in pure liquids. There are two proposed mechanisms for the effect of cavitation near surfaces: micro-jet impact and shock-wave damage.

Because asymmetric environment near interface a deformation of the cavity during collapse is involved. This deformation is self reinforcing and sends high speed stream of liquid at the surface at speed of about 100 m/s and such impacts leave characteristic micro pitting on surfaces. The second mechanism of cavitation-induced surface damage invokes shock waves created by cavity collapse in the liquid. The existence of both mechanisms has been established, but their relative importance is a matter of debate and probably depends on the method by which cavitation is produced. The impingement of micro-jets and shock waves on the surface creates the localized erosion responsible for the ultrasonic cleaning and many of the sonochemical effects on heterogeneous reactions. Moreover the shock waves caused by homogeneous cavitation cause strong high velocity particles impacts that can drive metal particles to melting in the point of collision reaching temperatures up to 3000 °C. Also ultrasonic irradiation containing metals powders leads to dramatic changes in morphology due to high velocity interparticle collisions causing smoothing of individual particles and aggregation of them in large aggregates.

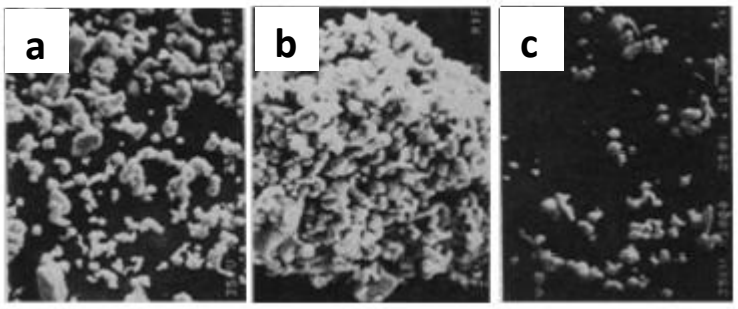

Fig.: 1.19: The effect of ultrasonic irradiation on the particle agglomeration and surface morphology on Ni powder. (a) no sonication, (b) sonication for 15 min and (c) sonication for 150 min.

1.7 Zeta-potential

Most particles dispersed in an aqueous system will acquire a surface charge, principally either by ionization of surface groups, or adsorption of charged species. These surface charges modify the distribution of the surrounding ions, resulting in a layer around the particle that is different to the bulk solution. If the particle moves, under Brownian motion for example, this layer moves as part of the particle. The zeta potential is the potential at the point in this layer where it moves past the bulk solution. This is usually called the slipping plane. The charge at this plane will be very sensitive to the concentration and type of ions in solution.

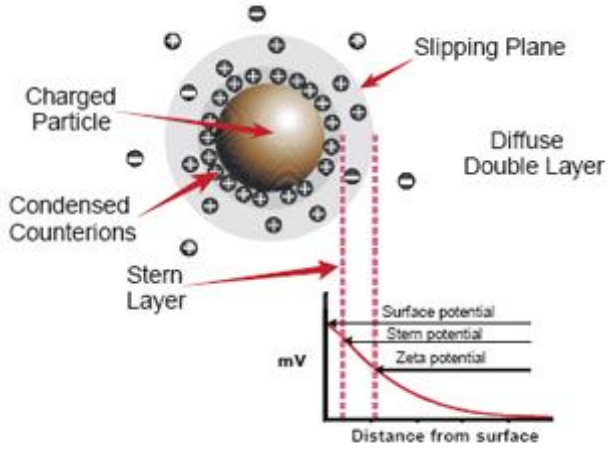

Fig. 1.20: Schematic showing the charge distribution of charge around a particle [25].

Zeta potential is one of the main forces that mediate interparticle interactions. Particles with a high zeta potential of the same charge sign, either positive or negative, will repel each other. Conventionally a high zeta potential can be high in a positive or negative sense, i.e. <-30mV and >+30mV would both be considered as high zeta potentials. For molecules and particles that are small enough, and of low enough density to remain in suspension, a high zeta potential will confer stability, i.e. the solution or dispersion will resist aggregation. The Faraday gold sol made in the 1850's now in the science museum in London, is still a stable dispersion, particle aggregation being slowed to an imperceptible rate due to its high zeta potential.

Typical applications are in the formulation of particulate dispersions. Zeta potential can be used to assess the effect of each additive in the formulation. Additives can have surprising effects; some materials sold as dispersion agents have been known to reduce the zeta potential in particular formulations. It is not always possible to predict the effect or the magnitude of the effect of an additive. The Zeta potential can also be used to increase shelf life by assessing the impact of product changes during storage, e.g. hydrolysis or gas ingress.

2 Motivation and aim of the study

Passivity of metals and alloys is the most central concept for studies of corrosion and materials with special passive properties serve many practical uses of large importance for the society.

In the light of this vast exploitation of metals and alloys that are employed both in daily life and in advanced engineered applications, human exposure and any potential negative effects on health and environment due to the these materials have become an issue of concern. A recent example, which is of substantial importance also to this research project, is the implementation of new chemicals legislation within the European Union, REACH.

2.1 Background and motivation

Via the initiatives of foresighted people from the stainless steel industry, research projects on the metal release from various grades of stainless steels were initiated in collaboration with the former Division of Corrosions Science at the Royal Institute of Technology, KTH. The aim was in this case to generate data that clearly proved what was obvious to people working with this material but not understood by legislators; alloys such as stainless steels have essentially different properties from the pure metals and an alloy does not behave as a mixture of the individual constituent elements. In order to meet the new demands of REACH, testing on metal release from stainless steel was performed in simulated biological media, aiming at to some extent mimic various body conditions. The results obtained were then supposed to be used within the risk assessment of stainless steels. As a part of the projects dealing with stainless steels, the particulate form of these materials was subject to research. The particulate form of metallic or metal-containing materials is highly relevant for human exposure through inhalation and following transportation into lungs or ingestion in the gastrointestinal tract. In the case of stainless steel alloy particles, the exposure scenario is commonly related to several occupational activities during production and further handling by downstream users.

Ever since the first pilot studies on metal release from stainless steel particles, several projects have resulted in published data concerning the metal release process from metal-containing particles within the framework of human health and environmental risk assessment.

With much more experience and understanding for the release processes of the particulate form of metal particles (including, pure metals, alloys, oxides and metal compounds), new research, with the goal to deeper understand the extraordinary passive properties of

stainless steel in this particular form as well as the model system, was initiated at the Division of Surface and Corrosion Science at KTH. This Master Thesis work is a part of that research effort that also includes a systematic study of the components in ALF media (one by one and in synergy), an investigation of the microstructure of stainless steel particles of various sizes, and pioneer studies with real-time metal release investigations on particles.

2.2 Aim of the Master Thesis work

As a part of this joint research effort, this Master Thesis covers the electrochemical properties of stainless steel particles as a measure of passivity. The experimental approach of this project is to combine electrochemical studies and subsequent metal release measurements with an ultimate goal to connect those methods in order to better understand the passive/reactive behavior of stainless steel particles. This approach to investigate metal particles is unique and was never fully adopted. The set of experimental methods was applied for the investigation of samples of different particle size, different microstructure and various degree of pre-treatment by a sonication procedure. In order to succeed in this, several practical issues related to the experimental handling and interpretation of data had to be considered in the design of the study.

Parts of the actual work, which was also included to a minor extent in this master thesis report, was to spend some time on creative thinking about how to perform metal release studies (in real-time as well) on particles under electrochemical control. Some of the ideas were realized and model cells were built and tested.

Passivity of metals and alloys is a widely studied field of research, however, the passivity/reactivity of the particle form of metals and alloys is very little examined. The literature regarding any influence on passivity and reactivity due to a reduction of dimension and particle size is very poor. Stainless steel particles with extraordinary passive properties have previously been extensively studied and there is already some knowledge about the behavior and performance of this material in simulated human exposure and contact. The particles serve as a good reference material for passive type of alloys in particle form. Therefore, an improved knowledge of the passive/reactive properties of this material is essential, also to gain a deeper understanding for other materials in this form.

The overall aim of this Master Thesis project is to deal with these gaps of knowledge and to provide a better understanding of the passivity and reactivity of the particulate form of 316L stainless steel particles of different particle size.

2.2.1. Brief description of experimental design and the report

This study comprises the generation of data through electrochemical methods, for instance linear sweep voltammetry and potentiostatic measurements. The design of a working electrochemical procedure was the first challenge that this project dealt with, since the working electrode should guarantee the reproducibility of the test and minimize the background current. In addition, the influence of particle size, solution pH, solution composition, metal microstructure on the passivity and reactivity was investigated. The electrolytes used in the study were of relevance for exposure to the human body and mimicked to some extent the conditions at exposure via the inhalation/ingestion route. This project also provides a detailed investigation and characterization of the 316L stainless steel particles under exam, in order enable correlation of results from electrochemical measurements with material characteristics, such as bulk and surface composition. In addition, the results from the electrochemical techniques (OCP and polarization) were discussed in relation to metal release measurements, allowing us to connect the corrosion process to the dissolution process.

As explained before the passivity in terms of a protective surface oxide, is what stop or at least hinder the corrosion process on a metal or ally in a humid environment. The literature comprises plenty of studies regarding the alloying phenomena and passive properties for bulk materials even though the mechanisms behind the actual formation of the passive surface oxide layer are yet to be fully defined. This mechanism is in fact depending from a wide range of parameters, such as material, pH, solution composition, temperature, exposure time, environment and also dimension/size and morphology of the sample.

This study is focused on the role played by the dimension parameter. It provides an exploration of the influence of particle size on the passive properties of two different micron-sized 316L stainless steel particles, fine-sized (< 5µm) and coarse (< 45µm) respectively. The particulate form involves other dimensions and somewhat different characteristics to the material in terms of particle size, shape, morphology, surface area, degree of agglomeration, differences in the surface oxide, impurities, differences in the microstructure, etc.

The experimental part of this Master Thesis project provides an investigation of the passivity and reactivity for stainless steel in particulate form. Due to the originality of this topic it was impossible to find extensive reading material from the literature concerning the same field of interest. Therefore this study also includes the development of the electrochemical procedure used to generate the data. Hence there is a chapter reporting the pilot studies

(Chapter 3), in which all the failed and successful set-ups are listed. The electrochemical tests of particles in the different media and the associated release tests and SEM characterization are compiled in Chapter 5. In this report it was considered as preferential to deal with the topic merging the results and discussion part into one section. Hopefully the choice to discuss results right after they are displayed could facilitate comprehension of the experimental findings and ease up the reading of this report.

3 Combining electrochemical and metal release investigations – pilot studies

The electrochemical study of materials in the particulate form is a challenge since it requires the development of a working electrode able to connect the particles into an electrical circuit. There are several practical issues adopting electrochemical measures on particle samples and data interpretation becomes complicated due to the particle form. To overcome such difficulties, the experimental set-up must be relatively simple, robust and reliable. The literature within the field of particles and electrochemistry is scarce and very little information can be found related to any fragment of the issue.

On the other hand, metal release testing has been developed and performed for many kinds of particle materials and solution systems. And much experience in the experimental handling of such systems together with insights and knowledge in data interpretation combined with thorough material characterization has been gained and developed during the last few years at the Division of Surface and Corrosion Science, KTH.

It is relatively conventional to analyze the electrolyte in electrochemical testing for metals after corrosion testing of bulk materials. Since almost no electrochemical measurements have been done for metal particles, the connection of electrochemical data and metal release results is a unique approach that has never been fully explored or adopted within material's research.

3.1 Electrochemistry on particles and endpoint release measurements

The first part of this Master Thesis project was focused on the design of a reliable working electrode, which had to be simple enough to be reproducible and should give as low background current as possible. In the normal case, using the bulk sample as working electrode, the connection with the potentiostat is fairly easy. In the case of particles, it is practically difficult (or impossible) to connect single particles to the circuit to function as working electrode. Therefore it was necessary to design a bridge between the circuit and the particles, able to guarantee the electrical connection without influencing the measurements. Various and different ideas were proposed; from sol-gel deposition onto platinum surface to PTFE vessel charged with defined amount of particles. The most important ideas were realized and tested and those are described in the following.

If only electrochemical testing of metal particles could be made feasible, the endpoint analysis of the electrolyte used for the test, would easily be analyzed as well.

The "cup"

The "cup" set-up consists of a glass vessel (see figure 3.1) that encapsulates the particles and a wire is placed as a stick into the particles in the cup. The function of the wire is to establish electrical connection. The material of the wire was at the beginning a tin alloy, but given the high passivity of the particles it was found to not be suitable for this application. The tin wire was then substituted with a platinum wire that which avoided the preferential corrosion of the wire, still the connection was unstable. Furthermore, for ultrafine 316L stainless particles tested in this configuration, the charging process in the vessel resulted in floating particles which could not be avoided.

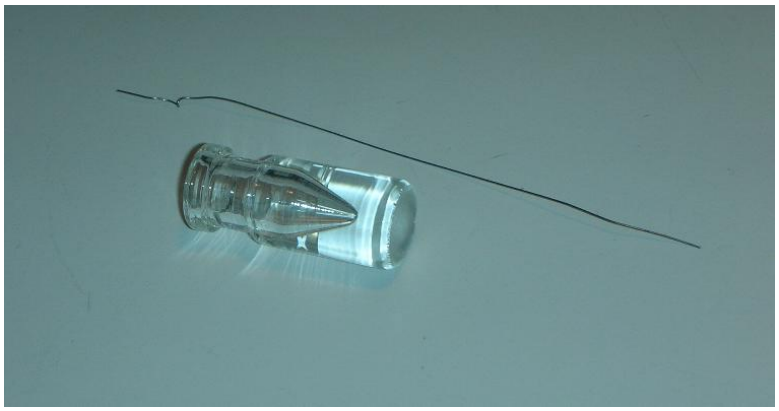

Fig.3.1: Picture of the "cup" configuration.

Fig.3.2: Picture of the "modified cage" configuration.

Based on the combined ideas of trapping particles in a cage-like volume (to be explained and described further in the next section), the "modified cage/cup" was designed. The application was meant to be electrochemical measurements with a better contact between particles and the surrounding solution. The vessel (see figure 3.2) presents at one end a membrane, whose function is to keep particles close to each other (creating electrical

connection) and at the same time putting them in contact with the solution, and at the other end a platinum wire. This configuration was promising, but the connection was unstable and the membranes could be used one time only, hence this set-up was at the end abandoned.

The paraffin impregnated graphite electrode, PIGE

In a previous work Y. Hedberg investigated the possible techniques available for the electrochemical treatment of metallic particles. Among the various procedure tested the paraffine impregnated graphite electrode (PIGE) was found to be advantageous for several reasons: i) the relatively low background current, ii) the advantageous fixing and iii) great electrical contact between particles and working electrode. The PIGE was also tested without loading any particles (blank), in order to see if the paraffin electrode affects the measurement. "Events" in blank measurements occurred in the first two blank measurements but decreased when the electrode was re-used more often. However, it is important to measure blank potential-current curves for this set-up and to exclude any oxidising effect deriving from this electrode. Thus events and differences in particles could clearly be seen with this set-up. Since the PIGE is soft it is difficult to fix the particles on the electrode only by dipping or pressing. A short (ca. 30 seconds) warm air treatment was found to be the best method to fix the particles on the PIGE by dipping. Then the particles that were at the sides of the PIGE were carefully removed.

3.2 Continuous monitoring of metal release from particles under electrochemical control

It is not a straightforward task to continuously measure metal release from metal particles under controlled electrochemical conditions. In fact, it is not always easy to measure the metal release from particles in a solution. The particulate form also makes normal electrochemical studies crucial to perform and results can be difficult to interpret. When studying particles, several parameters needs to be taken into account such as the particle size, the size distribution, agglomeration state, the loading of particles etc, all of them affecting the sample area. The surface condition of a particulate sample cannot be controlled or pre-treated. The particles have to be exposed in as-received condition and therefore it is essential to know something about the particle history, for example the production, handling, and storage procedures. A thorough characterization of the sample particles is needed to enable understanding of data and relevant interpretation of results.

As a part of this Master Thesis work, some creative thinking related to the experimental difficulties of combining continuous metal release measurements from a material sample

under electrochemical control. This topic was actualized because there was a possibility to use a special technique, atomic emission spectroelectrochemistry, available at École National Supérieure de Chimie de Paris, ENSCP Paris Tech, which actually measure the concentration of metals in solution flowing through a special cell were a bulk sample is exposed and controlled by a potentiostat. The research challenge was to adopt this technique to particle samples.

The continuous measurement of metal release from particles under electrochemical control consists of a few practical difficulties that need to be solved…

- ✓ How to expose particles in a flowing solution and at the same time enable continuous detection of released metal concentrations?
- ✓ How to manage to control particles electrochemically, i.e. how can we get electrical connection, and how to do this without affecting the desired particle/solution system (it should still be relevant for the simulated exposure scenario)?
- ✓ How can the continuous release measurement be combined with electrochemical study of particles?

To elaborate the experimental difficulties mentioned above, three different approaches to handle particles in the atomic emission spectroelectrochemistry instrument were tested both in pilot tests at KTH and in the equipment at ENSCP. None of them is actually perfect and some ideas need to be further worked on or refined and further developed. It could also be that one way to expose one kind of particles may not be suitable to another material or particle type. The aim at this early stage was to not make things much more complicated than they have to be. A general requirement for the ideas in pilot tests was that the already existing equipment could be used with only few modifications.

3.2.1 Metal release in a flowing system

The basic idea of metal release testing in a flowing system is based on the principle of trapping the metal particle sample in a small volume, allowing for solution to pass through, based on the idea of a “cage”.

The syringe column

The idea with the syringe column was to create a little volume were a defined amount of particles could be put and exposed to a flowing solution going through the volume. The working name for this approach was “the cage” which actually quite well describes the idea of trapping the particles in the flow. The little volume compartment was built from two

syringes cut into two pieces with a Teflon tube, perfectly fitted into the two pieces of syringes keeping them together and making the construction tight. The idea of using syringes came from that syringe filters seemed to be a reasonable way to let a solution flow through but particles could not. The volume of the syringe column was 1 mL. The filters used here came from PALL, and was an Acrodisc syringe filter with a 0.2 µm Supor membrane. The diameter of the filter was 25 mm which was enough to enable the flow going through the column without building up too much of pressure in the system. Some photos of the column are shown in figure 3.3 below.

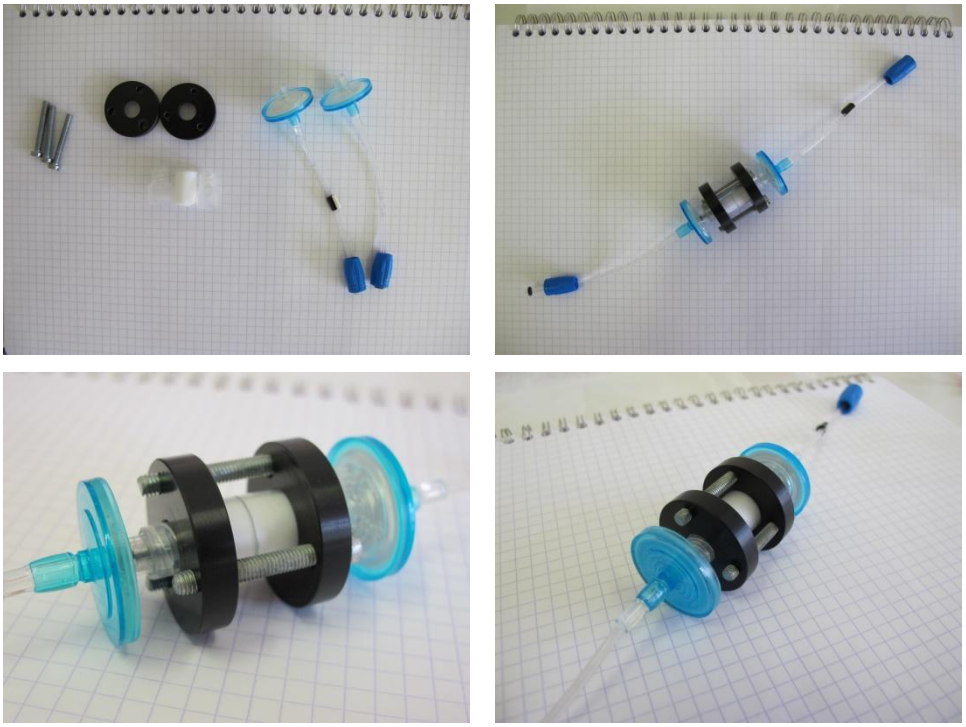

Fig.3.3: Pictures of the syringe column. This was one of the pilot ideas that resulted in a prototype used for continuous measuremens of metal release using the atomic emmission spectroelectrochemistry technique available at ENSCP ParisTech in Paris.

With the syringe column it was possible to obtain continuous data on released concentrations of metals from particles. The amount of particles can be controlled, hence the exposed surface area is known. Some disadvantages to be mentioned are that the syringe filters only can be used once and that the flow rate through the column has to be measured after the exposure. It is necessary to make a calibration measurement and run blank solution through the syringe column since the system affect flow conditions and thereby limits of detection can be affected. By doing this, it is possible to get some kind of idea on how the filters affect the released metal concentrations. Different filters can affect the form of the released metal so the selection of an appropriate filter is sometimes crucial since there are a large number of different filters available for purchase.

3.2.2 Metal release and electrochemical measurements in a flowing system

To design a cell that enables the continuous monitoring of metal release from a particle sample under electrochemical control is a challenging practical research problem with several practical problems. Combined ideas of trapping particles in a volume or just trying to create a bulk-like surface made of particles in electrical connection were some of the ideas that were either tested or banned.

The cage

The idea of a "cage" electrode was intended to work in the atomic emission spectroelectrochemistry system. The main components could typically have been: a vessel of PTFE, two membranes at the two ends of the vessel and a platinum wire running along the electrode ensuring the electrical connection. The main function of the vessel should be to host the particles without any leakage and the membranes were meant to hold the particles inside the vessel and to allow the flow of solution and dissolved metal ions created by a pump. The idea is basically a combination of the syringe column and the platinum wire connection adopted in the "cup" configuration previously described above. The design of this electrode is extremely complicated and the prototype was never tested.

The modified "cup" or the depression cell

One way to put a defined amount of particles in contact with the flowing solution in the atomic emission spectroelectrochemistry equipment was to build a little plate with a part of the area sunk to a slightly lower level. This idea was realized and a prototype was built and tested. In the little "cup", particles could be put and with a barrier (a membrane) in between the particles and the flow, the little "depression cell" could be mounted onto the normal flow cell to the atomic emission spectroelectrochemistry equipment, just as a regular massive metal sample. The depressed area was exactly of the same dimension as the window in the flow cell (0.5 cm^2). To get contact with the particles the sinkage was lined with platinum, see the photos in figure 3.4 below.

The depression cell was not worked with very much and one reason was the difficulty to find a suitable filter to cover the particles put in the sink age and trap them there so they would not get into the solution. In test experiments the cell seemed to work though, but there were problems with leakage after some time of exposure in the set-up. Further work is needed to evaluate which kind of membrane that can be used and that minimize the diffusion problems that likely occurs when the flowing (fresh) solution go through the

membrane and out again. The depression cell is not optimal but could be a way to monitor metal release from particles that to some degree are controlled electrochemically as well. The benefit of this cell would be that a known amount of particles could be put into the little deepening in the Teflon piece.

There were several ideas in similar direction as the one leading to the depression cell. One of them was the “modified cup” which was thought to be a particle electrode composed by a metal vessel with a hemispherical shape that was supposed to be attached to a wall of a specific cell. It should also use a membrane with the same function as the depression cell. The prototype of this design was never built due to issues related to the connection and mechanical stability.

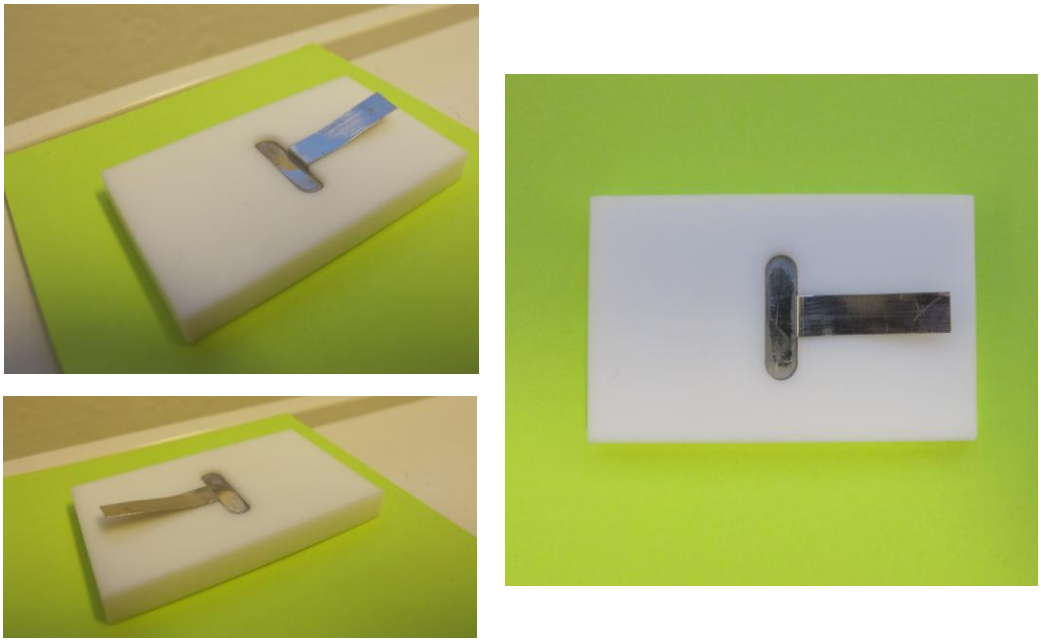

Fig.3.4: Pictures of the “depression”- or “modified cup” cell. This was one of the pilot ideas that resulted in a prototype used for continuous measuremens of metal release using the atomic emmission spectroelectrochemistry technique available at ENSCP ParisTech in Paris.

Carbon tape on graphite sheet

Since electrochemistry on particles was shown to work out fine using a paraffin impregnated graphite electrode (PIGE), an attempt to adopt this method to flowing conditions in the atomic spectroelectrochemistry equipment was made. Unfortunately, the “gluing” properties of the PIGE material was destroyed during the cutting procedure and the attempt failed.

Instead, the particles were mounted on normal carbon tape (which is conducting) on a little graphite sheet and then the particles could be exposed to the flowing solution in the normal cell. With this approach it was possible to also get electrical connection that enables

electrochemical control of the particles during the exposure. This way of exposing particle in the flow cell is really simple but it seemed to be successful. Several measurements were made for two types of stainless steel particles at OCP conditions and during potential sweep. There were usually no problems with leakage if the graphite sheet was mounted properly. Electrical connections seemed also to be fine and there was no problem with manipulating the “metal surface made of particles” when connected to the potentiostat. The disadvantage with this, very simple and straightforward approach, is that the exact amount of particles exposed to the solution is not known. It can though be estimated from for example SEM images or just theoretically calculated based on particle diameter and particle distribution.

The components of the carbon tape/graphite set-up are shown in the photographs belof, figure 3.5.

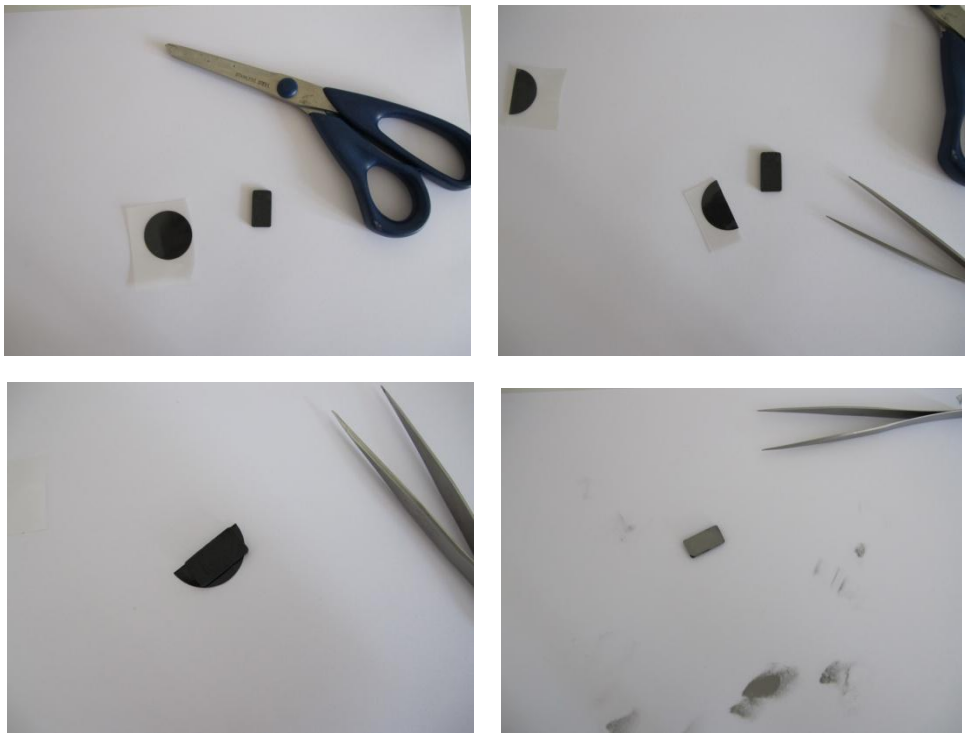

Fig.3.5: The way to mount particles on carbon tape on a grpahite cheet that could be used similar to a bulk sample in continuous measuremens of metal release under electrochemical control using the atomic emmission spectroelectrochemistry technique available at ENSCP ParisTech in Paris.

4 Materials, experimental techniques and procedures

This chapter provides a complete summary of currently available data on various material parameters for the two different 316L stainless steel particles of different sizes investigated. The information partly comes from the manufacturers of the respective materials and from different kind of analyses performed during previous studies that were already published in the scientific literature. Also new (preliminary) findings from further characterization of the materials are reported.

The thorough characterization of both the surface and physical properties of the materials under exam is crucial for the interpretation of results that were obtained within this work, since particle properties and surface characteristics govern the metal release process and any potential toxicity induced by particles. For instance, it is generally believed that a smaller dimension of a material influences many of its material properties, coming to its extreme in the nano dimension [(26)]. Whether or not this influence is also apparent for advanced engineering materials such as stainless steel in a slightly larger dimension is not fully clear. However, previous studies of the metal release pattern from these stainless steel particles proved that under the same conditions smaller particles show a larger release compared with coarser particles [(19)].

This chapter also describes the experimental procedures, the equipment and the methods used to investigate the passive properties of fine and coarse 316L stainless steel particles.

4.1 Stainless steel particles

The two types of stainless steel powder materials were manufactured by gas-atomization and were commercially available: the fine sized particles, in this work denoted <5 μm, came from the Sandvik Osprey Limited, and the coarse particles, which in this work are also called <45 μm, delivered by ARCAM AB, Sweden. This kind of steel particles is usually used for powder metallurgy applications such as the manufacturing of high precision components, for example within the automotive industry. Both stainless steel powder particles are of grade AISI 316 L.

4.1.1 Morphology, size distribution and surface area

The appearance and surface morphology of the 316L stainless steel particles were investigated by means of scanning electron microscopy (SEM). Figure 4.1 and 4.2 presents

SEM images for coarse and fine sized particles respectively, using the same magnification to enable a direct comparison of the particle size.

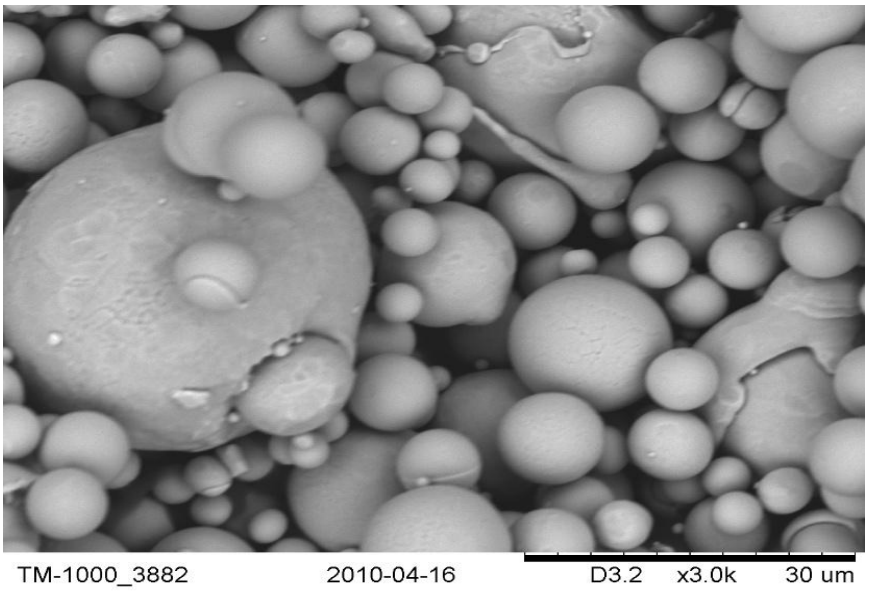

Fig.4.1: SEM image of the coarse (<45 μm) 316L stainless steel particles (magnification: 3000x).

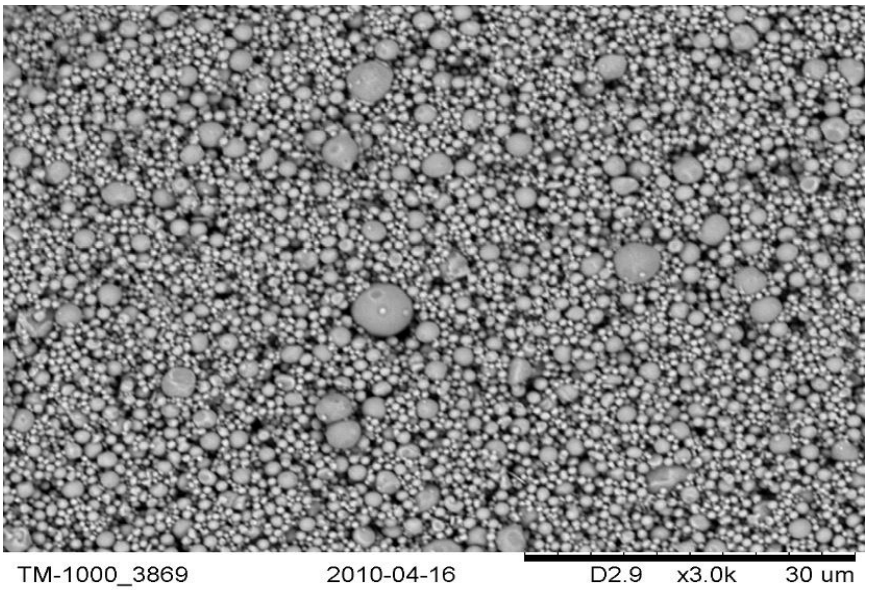

Fig.4.2: SEM image of the fine (<5 μm) 316L stainless steel particles (magnification: x3000).

Both fine and coarse 316L stainless steel particles show a spherical form due to the gas atomization process employed for their production. Furthermore, it is clear that the particles of the two size fractions coarse <45 μm and fine <5 μm really have a quite narrow size distribution as was also reported by the respective supplier, see table 4.1 and 4.2 below.

Table 4.1: Particle size distribution from sieve analysis (wt%) for coarse sized (<45 μm) 316L stainless steel particles as reported by the manufacturer [17].

Micron	*44*	*31*	*22*	*16*	*11*	*7.8*	*5.5*
< 45 μm	86.6	60.5	31.5	15.3	6.1	3.3	0.7

Table 4.2: Particle size distribution for fine sized (<5 μm) 316L stainless steel particles as reported by the manufacturer [18].

Powder diameter (μm)	*Fine particles (< 5 μm)*
D_{10}	1.1
D_{50}	1.8
D_{90}	3.6

In the table above the D_{90} value represents the largest diameter of 90% of the particle distribution, while the 50% and 10% of the particles have a diameter of less than the D_{50} and D_{10} values respectively.

A crucial quantity for a comparative study between different particles is the specific surface area. This quantity is dependent on the particle diameter and size distribution of the particles as well as the surface morphology such as roughness, eventual porosity etc. The values used in this Master Thesis study are reported in previous work performed by KTH [17]. The specific surface area was measured by means of BET (Brunauer- Emmett-Teller) analysis (adsorption of nitrogen in cryogenic conditions) and the results for the two 316L stainless steel particles are presented in table 4.3 below.

Table 4.3: Measured specific surface areas (by means of BET) for the 316 L stainless steel powders [18].

316 L powder	*Fine particles (<5 μm)*	*Coarse particles (<45 μm)*
BET area/m^2 g^{-1}	0.700	0.069

BET analysis was performed at Kanthal AB using a Micromeritics FlowSorb II 2300. The specific surface areas of the materials were in this study used to calculate metal release data per unit surface area of the exposed samples. It is well worth to note that the BET surface area related to the fine sized particles is ten times higher than the area of the coarse particles, and this fact will strongly affect the release rate of the two populations of particles.

4.1.2 Bulk and surface composition and phases of the material

The chemical bulk composition of the two 316L stainless steel particle materials was provided by the suppliers. This information is reported in table 4.4 below.

Table 4.4: Chemical composition of the 316L stainless steel powders in wt%. [18].

Powder	*C*	*Si*	*Mn*	*P*	*S*	*Cr*	*Ni*	*Mo*	*Fe*
< 5µm	0.048	0.65	1.4	0.027	0.008	18.5	11.6	2.3	65.5
< 45 µm	0.030	0.49	1.4	0.025	0.010	16.8	10.3	2.1	68.6

In previous studies using these test materials, the ratio of iron to chromium present at the surface of the materials was reported. The surface compositional analysis of the outermost surface layer was performed by X-ray photoelectron spectroscopy (XPS; UltraDLD spectrometer from Kratos Analytical) with monochromatic Al x-ray source (150 W) on areas sized approximately 700 x 300 µm. A comparison of relative proportions of iron to chromium in the bulk and surface of the coarse 316L stainless steel particles (based on ratios of (Cr/[Fe+Cr]) in wt% using the available results on surface and bulk composition) is shown in figure 4.1.

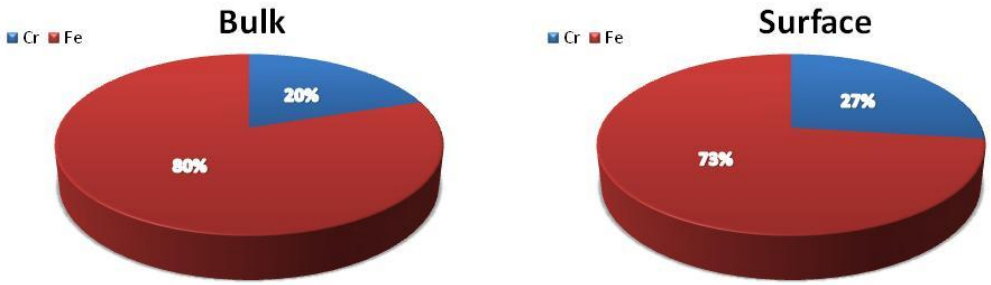

Fig.4.1: Relative proportion of chromium (Cr) and iron (Fe) in the bulk alloy (on the right) and the surface oxide (on the left) for the coarse (<45 µm) 316L stainless steel particles based on results on chemical composition of the surface and bulk [16].

The results from this surface analysis revealed oxidized iron and chromium to be the main components of the external layer of the passive film. In accordance with literature, the passive layer shows a surface enrichment of chromium.

Furthermore the microstructure of the particle materials was investigated by Electron Backscatter Diffraction (EBSD). The EBSD equipment used was a digital HKL Nordlys II F+ camera attached to a FEG-SEM Leo1530. A special sample preparation was needed to be able to embed and polish the particles of different size and avoid any electrical charging of the sample. This technique enables the comparison of scanning electron microscopy images, information on grain orientation and grain boundaries , and phase information (crystallography structure) simultaneously.

By means of the simultaneous use of EBSD, EDS (energy dispersive spectroscopy) and SEM, it was possible to carry out a study of the microstructure and the composition of the single stainless steel particles. This information is desirable since both microstructure and (phase)

composition largely influences the corrosion and release processes of the particles. The micrographs below were obtained by means of SEM for the two sizes of 316L stainless steel particles after etching with Vogel solution for 10 seconds and in both cases the particles show a very fine dendritic structure due to the gas atomization process employed in the production procedure, figures 4.2 and 4.3.

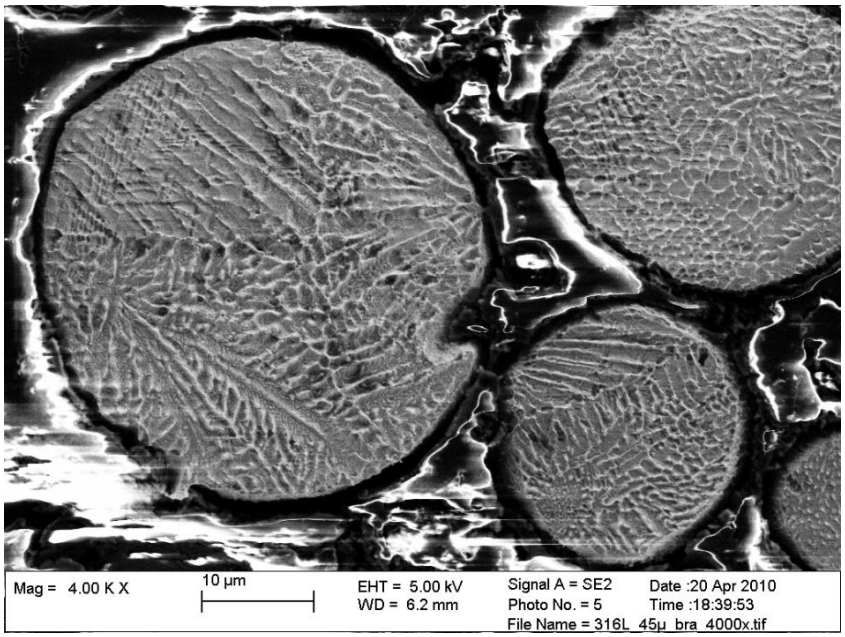

Fig.4.2: Cross section image of a few discrete particles of the coarse (<45 µm) 316L stainless steel material obtained by means of SEM after etching procedure.

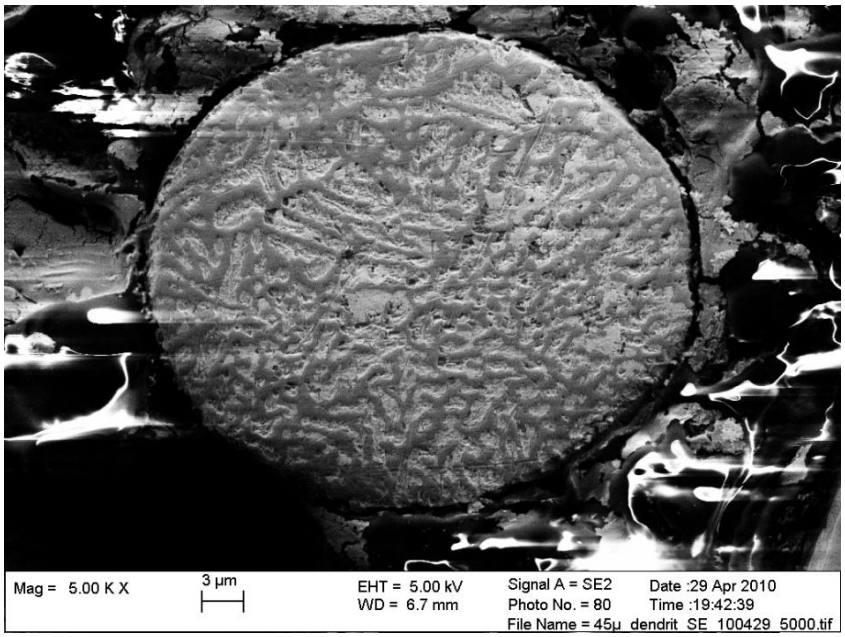

Fig.4.3: Cross section image of a discrete single particles of the fine sized (< 5 µm) 316L stainless steel material obtained by means of SEM after etching procedure.

Moreover, the EBSD investigation provided phase information for the two 316L particle types under exam, figures 4.4 and 4.5.

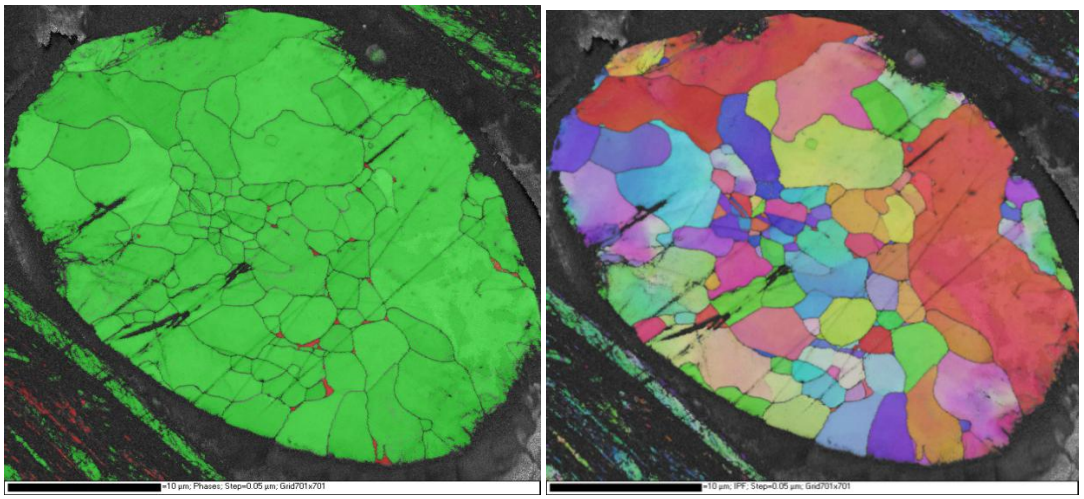

Fig.4.4: Phase image of the discrete particle from the coarse stainless steel material (<45 µm) obtained by means of EBSD. Green grains are austenitic and red areas are ferritic phases (left). The different colors in the image to the right represent different lattice orientations of the grains.

Figure 4.4 is related to the coarse 316L stainless steel particles. As reported in the first part of this section, this powder presents a large fraction of particles with a diameter of less than 45 µm. The results from EBSD phase analysis show these particles to consist of an almost complete austenitic and poly crystalline microstructure. By increasing the magnification, the fine sized 316L stainless steel particles were also possible to observe. The ferrite content in this powder sample seems to be quite elevated and cannot be neglected. Only the larger particles show an austenitic microstructure, while the small particles in this material are almost completely ferritic, see figure 4.5. The results indicate that with reduced particle size, the ferritic microstructure becomes more and more pronounced.

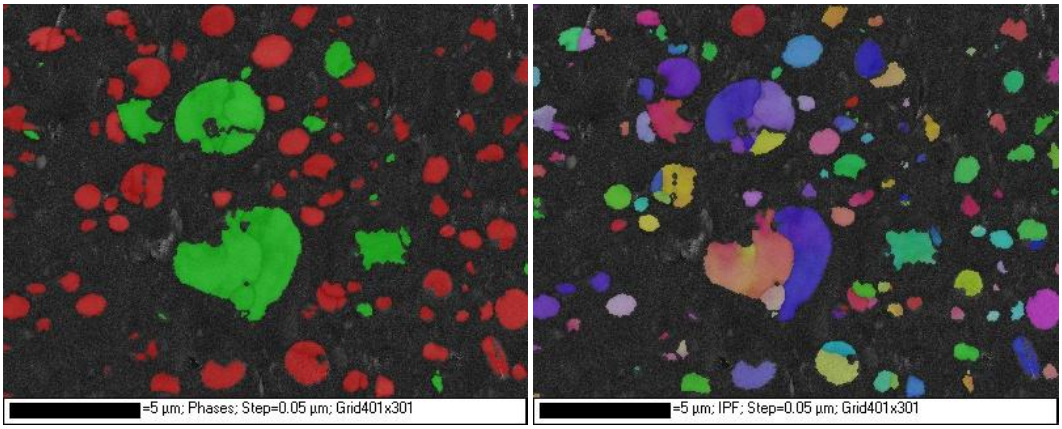

Fig.4.5: Phase image of the fine sized (<5 µm) 316L stainless steel particles obtained by means of EBSD. Green grains are austenitic and red areas are ferritic phases (left). The different colors in the image to the right represent different lattice orientations of the particle grains.

Furthermore many of the particles are present in a mono crystalline form, even though some of them are still poly crystalline. The magnification of a single particle in figure 4.6 below, shows for instance an almost completely ferritic particle with some few austenitic grains and lattice orientation of the grains obviously varies even at this miniscule dimension.

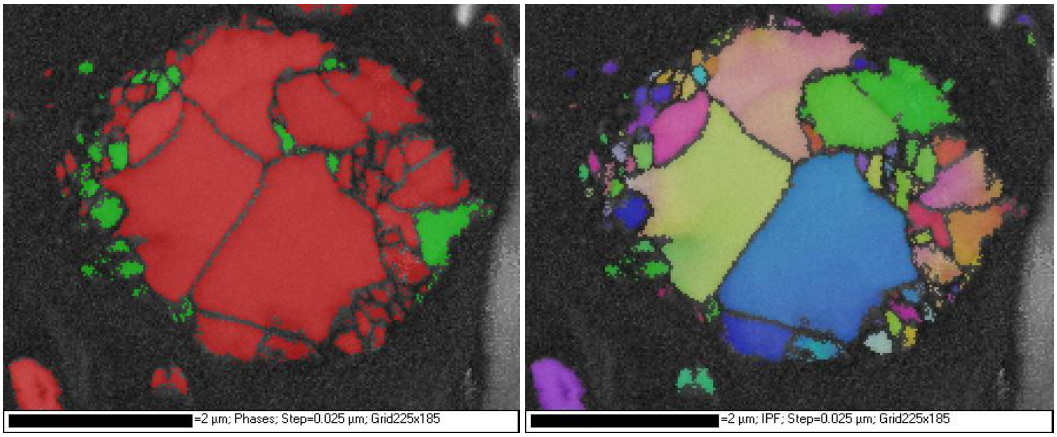

Fig.4.6: Magnification of a discrete 316L stainless steel particle (fin sized <5 µm) obtained by means of EBSD. Green grains are austenitic and red areas are ferritic phases (left). The different colors in the image to the right represent different lattice orientations of the particle grains.

The results from the particles are interesting to compare to similar results for bulk 316L stainless steel (a massive sheet sample) using the same technique, figure 4.7.

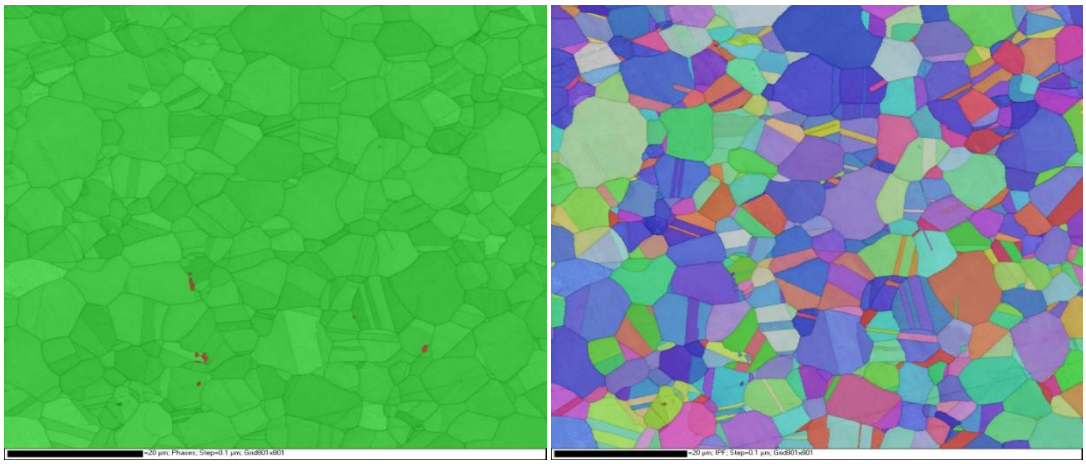

Fig.4.7: Micrograph of a 316L stainless steel bulk sample (massive sheet) obtained by means of EBSD. Green grains are austenitic and red areas are ferritic phases (left). The different colors in the image to the right represent different lattice orientations of the particle grains.

The structure of 316L stainless steel bulk material (a polished massive sheet sample) is completely austenitic beside some few inclusions of delta ferrite, which is a common feature for austenitic stainless steels. The ratio of ferrite to austenite in the bulk material is far lower than the one observed for the stainless steel particles. Moreover, as expected, the phase structure is poly crystalline for the bulk 316L stainless steel material and shows many twin grains, typically for the austenitic structure.

In all, the results from this preliminary EBSD investigation of the 316L stainless steel particles indicate that large fractions of ferrite are present in the smaller stainless steel particles. Furthermore, the amount of ferrite seems to increase with a reduction of the particle size. Consequently both austenitic and ferritic phases coexist in the two particle populations of different size. The microstructure of the smallest particles was either mono crystalline or in the poly crystalline form for the larger particles and for the massive sheet and the different grains show different orientation. Even discrete small (<5 μm) single particles contained grains of different phases. This particular microstructure could be related to the large cooling rate associated with the production procedure. The EBSD investigation could not at this stage clarify whether the ferrite observed in the particles was of delta or alpha phase.

4.2 Test media

The various test media used as electrolyte for electrochemical investigations in parallel with metal release studies, were all prepared using ultrapure water (18.2 $M\Omega cm^{-1}$) and chemicals of analytical grade. All test vessels were acid-cleaned (10% HNO_3) during at least 24 hours, rinsed 4 times with ultrapure water and dried in ambient air in the laboratory to avoid any risk of contamination.

Table 4.5: Chemical composition (g/L) and pH of the test media used for electrochemical investigations and subsequent metal release of 316L stainless steel particles [17].

Chemicals	*NaCl 3 g/L* *pH 5*	*ALF* *pH 4.5*	*GST* *pH 1.5*	*HCl 0.7%* *pH 0.9*
$MgCl_2$	-	0.050	-	-
NaCl	3	3.21	-	-
Na_2HPO_4	-	0.071	-	-
Na_2SO_4	-	0.039	-	-
$CaCl_2$-$2H_2O$	-	0.128	-	-
$C_6H_5Na_3O_7$-H_2O	-	0.077	-	-
NaOH	-	6.00	-	-
$C_6H_8O_7$	-	20.8	-	-
H_2NCH_2COOH	-	0.059	-	-
$C_4H_4O_6Na_2$-$2H_2O$	-	0.090	-	-
$C_3H_5NaO_3$	-	0.085	-	-
HCl 25%	-	-	0.89	7

Two of the test media has been extensively used in previous studies of metal release at simulated biological conditions performed at the Division of Surface and Corrosion Science, KTH; Artificial lysosomal fluid, ALF, simulates the intracellular environment present in lung cells during an inflammatory response. Artificial gastric fluid, GST, is a simple model solution of the gastric fluid in the stomach, which in reality basically consist of hydrochloric acid. The two solutions aim to mimic certain conditions related to an inhalation scenario where the particles enter the body through the respiratory system and/or become ingested in the gastrointestinal tract. It should be mentioned that the reliability of this simulation holds to some parts. In practice, the real body fluids are difficult to replicate and certain approximations have to be made [(27), (28)].

The two other solutions used within this project where selected because of their ability to serve other purposes; the 3 g/L sodium chloride was chosen as a solution for initial tests and optimization of experimental parameters since its simple composition enabled understanding of the experiments. Yet the 3% sodium chloride solution worked as electrolyte and its chloride content was to some extent similar to the more complex ALF. The 0.7% hydrochloric acid is basically just a more aggressive version of the GST and its purpose was to trigger any transpassive dissolution of the test materials under electrochemical testing.

4.3 Experimental procedure

The following paragraphs describe in detail the experimental procedures for the electrochemical investigations of the 316L stainless steel particles and the subsequent metal release studies performed within this project. The different analysis methods and the instrumentation used are also presented.

4.3.1 Electrode preparation

As it was discussed in the previous section regarding the pilot studies within this project, the design of a reliable working electrode with particles was a key issue for this project. For the lab investigation of 316L stainless steel particles, the configuration used by Y. Hedberg [(29)] in preliminary electrochemical studies on these particles was chosen. This set-up combines a relatively low background current, an easy fixing technique of the particles on the electrode and an appropriate electrical contact between the particles and working electrode matrix.

The working electrode consists of a rod made from graphite and paraffin. This matrix enables good conduction and the possibility to fix particles on the tip of the rod. The fixing of the particles on the tip of the electrode is a relatively simple procedure; first the tip of the paraffin stick is cleaned by a quick grinding, then it is heated up using of a hot flow of air (using a hairdryer), and when the tip is slightly melted, the stainless steel particles could be pressed into the tip surface.

For the electrochemical investigations of a specific amount of 5 ± 0.5 mg of stainless steel particles was pressed onto the electrode. The particles was weighted before the fixation using a Mettler AT20 microbalance with a readability of 2 μg, see figure 4.8.

Fig.4.8: The Mettler AT20 microbalance used to weigh the 316L stainless steel particles.

The particles, which in this way were successfully fixed on the tip of the electrode, could now undergo the electrochemical studies connected to the circuit, and moreover this configuration holds perfectly when immersed into the test media/electrolyte.

The configuration of the experimental set-up used for the electrochemical studies of stainless steel particles is shown in figure 4.9 below.

The working electrode (particles fixed on the paraffin impregnated graphite electrode) was immersed into 50 ml of test media serving as the electrolyte and placed in a glass beaker, connected with a reference electrode (Ag/AgCl rel SHE) and a counter electrode, in this case a platinum wire. The electrochemical testing of the particles, including Linear Sweep

Voltammetry (LVS) and potentiostatic tests, was performed using a Metrohm micro-Autolab type II potentiostat at ambient room temperature, 20 C°.

Furthermore, the system was shielded from external noise, such as the influences of lamps and other electric equipment, during the electrochemical tests using a Faraday cage made by wrapping aluminum foil around the experimental set-up.

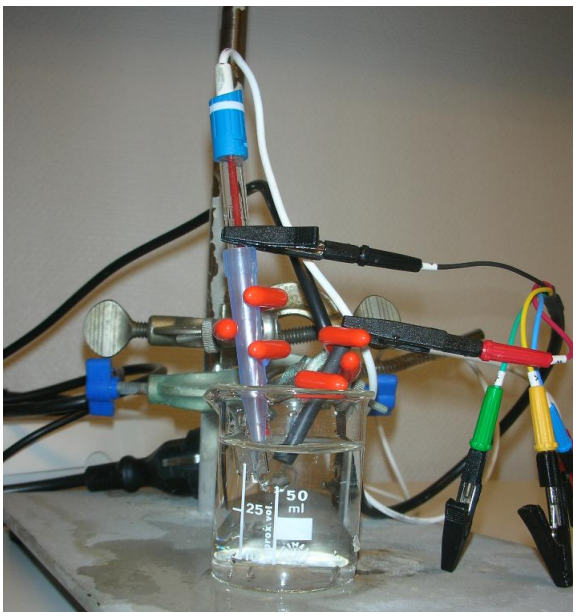

Fig.4.9: Experimental set-up for the electrochemical investigations of 316L stainless steel particles with the particles fixed on a paraffine impregnated graphite electrode as working electrode, a platinum wire as counter electrode and a Ag/AgCl reference electrode.

4.3.2 Separation of austenitic and ferritic particles

As previously mentioned, the characterization of the test materials showed that the 316L stainless steel particle samples contains a variable fraction of ferrite. Since the austenite and the ferrite phases show different magnetic properties, this feature was exploited to separate the austenitic particles from the ferritic ones in order to test them separately.

The separation procedure was managed by using two magnets and a number of PE flasks. The technique used was quite rudimental, but apparently effective. In principle the particles were poured into a flask and there after the magnet was placed on the outside of the vessel catching the ferritic particles inside the flask. Already at this stage it was possible to actually observe a separate fraction of the powder particles moving towards to the side of the vessel were the magnet was sited. The flask was then tilted in order to pour out the non-magnetic austenitic particles not affected by the magnetic field. Obviously the powder still inside the vessel was designated as rich in ferrite phases and the one outside the vessel rich in austenite. The process was repeated for until a sufficient amount of particles of both populations were obtained.

To verify if the process managed to actually separate the two phases from each other, samples were analyzed by means of SEM. The images below show the two particle populations assumed to be rich in austenite and ferrite, figure 4.10 and 4.11 respectively.

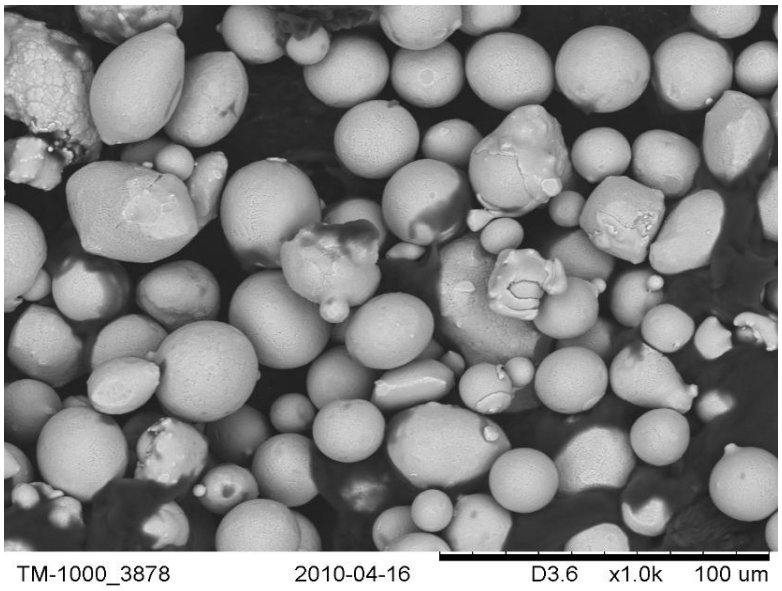

Fig.4.10: SEM image of a particle population from the yield by a magnetic separation procedure, assumed to be rich in austenite.

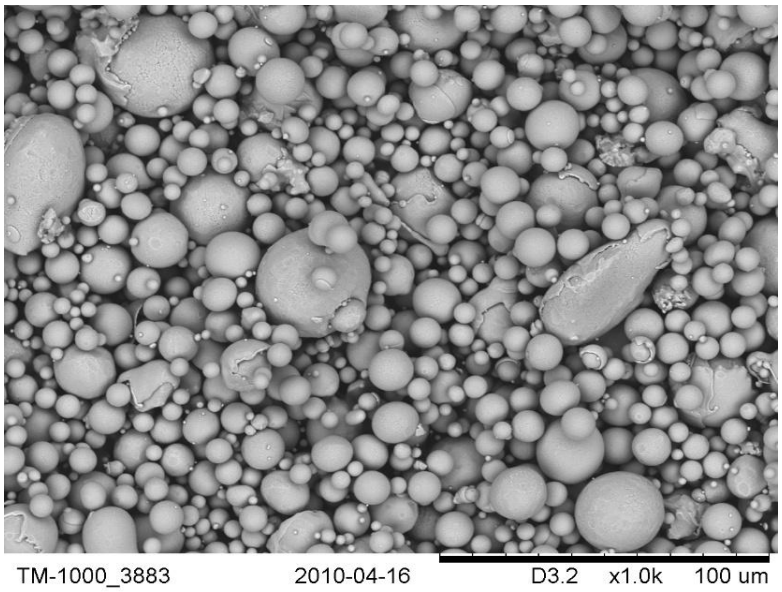

Fig.4.11: SEM image of a particle population from the yield by a magnetic separation procedure, assumed to be rich in ferrite.

The SEM images of the assumed austenitic and ferritic particles show two particles populations with a clearly different size distribution.

Using the same magnification figure 4.10 displays the austenitic particles of a quite narrow size distribution with an average size that is larger than that of the ferritic particles in figure

4.11. The latter one, also presents a more wide size distribution and a larger fraction of fine particles. Since the ferrite fraction seems to increase with a reduction of the particle size it is logical to assume that the two particulate samples are actually rich, in austenite and ferrite, respectively. It is interesting though to observe how the ferritic particle population in figure 4.11, besides a larger fraction of fine particles also contains a noteworthy fraction of quite coarse particles. This indicates the presence of some austenitic particles left in the ferritic population. This could influence the electrochemical behavior of the powder and it must therefore be taken into account.

4.3.3 Linear sweep voltammetry (LSV) investigations

This electrochemical technique is practically proceeding by applying a potential ramp to the sample with certain prerequisites such as start or end condition for the potential sweep or a fixed time duration for the sweep.

This procedure aims to find a correlation between the corrosion process associated with the polarization, and the current response during the potential sweep reflects the electrochemical reactions as a possible part of the metal release process.

In this work the micro-AUTOLAB potentiostat was set to start the linear sweep from the open circuit potential value (OCP), and end at 1 V with a scan rate of 0.2 mV/s. Due to this choice of input parameters, the duration of the different experiments could vary largely depending on the OCP value and for this reason it was necessary to normalize the data in terms of released metal concentration with the time and compare the data to the data to the respective time periods in previous metal release studies. For example, the duration of LSV test was ranging from twenty minutes for coarse particles in 3% NaCl, up to one hour and a half, for the fine sized particles in 0.7% HCl. Usually a stable OCP value was obtained after about half an hour in the electrolyte.

In addition to the careful monitoring of different time durations for the linear potential sweeps, the pH of the electrolyte was controlled before and after the test, in order to further help the interpretation of obtained results.

The number of replicate LSV measurements for each particle type and test solution varied though the number was never inferior to three. For example, technical problems or difficulties in reaching a stable OCP value sometimes made it necessary to repeat the test several times. Moreover the results obtained for some test media showed a broad variation which made further repetitions of the LSV test necessary.

The following figure gives a schematic overview of the electrochemical tests performed on 316L stainless steel particles using linear sweep voltammetry, figure 4.12.

pH:
5.0 ± 0.2
4.5 ± 0.2
1.5 ± 0.2
0.9 ± 0.2

Solutions:

3% NaCl; ALF; GST and 0.7% HCl

Acid cleaning:
Cleaning of all used equipment with 10% HNO_3, at least 24h

Sampling:
Centrifugation at 704 rcf for 10 min and acidification to pH <2

Loading:
100 mg/L
(50 ml solution)

Experimental set-up:
Potential range starting from the OCP value and ending at 1V, scan rate of 0.2 mV/s.
Waiting time for OCP, 30 min.
pH measurements before and after the test

Materials:
SS AISI 316L in particulate form (<45 and <5 μm in diameter)

Fig.4.12: Compilation of the most important test parameters and settings of the experimental procedure for LVS test of 316L stainless steel particles in different media.

4.3.4 Potentiostatic investigations

The potentiostatic investigations of the 316L stainless steel particles were executed by applying a constant potential at a certain value for a fixed period instead of sweeping a potential range as in the case of LSV. The time period chosen for the potentiostatic tests was in this case set to 30 minutes and four different potential values were used: 0.4, 0.6, 0.8 and 1V respectively.

The aim of this test was to study the influence of the applied constant potential on the electrochemical reactions (corrosion) taking place under these conditions and also to correlate this information with corresponding results from LSV investigations and the metal released into the solution. For the fine sized 316L stainless steel particles, duplicate measurements were run while for the coarse particles three replicate tests. Before applying the constant potential, the particles were immersed into the electrolyte for 15 minutes in order to obtain a stable OCP. The pH of the test media was monitored before and after the potentiostatic tests.

Figure 4.13 below gives a schematic overview of the electrochemical tests performed on 316L stainless steel particles using the constant applied potential procedure.

Materials:
SS AISI 316L in particulate form (<45 and <5 μm diameter)

Acid cleaning:
Cleaning of all used equipment with 10% HNO_3, at least 24h

Sampling:
Centrifugaton at 704 rcf for 10 min and acidification to pH <2.

Loading:
100 mg/L
(50 ml solution)

Solutions:
GST (artificial gastric fluid)

Sampling time:
30 min of potentiostatic test and 15 min of OCP waiting time.

Experimental set-up:
Holding potential at 0.4, 0.6, 0.8 and 1.0V.
pH measurements before and after the test.

Fig.4.13: Compilation of test parameters and settings of the experimental procedure for potentiostatic testings of 316L stainless steel particles in different media.

4.3.5 Metal release investigations

Corrosion of the 316L stainless steel particles during the linear sweep voltammetry and potentiostatic tests is related to the electrochemical reactions taking place on the particle surfaces resulting in release of metal ions. In addition to this process, dissolution of the surface oxide present on the particles occurs and this process is strictly chemical and governed by other parameters such as the equilibrium conditions in the electrolyte and temperature. To assess the total amounts of metal released from the 316L stainless steel particles (both from the electrochemical reactions and dissolution of particles), the electrolyte used under electrochemical investigations was further analyzed by means of metal concentrations.

After the electrochemical testing of 316L stainless steel particles, the test media/electrolyte was poured into 50 mL centrifugation tubes and the particles that eventually came loose from the electrode tip during the electrochemical measurements could be separated from the solution by centrifugation at 704 relative centrifugal force (rcf) for 10 minutes, figure 4.14.

Fig.4.14: Picture of the two centrifuges (Eppendorf Centrifuge 5702 and Eppendorf Minispin) used to separate any particles from the test media after the electrochemical measurements performed within this work.

After centrifugation the supernatant, free of particles, was poured into polyethylene storage flasks and, if necessary, acidified with 65% HNO_3 acid to a pH below 2, in order to make sure that the released metal was conserved in its free form (completely dissociated and not complexed) which enables an accurate metal analysis. Concentrations of total concentrations of released iron, chromium and nickel were analyzed by means of flame atomic absorption spectroscopy (Flame-AAS) and in case the released extent was below the detection limit, the graphite furnace mode (GF-AAS) on the Perkin Elmer AAnalyst 800 instrument was used instead, figure 4.15. The measurements were based on three replicate readings for each sample and quality control samples of known concentration were analyzed consecutively.

Fig.4.15: The atomic absorption spectrometer, a Perkin Elmer AAnalyst 800, used to analyse released metal concentrations at the Division of Surface and Corrosion Science,KTH.

The results presented in this work are the concentrations of the tested elements as measured in the media separated from the particles, with any contribution from the blank subtracted. The detection limits for iron, chromium and nickel were 1.0 μg/L, 0.5 μg/L and 0.5 μg/L respectively.

Results of total metal release from the 316L stainless steel particles will later on be reported as metal release rates, in terms of metal concentration per unit area and immersion time period ($\mu g/cm^2\ h^{-1}$). The metal release rates were obtained by multiplying the released concentration, c (μg/L), with the solution volume, V (L).

Thereafter the result was divided with the BET the specific surface area, A (m^2/g), and the time of exposure, t (h), ($=(c \times V/(A \times 10000 \times t))$). This quantity does not only consider the metal concentration, but takes into account the time and the specific surface area in order to normalize the released extent of metal with respect of these two variables.

It should be noticed, that the metal release rate normally strongly varies with time, for passive metals in normal environments, it is often strongly decreasing with time. In this manner, more realistic information related to the release process can be obtained. This presentation of release data comes especially handy since the fine-sized particles and the coarse particles have large differences in their specific surface areas. Moreover, the time period for exposure to the electrolyte differs due to different OCP values affecting the length of the linear potential sweep.

4.3.6 Sonication investigations

This paragraph is focused on describing the experimental procedure employed to investigate the influence of the sonication process on the corrosion process of the stainless steel in particulate form. As discussed in the sonochemistry section the ultrasonic waves applied to a solution, either homogeneous or heterogeneous, cause a series of interesting phenomenon, such as cavitation bubbles or high energy collision between particles. Thus it is logical to speculate how the employment of such technique might affect the properties of the stainless steel 316 L in particulate form. The effects of the sonication process are explored using the same test configuration followed for the Linear Sweep Voltammetry investigation. Moreover it has been also attempted to determine the effect of the ultrasonic treatment on the zeta-potential.

Sonication procedure

Since the ultrasonic waves need a media in which travel to be effective, the particles are first dispersed in a solution of 2 mL of ethanol. Using 15 mL centrifuge tubes as vessels the dispersion is then treated with ultrasonic waves. In order to compare not only the effect of the ultrasounds, but also of the different techniques the sonication treatment is carried out by means of either ultrasonic bath or ultrasonic probe, employing using a VWR Ultrasonic Cleaner B-3001 Leuven, and a Branson Sonifier 250, respectively. The pictures of the two equipments are reported below.

Fig. 4.16: Image of the VWR Ultrasonic Cleaner B-3001 Leuven.

Fig 4.17: Image of the Branson Sonifier 250

The settings of the ultrasonic bath and sonic probe are the same used in a parallel project concerning the effect of sonication on the dissolution process, moreover they were chosen in order to render the measurements related to the different techniques comparable.

Usually the sonication process is carried out either using a sonic bath for 2 min or either using a sonic tip for 2 min (output =2 and duty cycle=10%). Although in specific cases the settings for the ultrasonic probe are changed in order to reach more harsh treatment conditions (output = 4 and duty cycle = 10%; output = 2 and duty cycle = constant). Then after the sonication treatment the dispersion are centrifuged in order for the particles to settle.

Electrode preparation

Since the particles are dispersed in a 2 mL ethanol solution it is impossible to employ the same technique followed before. Thus instead of pressing the particles on the tip of the PIGE, the electrode is prepared using an automatic pipette. So droplets of the dispersion are deposited on the top of the PIGE, this process is quite time consuming since the solution is deposited dropping 0.01 ml per time.

The choice of using ethanol as a dispersion media is related to the quick evaporation associated with this liquid. Furthermore the ethanol evaporation is aided using a hair-dryer The particles deposition appears to be uniform and stable, as proved by means of SEM observation. Afterward the electrodes obtained in this fashion are left for 20 hours in a desiccators in order to protect the sample from the external environment. The previous procedure have been successfully employed for the deposition of the ultrafine particles, although it cannot be applied to the coarse particles. Unfortunately due to the large size the dispersion of the 45 μm particles are not suitable to be deposited on the tip of the electrode.

Linear Sweep Voltammetry test and Zeta-potential measurements

Both techniques are employed in order to seek for the influence of the ultrasonic treatment on the surface and passivity properties of the stainless steel particles. By means of LVS it is possible to compare the polarization curves for the different cases and observe eventual variation in current range or OCP, while by means of zeta-potential it is possible to measure the changes in surface characteristics of the particles.
Moreover it is worth to mention that in order to obtain useful Zeta-potential measurement it is compulsory to satisfy different conditions, such as adequate ionic strength, and avoid cross contamination and too rapid settling of the particle. During this investigation it has attempted to create a procedure able to answer to all these requisites.

For the Zeta-potential measurement it has been used a Zetasizer Malvern 5.20 (figure 4.19).

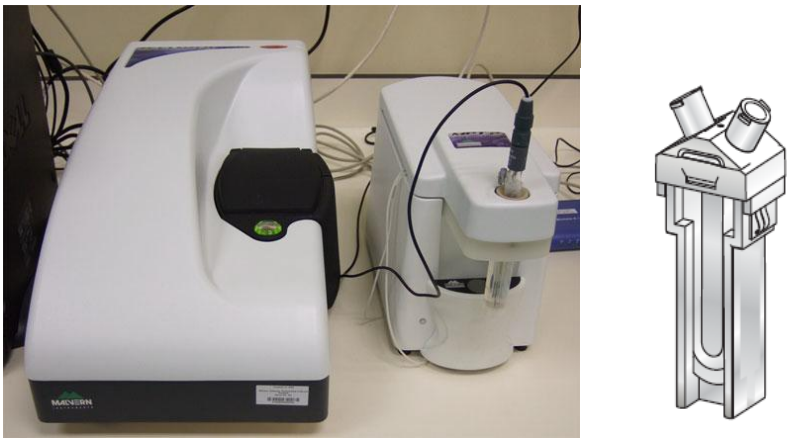

Fig. 4.19: Picture of the Zetasizer Malvern 5.20 (on the left) and a schematic of a specific disposable cell for Zeta-potential measurement (on the right).

The particles are dispersed in a 10 mM NaCl solution, the concentration of the chloride ions is crucial to reach the suitable ionic strength for an accurate measurement. Then the dispersion is poured in the specific cell for this instrument (figure 4.19) using an automatic pipette.

While for the LVS tests are carried out using the same equipment and configuration already described in the previous sections, moreover the settings employed for this investigation are reported below.

Experimental set-up:
Potential range starting from the OCP value and ending at 1V, scan rate of 0.5 mV/s.
Waiting time for OCP, 30 min.
pH measurements before and after the test

Materials:
SS AISI 316L in particulate form (<5 μm diameter)

Acid cleaning:
Cleaning of all used equipment with 10% HNO_3, at least 24h

Loading:
100 mg/L
(50 ml solution)

Solutions:
GST (artificial gastric fluid)

Fig. 4.18: Compilation of the most important test parameters and settings of the experimental procedure for LVS test of 316L stainless steel particles after the sonication treatment in GST.

5 Results and Discussion

The aim of this Master Thesis work is to generate results that can improve the understanding of extraordinary passive properties of 316L stainless steel particles. The experimental part of this project provides an investigation of two 316L particle samples from an electrochemical and metal release point of view with special focus on the influence of size on the passivity of stainless steel 316L in particular form. This study is a spin off project related to on-going research concerning the assessment of the potential health risks to humans posed by inhalation or ingestion of metal-containing particles. Therefore, the test media used within experiments are mainly artificial body fluids that simulate various conditions that the particles might encounter in contact with the human body, such as in the lung or stomach.

The test media used for study had to be optimized with respect to ionic strength and to obtain any results they also needed to be aggressive enough to allow the measurements. Furthermore the choice of test media/electrolyte was correlated to another Master Thesis project concerning the influence of different components of a simulated biological medium on the corrosion process of 316L stainless steel particles. Furthermore it is crucial to remember that no pretreatment, such as grinding or pre-oxidation, of the sample particles has been carried out before any experiment. This is an unfortunate prerequisite of the particulate form of the material under exam.

5.1 Linear sweep voltammetry and metal release investigations

In the following, results from electrochemical measurements on 316L stainless steel particles including open circuit potentials (OCP) and polarization curves, are presented and discussed in relation to the measured released metal concentrations under test.

5.1.1. Sodium Chloride 0.3%

The media under exam is a simple saline solution which was selected as a starting point for these measurements. The content of sodium chloride is the same as in artificial lysosomal fluid (ALF) and it is a relatively aggressive solution for bulk stainless steels given the high concentration of chlorides ions, even if the pH of 5.5 is quite close to neutrality.

In the 0.3% sodium chloride solution, a massive sheet sample of 316L stainless steel was tested in addition to the two particulate 316L samples, using the cell shown in figure 5.1 below. This sample was tested in as-received (aged) condition. Actually the oxidation due to

the age of the sample was pretty much desired in order to guarantee a preexistent passive layer since this somehow corresponds to the surface condition of the particulate 316L samples.

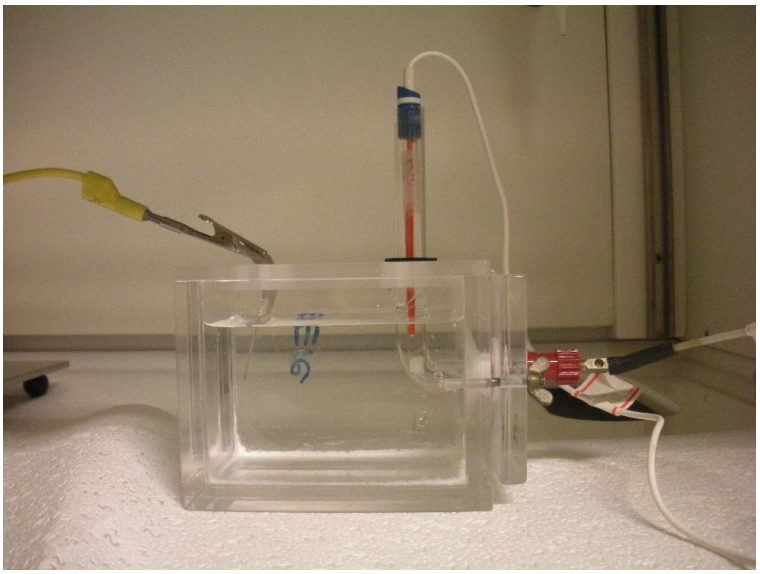

Figure 5.1: Picture of the electrochemical cell used for the testing of the massive sheet of SS 316 L.

For each case different replicas have been tested, though the typical results obtained during potential sweep from open circuit potential values up to 1 V are displayed in figure 5.2 for 316L particles of two different sizes, <45µm and <5µm respectively, in comparison with a massive sheet 316L sample.

The bulk stainless steel sample (aged massive sheet) showed the highest reactivity of the test materials in this solution and the measured pitting potential was around 400 mV, and the OCP approximately -100 mV. The results obtained for the bulk stainless steel sample were similar to values found in the literature reporting open circuit potentials in the range of -0.3 and -0.2 V and pitting potentials typically in the range of 0.3 and 0.5 V [(5)] in similar saline solutions.

On the other hand the two stainless steel samples in particulate form both showed a very passive behavior compared to the bulk sample; the particles exhibit a more narrow current range which are within three (<5µm) or four (<45µm) orders of magnitude higher than for that of the bulk material. Also the OCP values of the particles in the 0.3% sodium chloride solution are much higher than the -100 mV observed for the bulk stainless steel sample.

Based on these findings it is logical to assume that the two particle types experience very mild corrosion in this electrolyte and likely no or very little metal is dissolved from the samples.

Furthermore, the corrosion behavior seems to be affected not only by the particulate form, but also by the size of the particles under exam.

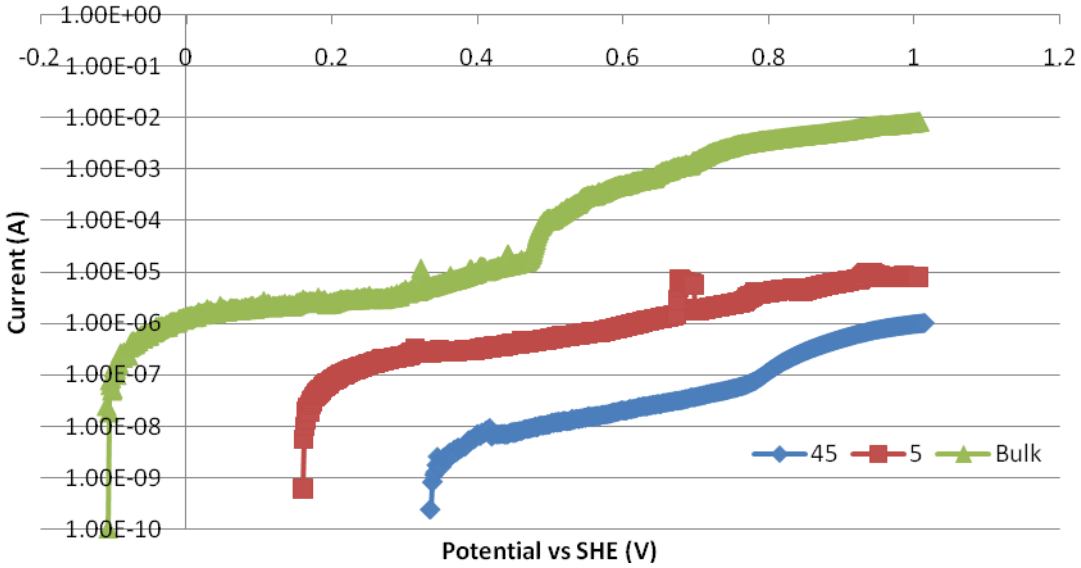

Fig.5.2: Polarization curves for stainless steel bulk, coarse (45) and ultrafine (5) particles in 0.3% sodium chloride solution. As it is possible to see the stainless steel in particulate form shows a stronger passivity than the bulk form. The latter in fact present a pitting potential just above 0.4 V and a corrosion potential around -0.1 V. While compoaring the two particle sizes it is clear that the coarse particles seems more passive than the finer.

The polarization curves recorded for the two particle sizes clearly indicate differences between the samples. The coarse particles, < 45µm, show the highest OCP values, varying in a range from 300 mV to 700 mV. Also the polarization curve remains in a lower range of current and at 1000 mV (the end of the potential sweep) the current is reaching a value in the order of 10^{-6}A. For the ultrafine particles, < 5µm, the OCP is measured around 200 mV, which is lower than for the coarse particles but still way higher than OCP of the bulk stainless steel. Although the current range is narrow for the fine particles, the polarization curve for these particles shows a higher activity than the coarse ones does, with a current that increases reaching an order of 10^{-5} at the end of the sweep. The same trend has been observed for all the replicate measurements for these sample materials in 0.3% sodium chloride.

Moreover it is worth to point out that the polarization curves reported have in the y-axis the current (A) and not the current density (A/m^2), therefore the current values that were discussed are not normalized with respect to the area. In fact during this Master Thesis project it has been assumed for the electrochemical test that the particles deposition on the tip of the PIGE had the same area both for coarse and fine particles, regardless of the size. Although this assumption is reliable since the particles are deposited onto the electrode in a layer structure, it is worth to remember that the exposed area for the UF particles is actually

larger than for the coarse ones. Thus if we had the actual current-density in the y-axis , the polarization curves for the two sizes would be much closer to each other.

The previous assumption applies also for the case of the massive stainless steel sheet, indeed the electrochemical cell used for the test allows the solution to come in contact with the sample only through a narrow window of the same dimensions of the PIGE. To conclude it is safe to say that, given the large difference in current range for this solution, even using the current-density the UF particles would still lay on higher current ranges than the coarse ones, although the difference would be more subtle. After the linear sweep measurements, the electrolyte was analyzed by means of released metal concentrations of the main alloy constituents iron, chromium and nickel, in order to verify the released amount of these three metals. In figure 5.3 below, the three graphs show the mean metal release rate per unit surface area (of the 5 mg particles that were fixed on the electrode tip) and hour of exposure in 0.3% sodium chloride (µg/cm^2/hour) for iron, chromium and nickel respectively.

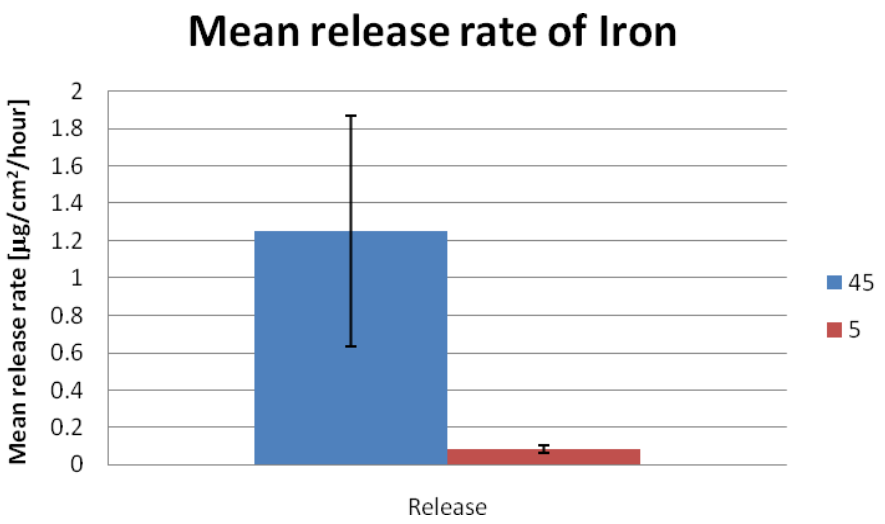

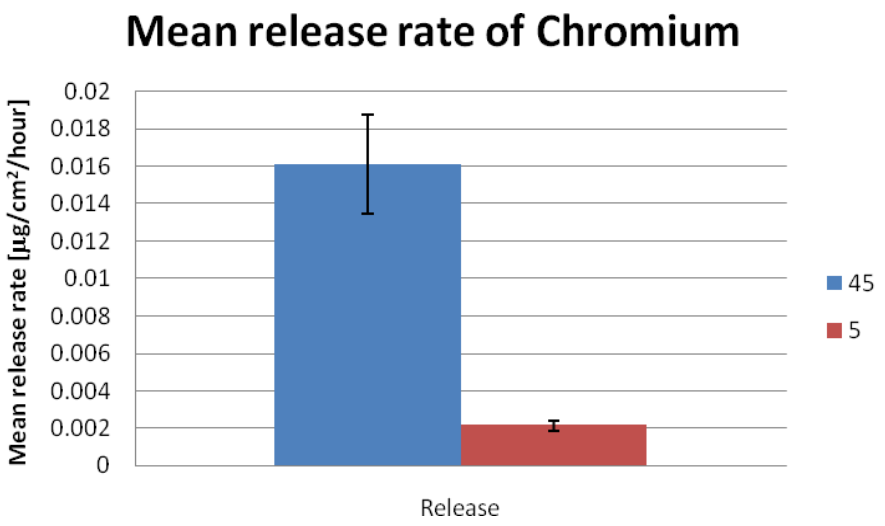

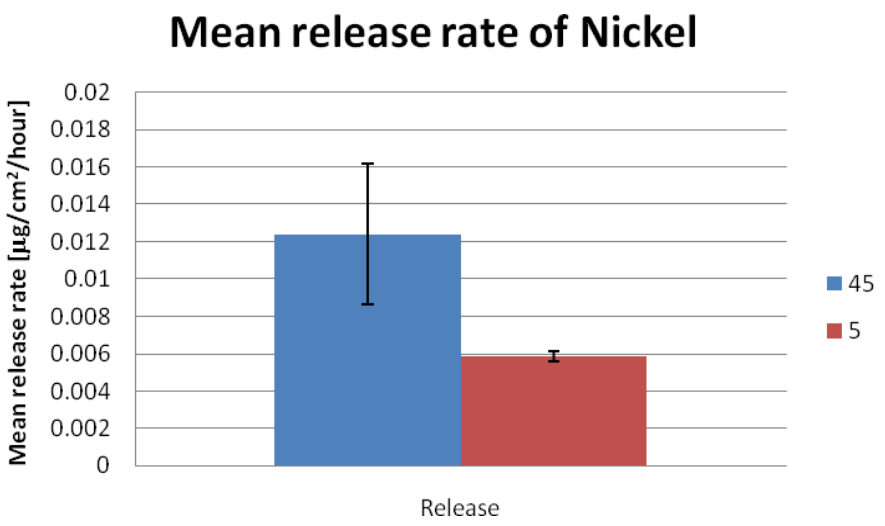

Fig.5.3: Mean release rate (µg/cm^2/hour) of iron, chromium and nickel in 0.3% NaCl-solution. for every elements the release related to the coarse particles results way higher than for the finer. Furthermore the release of the alloy elements is two orders of magnitude lower than for the Iron.

Results in terms of release rates of iron, chromium and nickel from the two sizes of 316L particles show all over higher release rates for the coarse (<45 µm) particles than for the ultrafine particles (<5 µm). These results indicate an opposite behavior compared to previously reported data after 1 week exposure of the same 316L stainless steel particles in ALF (without any applied potential), in which the higher release was seen for the ultrafine particles. (Midander et al 2007, 2009).

Considering instead the measured released amounts of iron and chromium with time (µg/h), obtained by multiplying the release rate for the ultrafine particles with a factor of ten, the difference in surface area), the level was about the similar for the two types of particles. It is the normalization with surface area (ten times larger for the fine particles) and the time (the fine particles were in the solution during a longer, sometimes almost twice longer, time period due to the larger sweep range for the PSV test) that contribute to the ten-fold difference in results of iron and chromium release rate.

Also the release rate of nickel per unit surface area and time period, is higher for the coarse particles (<45 µm) than for the ultrafine ones, however, the difference it not as much as ten times in this case. In fact, the released amount of nickel, in terms of measured released amount (µg/h), is about five times higher for the ultrafine 316L particles! The relatively higher release of nickel from ultrafine particles is suggested to be related to the higher activity for these particles observed under polarization in the LSV-test. However, the metal release data are very crucial to interpret in relation to the results obtained for the electrochemical investigation. For example, the activity under LSV testing is reflected both

by the OCP (or the range of the linear sweep) and the current response on the applied potential during the sweep. The current in these measurements is related to the exposed surface area of the particles and even though the amount of particles fixed on the electrode tip (5 mg) is known, the accessible surface area of the particles may not be the BET specific surface area. The particles are to parts embedded in the electrode material, which of course, reduces the actually exposed surface area. However, it is likely that the surface area of the ultrafine particles on the electrode is much larger than the area of the coarse ones.

The release rate of 316L stainless steel powders does not change with the same entity for the different elements. The release rate of iron is approximately 10 times higher than the measured chromium and nickel release as indicated by the ordinates of the graphs in figure 5.3. Generally, the extent of released metal was low, especially for Cr, which likely is found enriched in the oxide and alloy surface layer, according to the literature (Herting et al 2006, 2007).

The influence of an applied potential on the released amounts of metal has not been extensively studied for particles. The results of metal release after exposure in solution during applied potential or a potential sweep presented in this Master thesis can be regarded as pilot measurements and the interpretation of this data is preliminary. The influence of several parameters such as the surface area of the particles mounted on the electrode as well as the time for the potential sweep etc, could not be completely controlled in this study for several practical reasons.

To conclude, the results from linear sweep voltammetry investigations of bulk 316L stainless steel and 316L stainless steel particles of two sizes in 0.3% sodium chloride point out the particle form to exhibit much higher passivity compared to the bulk (massive sheet) material. Concerning the differences between the two size fractions of the particle material it was observed that with a reduction of the size the reactivity in enhanced. However, subsequent metal release measurements indicate the opposite, with higher release rates per unit surface area of the particles observed for the coarser particle type. This result could be an artifact of the normalization by specific surface area (which could not be completely controlled) and the variation in time duration for the exposure due to the different range of potential sweep. Another reason for the contradiction between electrochemical measurements and metal release data could be the different ratio of surface area (of particles) to solution volume which is a parameter that in this investigation was difficult to practically resolve. It could also be that the surface oxide on the coarser particles is to a larger extent chemically dissolved in the 0.3% sodium chloride. This process in not of

electrochemical nature which means that it is not visible in the linear sweep voltammetry recordings that is only a measure of the pure corrosion process taking place on the surface. The fact that the finer stainless steel particles contain a substantial fraction of ferrite is something that could affect both the release data and the results from electrochemical measurements. Therefore the austenite particles and the ferrite particles were investigated separately.

Austenitic and Ferritic particles

From the literature, the alpha ferrite is known to be less corrosion resistant compared to the austenite phase due to the differences in chemical composition of the two phases respectively. In this study the two types of 316L stainless steel particles examined have a very similar composition and according to general knowledge the materials should be austenitic. Yet there are ferritic particles present as was previously mentioned in the materials section 4.1.2. Whether the ferritic particles in the studied particulate materials have a different composition compared to the austenitic ones or not, is not fully clarified and needs to be further investigated. Anyhow, the passive tendencies of the two phases as particles separated from each other was studied with the aim to clarify their respective influence on the behavior of the 316L stainless steel particles

The following graphs show the polarization curves recorded by linear sweep voltammetry for particles of the two phases that extracted from the coarse (<45 µm) sized 316L stainless steel particles.

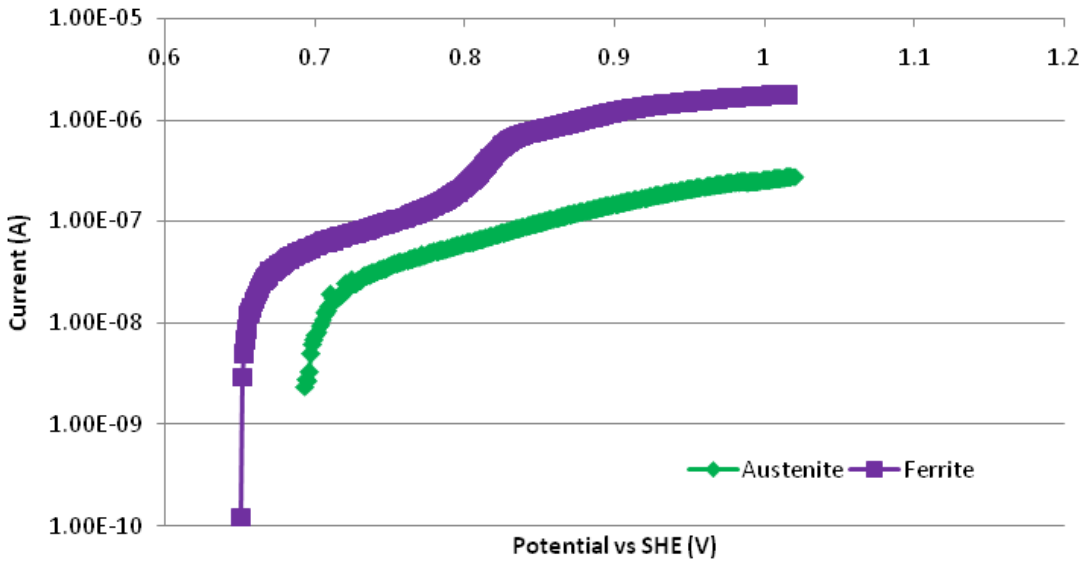

Fig.5.4: Polarization curves for the austenitic and ferritic phases of coarse 316L stainless steel particles separated from each other in 0.3% sodium chloride solution. No relevant difference has been observed between austenite and ferrite. Despite the current range is slighlty lower for the austenite, the OCPs values are quite close.

Figure 5.4 show high OCP values of the austenitic and ferritic phases, in the range of 650-700 mV. The OCP values for the two phases are also very similar to each other. The current range is higher for ferrite, slightly more than 4 orders of magnitude over the sweep from OCP to 1V, indicating a higher reactivity of the surface than for the austenitic particles with a current range of about 3 orders of magnitude. Still both phases show a strong passivity.

The polarization curves of the austenitic and the ferritic particles are compared with those of the coarse and fine sized 316L stainless steel particles in figure 5.5. It is obvious from this comparison that the separated phases show even more passive properties than the size fractions of stainless steel particles with higher OCP values. However, the influence of the different phases in the OCP values for the fine and coarse particles respectively is not straight forward to interpret. The differences in current ranges between the two phases are in line with what is observed for the coarse and fine particles; Fine sized particles (<5 µm) constitutes to a larger extent of ferritic particles than the coarser particles. Considering the current range, a similar activity is observed for the fine sized particles and the separated ferritic ones (about 4 orders of magnitude). The coarser particles are less reactive (they also contains less of smaller sized ferritic particles) and the current range (in about 3 orders of magnitude) is likely this limited due to less reactivity of the austenitic particles, predominantly present in this material.

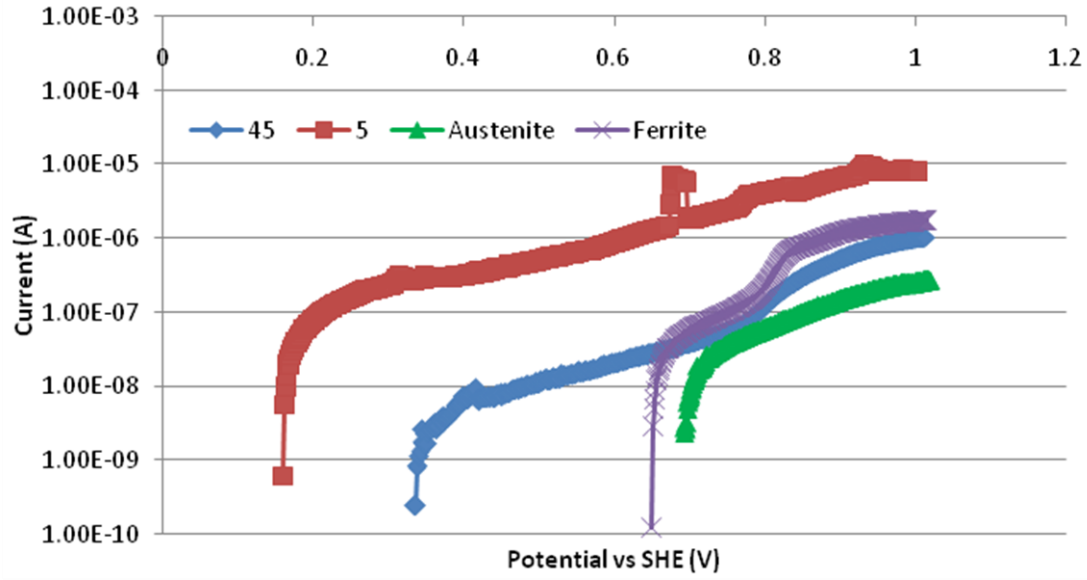

Fig.5.5: Polarization curves for stainless steel coarse (<45 µm) and fine sized (<5 µm) particles, and particles of the austenitic and ferritic phases separated from each other in 0.3% sodium chloride solution. The behavior of austenite and ferrite is much closer to the one of the coarse particles than to the finer particles.

Furthermore the two particle phases were characterized from a metal release point of view. However, the specific experimental conditions for the test of austenitic and ferritic particles were not well-controlled (for example the amount of particles mounted, their size etc) which make results not possible to interpret. Better controlled metal release investigations are needed to draw any further conclusions in this topic.

Table 5.1 below summarizes results from electrochemical studies and metal release investigations. Typical open circuit potentials and current ranges are given for the coarse, fine, austenitic and ferritic particles. Release rates calculated from data from metal analysis are represented in terms of released amount of metal (μg) per surface area unit of the particles mounted on the electrode tip (cm^2) and the time of exposure in the solution (including 30 min for obtaining a stable OCP and thereafter the time duration of the potential sweep). Also metal analysis raw data is found in the table of next page.

Table 5.1: Summary of the results obtained for fine and coarse 316 L stainless steel particles and the separated austenitic and ferritic particles in 3g/L sodium chloride.

	Coarse 316 L particles <45 μm	*Fine 316 L particles <5 μm*	*Austenitic particles*	*Ferritic particles*
OCP range (mV) Max; min	543 ± 107	146 ± 61	670 ± 19	650 ± 10
Max current (A) (typical)	1.05E-06	9.68E-06	1.50E-07	1.46E-07
Fe release μg/cm² particles/h	1.2500 ± 0.6162	0.0830 ± 0.0180	-	-
Cr release μg/cm² particles/h	0.0161 ± 0.0027	0.0021 ± 0.0003	-	-
Ni release μg/cm² particles/h	0.0124 ± 0.0093	0.0059 ± 0.0003	-	-
Fe release μg/cm² electrode/h	22.2930 ± 10.9894	14.8025 ± 3.2067	55.5414 ± 8.2374	52.4841 ± 16.5768
Cr release μg/cm² electrode/h	0.2873 ± 0.0474	0.3823 ± 0.0510	1.6306 ± 0.3491	1.6260 ± 0.7854
Ni release μg/cm² electrode/h	0.2210 ± 0.1738	1.0455 ± 0.0491	1.4564 ± 0.4567	1.3667 ± 0.8952

5.1.2 Artificial Lysosomal Fluid

The artificial lysosomal fluid, ALF, simulates intracellular conditions in lung cell following phagocytosis and represents a relatively harsh environment that arises upon inflammation with a pH around 4.5 [28]. The precise composition is reported in the experimental section 4.2. In ALF, electrochemical tests and subsequent metal release analysis were performed for the ultrafine (<5µm) and coarse (<45µm) 316L stainless steel particles.

During the initial exposure period at open circuit conditions, a decreasing OCP was observed for the ultrafine particles reaching values around -200 mV, while for coarse <45 µm particles the OCP keep a more stable value around 600 mV. The current response when sweeping the potential range from OCP up to 1V is displayed in figure 5.6 below for the fine and coarse 316L stainless steel particles.

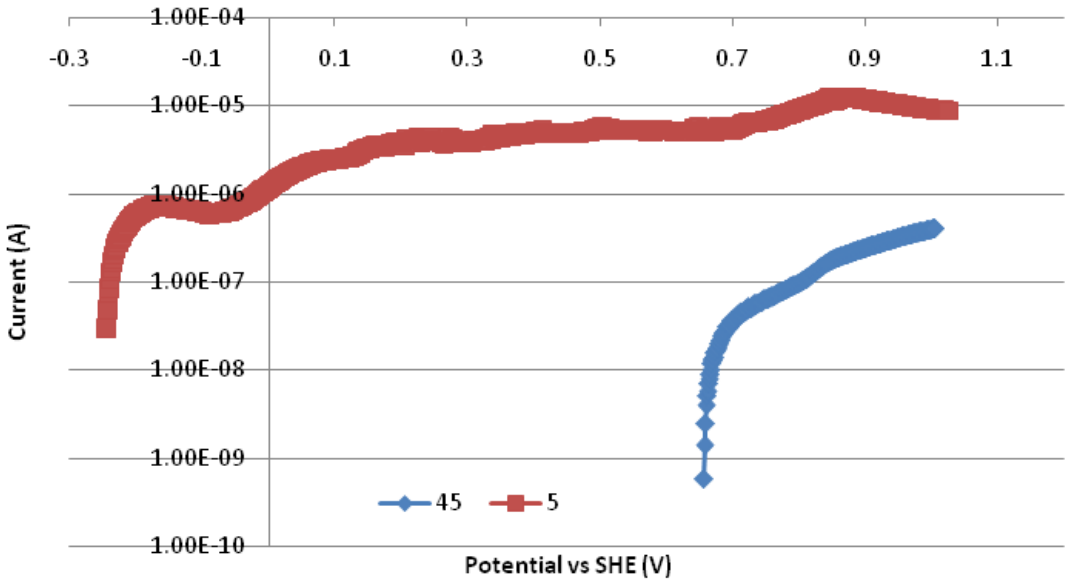

Fig.5.6: Polarization curves for stainless steel coarse (45) and ultrafine (5) particles in ALF. In this solution the difference among the two sizes is quite evident. The OCP values differ of almost 1 V, furthermore also the current ranges point to stronger activity for the finer particles.

In ALF, the two size fractions of 316L particles show clearly different electrochemical tendencies, although they remain quite passive with a relatively low current range (2-3 orders of magnitude, slightly lower than in 0.3% NaCl).

The gap between the OCP values of the fine and coarse particles reaches a value around 800 mV, but also the polarization curves appears extremely different from each other. The fine particles are way more active than the coarse ones. This means that in ALF, the influence of size is crucial for the corrosion behavior, and a reduction of the particle size means an increase of the reactivity. When comparing the polarization curves for ALF with the ones

recorded in NaCl it appears that, even if the OCP values changes, the current range is quite similar in the two different media.

It is important to mention that for ultrafine particles the highest current observed did not change significantly while the average current varied in the different replicate tests. The higher activity of smaller particles observed in ALF could maybe be explained by a more pronounced dissolution of ferritic particles or a stronger size-dependence, as suggested by the literature [19]. As for the previous solution it is interesting to consider how the polarization curves should change if, instead of the current (A), the current-density (A/m^2) was employed.

For the ALF as displayed in figure 5.6 the influence of the particle size is crucial, although it is important to remember that normalizing the current for the exact area of the electrode the current range for the UF particles would be closer to the one for the coarse particles. The electrolyte in electrochemical tests of particles was analyzed by means of released metal concentrations of iron, nickel and chromium respectively.

In figure 5.7 below, the three graphs show the mean metal release rate per unit surface area (of the 5 mg particles fixed on the electrode tip) and hour of exposure in ALF for iron, chromium and nickel. In general the release rates in ALF are higher than those observed in 0.3% NaCl. This is somehow expected based on the findings of a parallel Master thesis work that investigated the effect on metal release from the same particles as studied here, by the individual chemical components of ALF (ref Maggie 2010).

The release rate of iron in ALF is about double the ones in 0.3% NaCl and chromium release is also of similar magnitude. However the ultrafine particles release substantially more chromium than the coarse particles, the opposite behavior of what was previously observed in NaCl and for the other elements. Still the released amount of chromium does not reflect the bulk composition of the alloy, since the less noble Fe is selectively dissolved. It is very interesting to notice that nickel is released to a large extent in ALF compared to in NaCl.

The release rates of nickel from the fine sized and coarse 316L particles follow the same pattern as iron release and the rates are roughly one third of the iron release rates. This result indicates an enhanced dissolution of nickel in ALF which is in accordance with work by Chiba et al, who found that the release of nickel was much higher than release of chromium, with subsequent enrichment of the latter in the surface oxide.

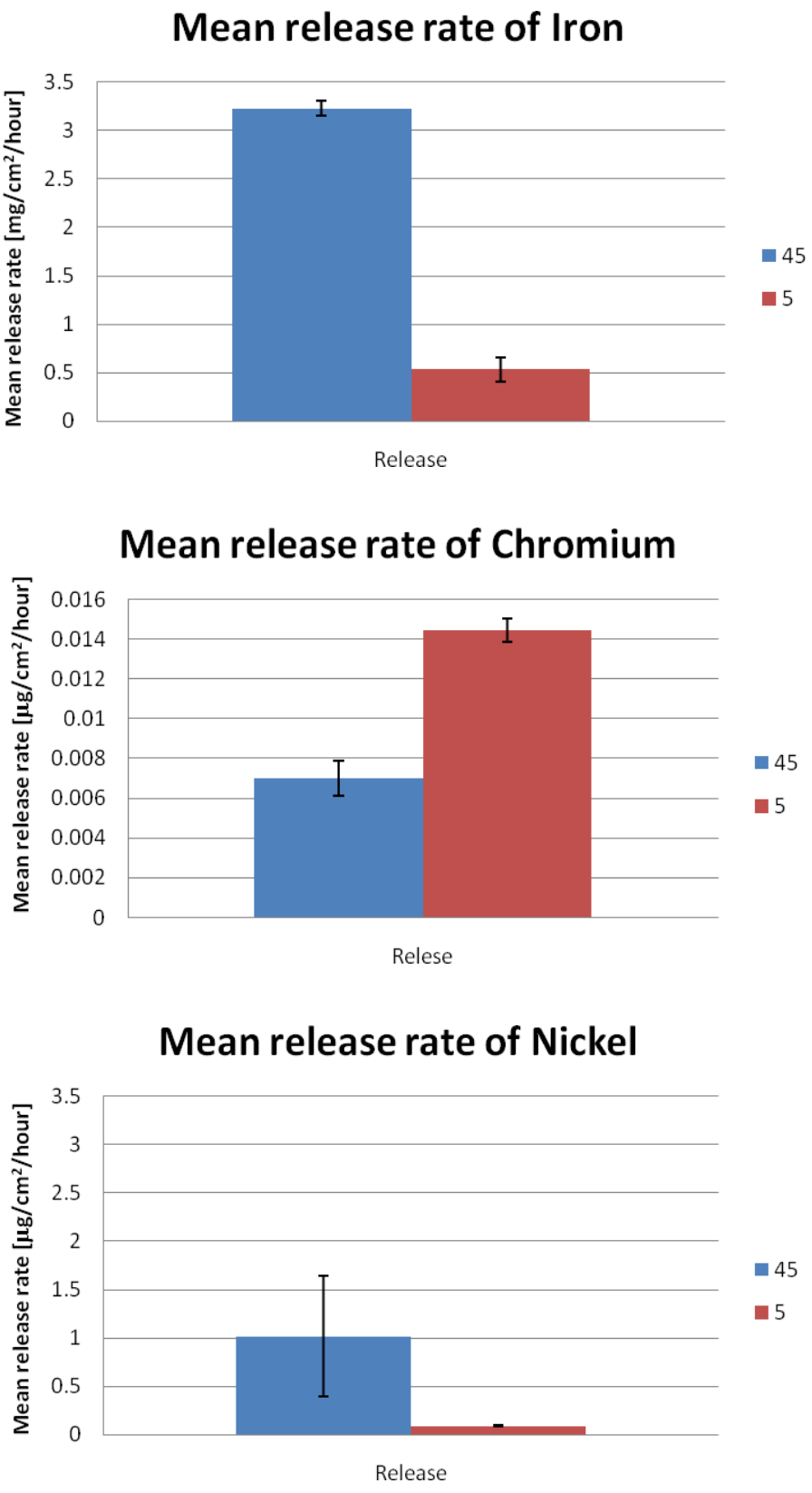

Fig.5.7: Mean release rate (µg/cm^2/hour) of iron, chromium and nickel in ALF. Except for Chromium the release for coarse particles is larger for coarse particles, although is very interesting to observe how the release of Nickel is now of the same order of magnitude of Iron, probably due to the high complexation ability of ALF for this element.

Again the findings of the parallel Master Thesis project confirm the high levels of released nickel in ALF obtained in these tests. This investigation of the influence of single components of the ALF solution tested on stainless steel particles, indicate that this larger release rate is caused by the strong complexation properties of citric acid and sodium citrate present in the solution. Another interesting result, also seen before, is that the different elements do not change their release concentrations with the same entity. Hence the composition of the surface layer changes as well, although in this case the released extent of nickel is more similar for the two particle sizes.

Austenitic and Ferritic particles

Separated particles of austenite and ferrite were tested also in the ALF. As seen previously in 0.3% NaCl, the two phases do not show any particular differences, figure 5.8. Although both polarization curves indicate a strong passivity of the two phases, the potential sweep for ferrite particles results in a slightly higher current response indicating a higher reactivity for this phase.

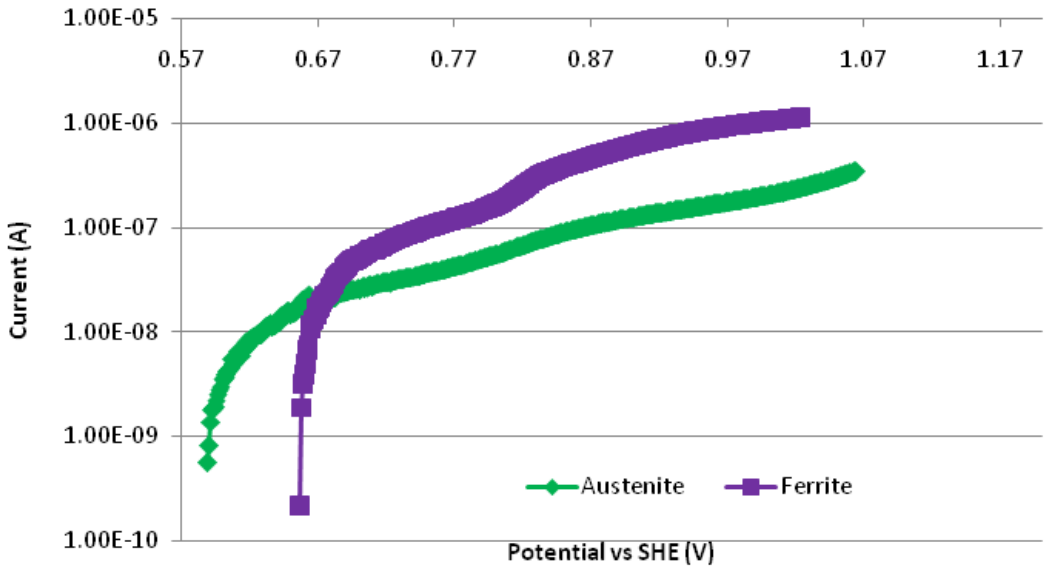

Fig.5.8: Polarization curves for the austenitic and ferritic phases of coarse 316L stainless steel particles separatedf rom each other in ALF solution. As in NaCl the difference among the two phases is not relevant, the OCP values are very close and the current ranges as well.

Figure 5.9 show that the OCP values stay within the same range as the coarse particles no matter austenite or ferrite content. The OCP values obtained for austenitic and ferritic particles are very close to the ones for the coarse <45µm particle, while they are quite distant from the OCP of the ultrafine size fraction. Concerning the current range the austenite seems the less reactive, while the ferrite stays in the middle between the fine and coarse particles. As previously suggested, the different phases of particles seem to affect the

reactivity of 316L stainless steel particles, even if the influence of size in much stronger (both for OCP and shape of the curve) in this case.

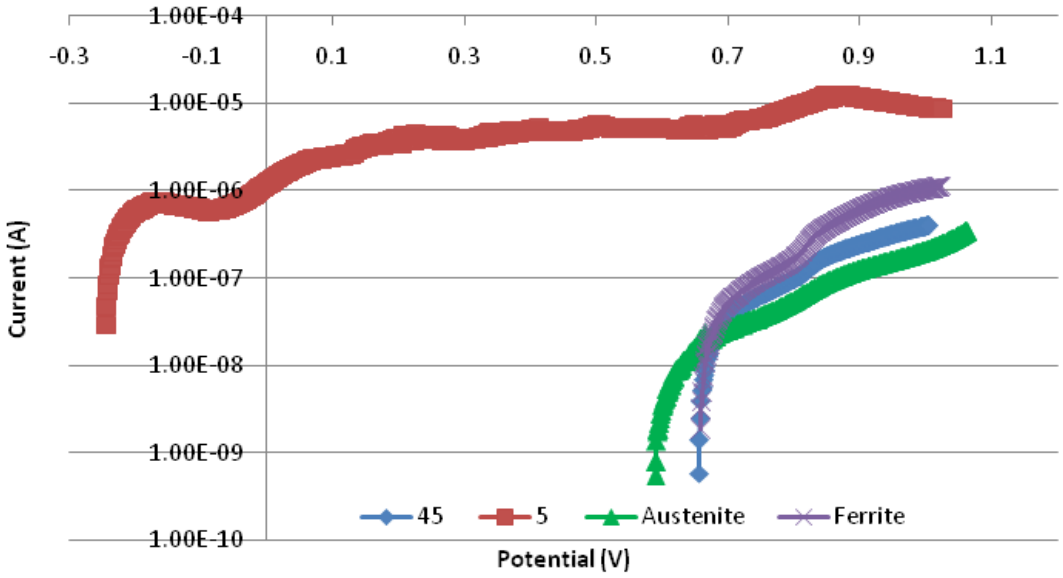

Fig.5.9: Polarization curves for the stainless steel coarse (45), fine (5) particles, austenitic and ferritic phases in ALF solution. Also in ALF both ferritic and austenitic phases keep a similar behavior to the coarse particles.

Table 5.2 summarizes results from electrochemical studies and metal release investigations. Typical open circuit potentials and current ranges are given for the coarse ones, fine, austenitic and ferritic particles in ALF. Release rates calculated from data from metal analysis are represented in terms of released amount of metal (µg) per surface area unit of the particles mounted on the electrode tip (cm^2) and the time of exposure in the solution (including 30 min for obtaining a stable OCP and thereafter the time duration of the potential sweep). Raw data from the metal analysis is compiled in the table in the next page.

Table 5.2: Summary of the results obtained for fine and coarse 316 L stainless steel particles and the separated austenitic and ferritic particles in ALF.

	Coarse 316 L particles <45 μm	*Fine 316 L particles <5 μm*	*Austenitic particles*	*Ferritic particles*
OCP range (mV) Max; min	586 ± 72	-273 ± 43	589 ± 34	657 ± 56
Max current (A) (typical)	4.21E-07	1.22E-05	3.45E-07	1.12E-06
Fe release μg/cm² particles/h	3.2286 ± 0.0808	0.5304 ± 0.1248	-	-
Cr release μg/cm² particles/h	0.0070 ± 0.0009	0.0144 ± 0.0006	-	-
Ni release μg/cm² particles/h	1.0183 ± 0.6263	0.0915 ± 0.0101	-	-
Fe release μg/cm² electrode/h	56.5000 ± 1.4142	92.8125 ± 21.8319	44.7500 ± 12.3744	48.0087 ± 6.3640
Cr release μg/cm² electrode/h	0.1225 ± 0.1520	2.5281 ± 0.1052	0.2717 ± 0.0322	0.5412 ± 0.0555
Ni release μg/cm² electrode/h	17.8210 ± 10.9602	16.0177 ± 10.9602	21.5710 ± 5.6568	43.5710 ± 3.1820

5.1.3. Artificial Gastric Fluid

Artificial gastric fluid, GST, mimics the very harsh digestion milieu of high acidity in the stomach (Hamel et al 1998, ASTM 2003). The solution pH is 1.5 and compared with the other test media used within this work, GST is very aggressive solution. Its composition is simply 0.1% hydrochloric acid, still the solution is relevant model media.

No 316L stainless steel bulk material was tested in GST since this media as electrolyte is too aggressive rendering the measurement useless. The media represents a harsh condition even for the stainless steel in particulate form. For instance the electrochemical studies in GST, figure 5.10, show reduced OCP values compared to those in NaCl and ALF and potentials at open circuit conditions reach values around 160 and -100 mV for coarse <45µm and fine <5µm particles respectively. In this medium, the difference between the two particle sizes is not as pronounced as in the case of ALF, in fact the gap between the OCPs is reduced to 260 mV compared to the almost 800mV in case of ALF. Furthermore the two polarization curves appears to be quite similar, indicating that under exposure in GST, the influence of size is not predominant, at least not for the polarization behavior of the particles. During polarization in GST the two sizes of particles seem more active than what was previously observed in three other test media. The current at 1V is in both cases slightly higher than 10^{-5}A, which was not seen in other media. Moreover the fluctuation in current response is much larger in GST, especially for the coarse particles and but also for ultrafine at the higher potentials. This is in line with what preliminary results of the continuous measurements of metal release during linear potential sweep by atomic emission spectroelectrochemistry.

The numerous peaks causing fluctuations in current response during the potential sweep, could indicate the formation of pits, meaning the breakdown of the oxide layer, and its subsequent repassivation, or the fall from the PIGE of some particles. The polarization curve of ultrafine particles remains during the initial part of the sweep on a higher current range than the coarse particles. At around 1000 mV, the two curves reach the highest current which is practically the same for both particle sizes. Beside the repassivation of any eventual pits, the slope in the last part of the sweep is increasing, which could be seen as a sign of reactivity of the particle's surface. However, this slope ends in a plateau at potential values around 1100 mV with currents in order of 10^{-5}, indicating that the pitting potential and the breakdown of the passive layer is not yet reached.

Given the similarity of polarization behavior for the different particle size it logical to speculate how the curves should appear using current-density (A/m^2) instead of current (A). As stated in section for the 3 g/L NaCl, the UF particles deposition on the electrode presents a larger exposed area than for the coarse ones. Thus normalizing the current for the area could decrease further the gap between the two particles sizes. In this case it is even possible assume that the current-density ranges for the UF particles might be lower than

for the other size. This might be in accord with the more numerous features shown by the fine particles, although not with the lower OCP value.

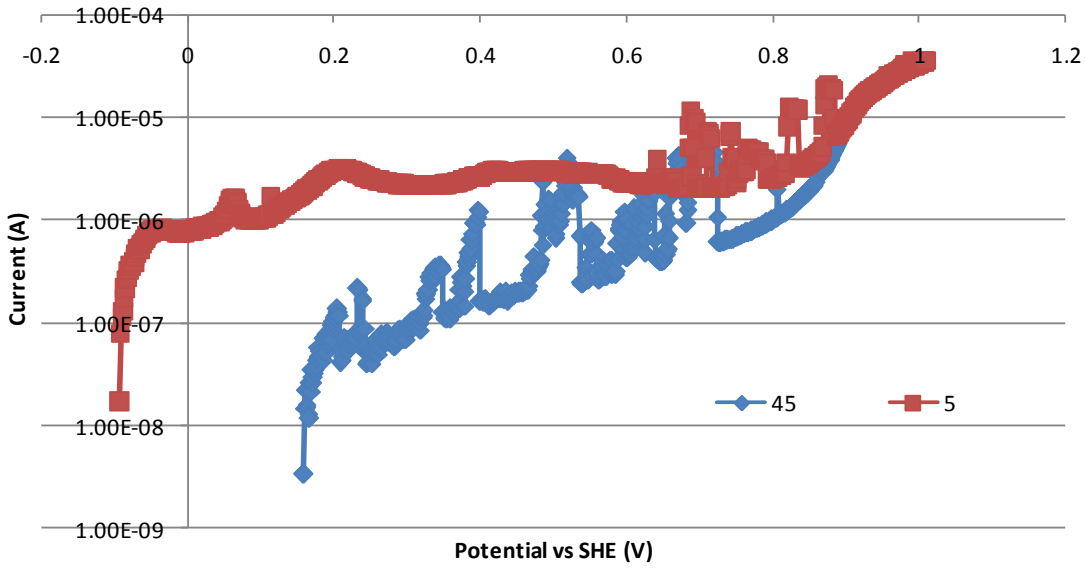

Fig.5.10: Polarization curves for stainless steel coarse (45) and fine (5) particles in GST solution. The OCP values are still quite different indicating a more passive behavior for the coarse particles, although the curent ranges are now much closer.

The electrolytes used in the sweep voltammetry tests were analyzed by means of iron, chromium and nickel and the results expressed as release rates (µg/cm^2/hour) are displayed in figure 5.11 for ultrafine and coarse 316L stainless steel particles.

The release rate of iron in GST did not increase significantly in this acidic media and the rate is in the same order of magnitude as observed in ALF. In general the release rates are still higher for the coarser particles than the ultrafine ones. This is likely an effect due to the normalization with surface area and time of exposure which both contribute to the higher release rate for coarser particles (both the surface area is smaller and exposure time shorter for the coarse particles, as discussed in section 5.1.1. The released amount of chromium is higher in GST than in ALF and opposite to the results in ALF, the coarse particles show the higher release rate for chromium. The most striking results of metal release in GST is that the nickel release is now lower than the one for ALF. This confirms the high complexation ability of the previous solution, in fact although the pH dropped to 1.5 the release extent does not increase, but it even decreases. Moreover it is interesting to observe how the release of chromium and nickel now differs of almost one order of magnitude. If on one hand the chromium release extent increases, pointing out a weakening of the protective oxide layer, on the other the nickel stays on release rate comparable to the mildest solution (3 g/L NaCl). The latter result is, according to literature, due to the segregation of nickel in the alloy surface beneath the passive layer [8].

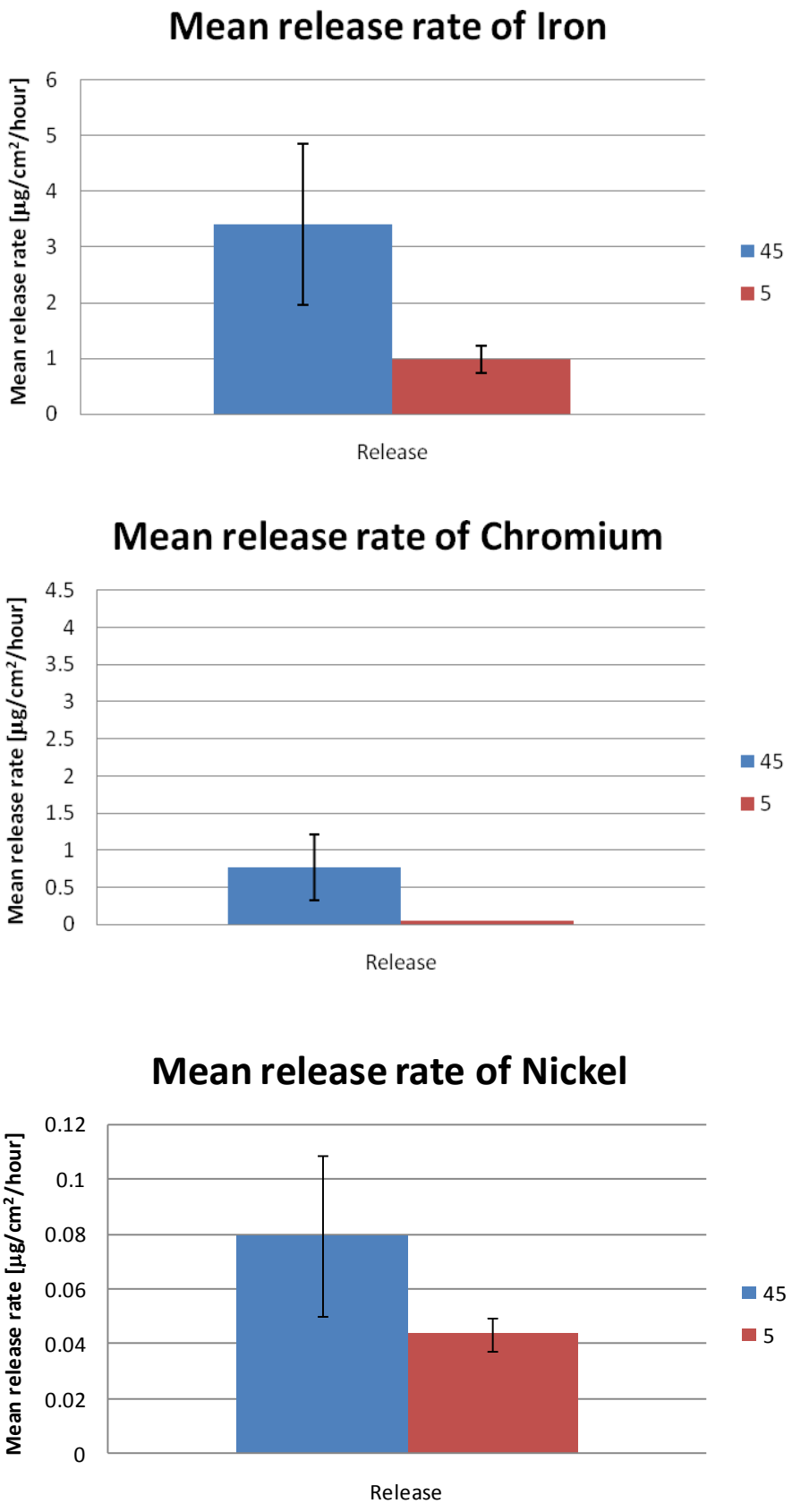

Fig.5.11: Mean release rate (µg/cm^2/hour) of iron, chromium and nickel in GST. For each elements the coarse particles show a larger release extent, although it is important to notice that the release of alloy elements is raising. This fact indicates that the oxide layer is weakening.

It is worth to mention that, while the polarization curves of the two particle sizes tend to converge at similar, relatively high average currents, the difference between the released amounts of iron remains stable. From this observation it is logical to assume that the release process for this element is weakly influenced by the applied potential. Hence the release of iron could be assumed to depend exclusively from the material, particles size and test media, but not from the polarization behavior.

To conclude, the results from exposure and linear potential sweep tests in GST show that it is not possible to predict the released metal concentration from the bulk or the surface composition.

Austenitic and Ferritic particles

Thanks to the use of magnets and to SEM characterization it was possible to create two populations of particles with a high fraction of respectively austenite and ferrite. Therefore the different behavior of the two phases has been tested also in the GST solution. The results of linear sweep voltammetry tests show an uncanny different behavior for the two phases as reported in figure 5.12 below.

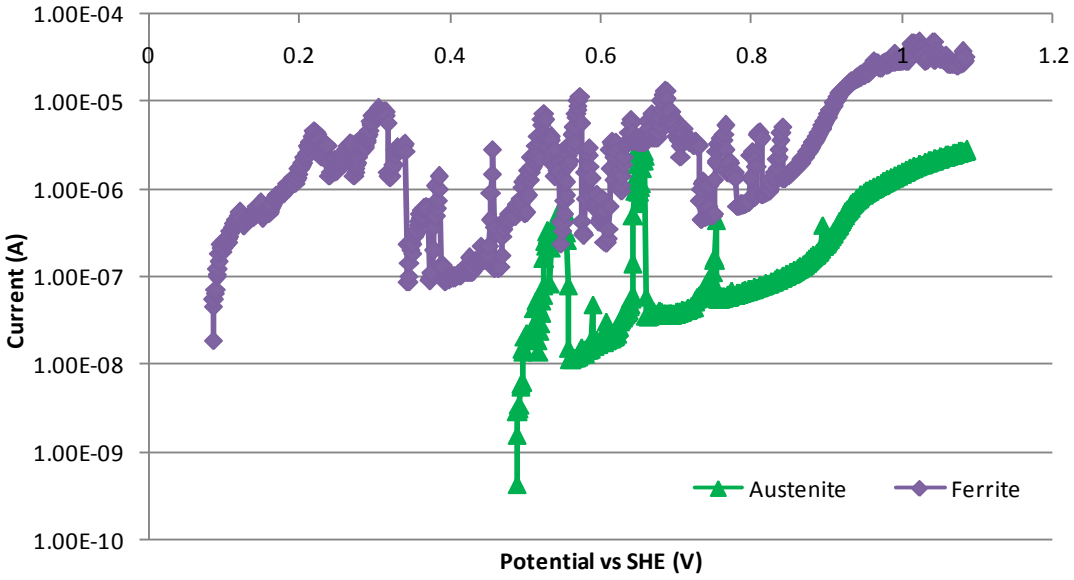

Fig.5.12: Polarization curves for the austenitic and ferritic phases of the coarse 316L stainless steel particles in GST solution. Both curves show an intense activity, although the OCP value for austenite is quite higher than for the other phases, moreover for the first time the current ranges differ remarkably.

The OCP values for the austenitic and ferritic particles separated from each other are quite different from each other and also the two curves show large differences. First of all both the average and highest current are higher for the ferrite, and this behavior remains during the whole sweep. Current response for ferrite is all over on a higher level than for the austenitic particles. The strong passive behavior that was previously shown by both the phases in ALF and NaCl, is no more present since the GST is a much more aggressive solution. The OCP of austenite particles remains on a quite high value also in this solution, almost in the same range as for the coarse particles in ALF.

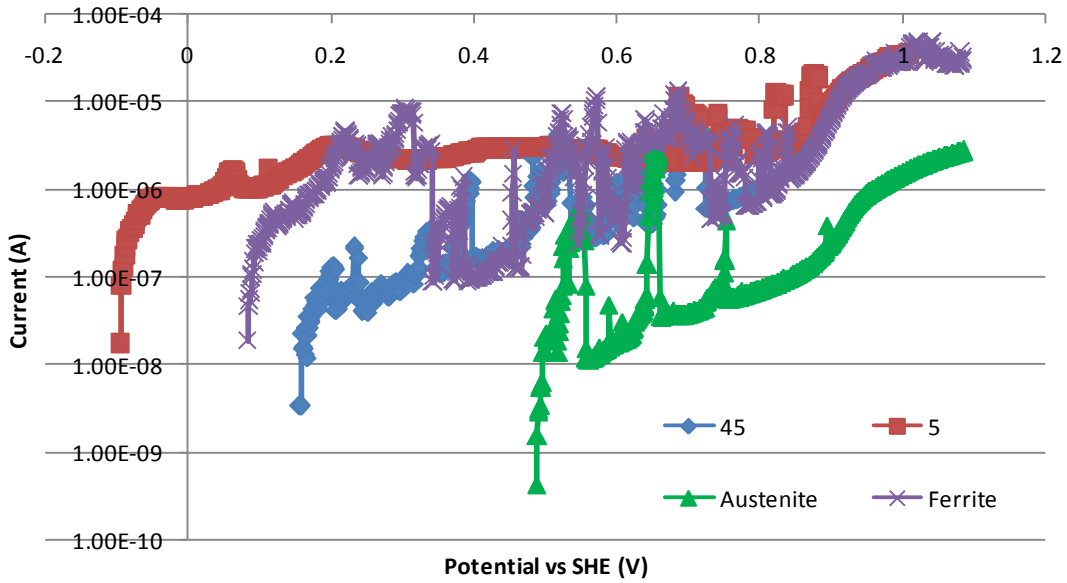

Fig.5.13: Polarization curves for stainless steel coarse (45), fine (5) particles, austenitic and ferritic phases in GST. As it is possible to see the behavior of the coarse particles appears to be led by the ferritic phase, while the austinetic phase keeps a more passive behavior.

Similar to results from testing in the other media, the austenite behaves as a more noble material with a higher OCP and a lower current range than ferritic particles. On the other hand the ferrite appears to be a sort of middle way between the coarse 45µm and ultrafine 5µm particles at the beginning. At a potential of 400 mV the polarization curve for the ferrite seems almost superposed to the one for the coarse particles, indicating that the ferrite has a strong influence on the behavior of the latter in this solution. Furthermore is interesting to see that passing to more aggressive solution such as GST, the influence of particle size seems weaker, while the dependence from the phase composition is considered to be increasing.

Table 5.3 summarizes results from electrochemical studies and metal release investigations. Typical open circuit potentials and current ranges are given for the coarse ones, fine, austenitic and ferritic particles in GST. Release rates calculated from data from metal analysis are represented in terms of released amount of metal (µg) per surface area unit of the particles mounted on the electrode tip (cm^2) and the time of exposure in the solution (including 30 min for obtaining a stable OCP and thereafter the time duration of the potential sweep). Raw data from the metal analysis is compiled in the table below.

Table 5.3: Summary of the results obtained for fine and coarse 316 L stainless steel particles and the separated austenitic and ferritic particles in GST.

	Coarse 316 L particles <45 μm	*Fine 316 L particles <5 μm*	*Austenitic particles*	*Ferritic particles*
OCP range (mV) Max; min	196 ± 55	-125 ± 45	488 ± 87	86 ± 34
Max current (A) (typical)	4.21E-07	1.22E-05	2.77E-06	3.22-E05
Fe release μg/cm^2 particles/h	3.4104 ± 1.4500	0.9864 ± 0.2455	-	-
Cr release μg/cm^2 particles/h	0.7721 ± 0.2455	0.0473 ± 0.0007	-	-
Ni release μg/cm^2 particles/h	3.7376 ± 1.4823	0.0436 ± 0.0007	-	-
Fe release μg/cm^2 electrode/h	59.6821 ± 25.3751	172.6250 ± 42.9567	-	-
Cr release μg/cm^2 electrode/h	13.5109 ± 7.6888	8.2877 ± 0.1202	-	-
Ni release μg/cm^2 electrode/h	65.4076 ± 25.9401	7.6250 ± 1.0607	-	-

5.1.4. 0.7 % Hydrochloric Acid

The relatively concentrated hydrochloric acid solution does not simulate any condition that could be found inside a human body. Even if its composition is similar to the artificial gastric fluid, the concentration of chloride ions is higher and the pH reaches a value around 0.9. The purpose for using the 0.7% hydrochloric acid as the electrolyte in electrochemical testing is only to try to break down the passive layer of the stainless steel particles in order to observe the subsequent dissolution of metal.

The results from the linear sweep voltammetry investigations of coarse < 45µm and ultrafine < 5µm 316L stainless steel particles in 0.7% hydrochloric acid are shown in figure 5.14 below. The OCP values in this electrolyte solution decreases (as expected) and reach the low values of 25 mV for the coarse particles and -200 mV for the ultrafine particles respectively. Hence the potential gap between the two particle sizes remains and it does not increase in the acidic hydrochloric acid compared to the artificial gastric fluid.

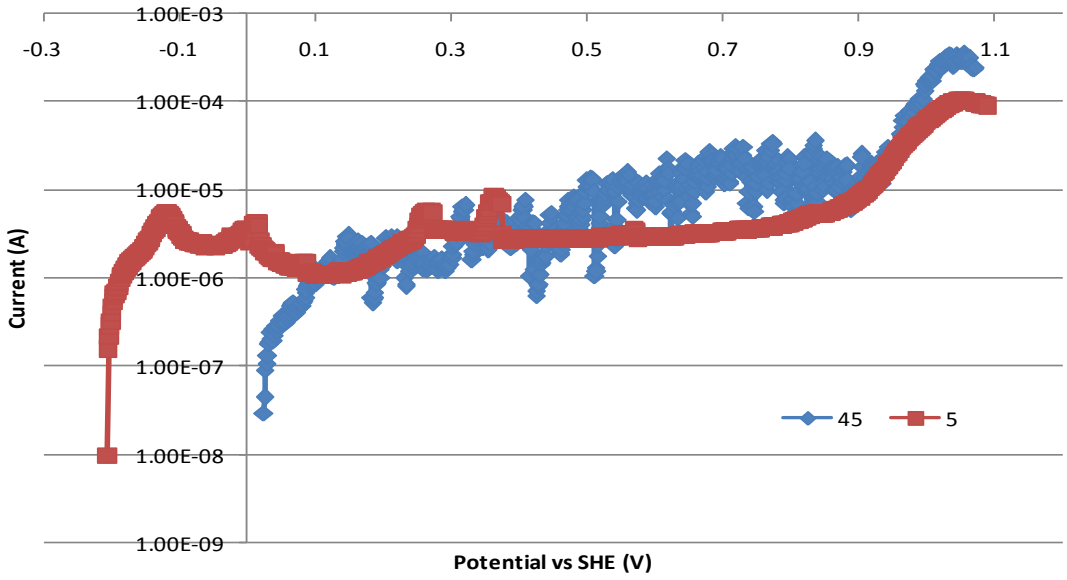

Fig.5.14: Polarization curves for stainless steel coarse (45) and ultrafine (5) particles in 0.7% HCl solution. Now the two curves are almost superposed and for the first time the finer particles do not possess the highest current, although the OCP for the coarse is still more noble.

From the polarization curves is it clear that, beside the different OCP values for fine and coarse particles, the shape of is quite similar. Actually it is interesting to note that for the first time the coarse particles reach a current that is higher than the current for the fine ones.

Similar to the linear potential sweep in GST, the polarization curves show fluctuations in current response indicating on on-going passivation/repassivation events that prove there is surface activity of the particles in this solution.

Around 900 mV the current start to increase rapidly until values of 0.248 and 0.1 mA for coarse and fine particles respectively is reached at potentials around 1.1 V. Even though the current thereafter stabilizes in a plateau, the value of the current is high enough to assume that there is an on-going corrosion process

occurring for both batches of particles. Oddly, it seems that the curve for coarse particles presents a higher background noise than the fine ones, a trend which was observed also in the replicas.

In this case it is safe to assume that considering the current-density (A/m^2)instead of the current (A) would shift the UF particles curve at a lower range than the coarse ones, since the former size possess a larger area for a constant volume.

As expected, the lowering of solution pH results in increased amounts of released iron and chromium, indicating a more intensive corrosion process on the particles, figure 5.14. These results report a noteworthy increase in the iron release, about a factor 10 times higher than in GST. Also the released amount of chromium is ten times higher in this media than in GST.

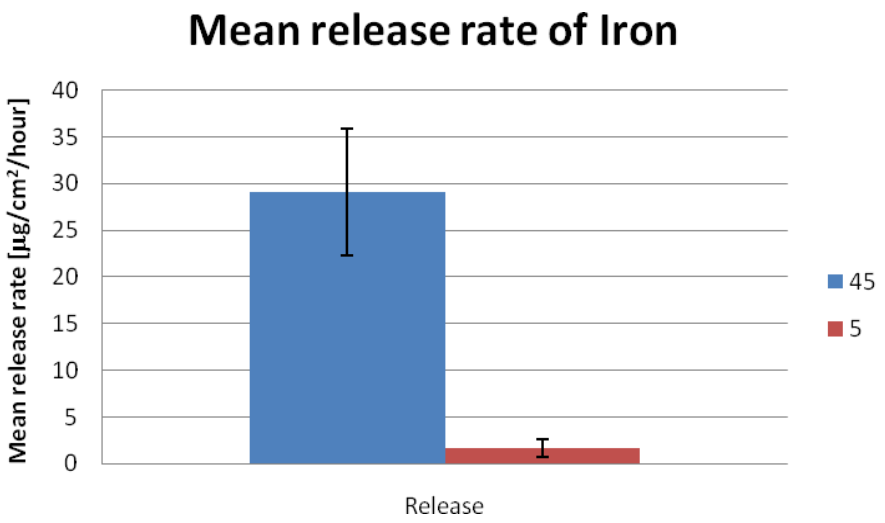

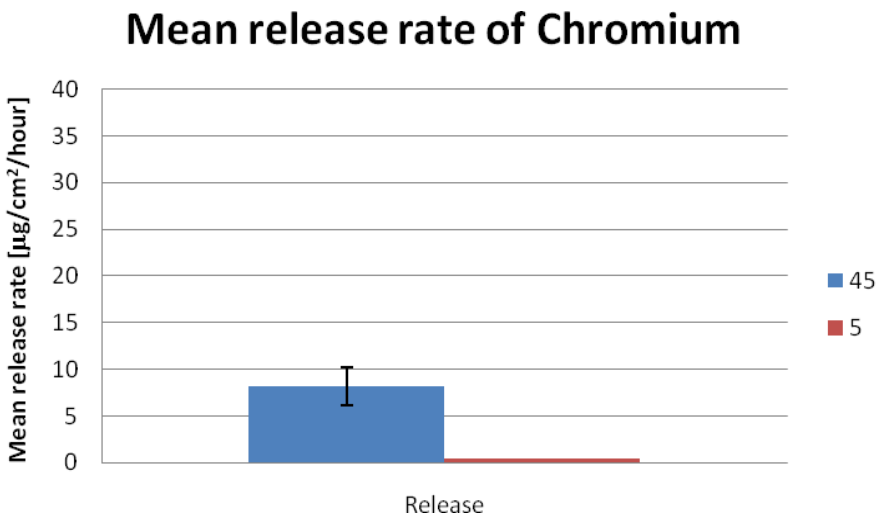

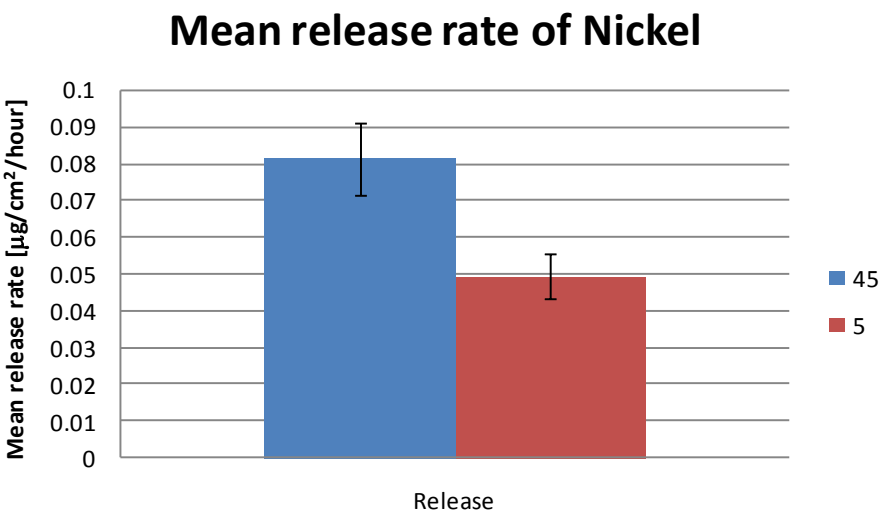

Fig.5.14: Mean release rate (µg/cm^2/hour) of Iron, chromium and nickel in 0.7% HCl. The release extent keeps being larger for coarse particles, although for Nickel the difference is reduced. Moreover the release of Chromium has reached the same order of Iron, indicating that the oxide layer is finally breaking down.

On the other hand, the release of nickel remains at similar rates as in previous solutions with an exception for ALF. This means there is a preferential dissolution of iron and chromium with a subsequent enrichment of nickel in the oxide and surface layer. It is interesting to observe that, even when pH is as low as 0.9, the release of nickel is still way lower in 0.7% HCl than in ALF. This indicates that the ALF media, as reported in the literature (Midander et al 2007, 2009), carries impressive complexation properties.

A general comparison of the two sizes of 316L stainless steel particles, clearly confirm the same release pattern as observed for the other media used within this study. The finer particles practically always show lower release rates, while the coarse ones exhibit release at a higher rate. This is both an effect of the 10 times difference in surface area of the two particle types (and following the surface area to solution volume ratio is not the same) and the different time duration of the experiment starting from quite different OCP values with a sweep up to 1V.

To prove eventual signs of corrosion/dissolution of the particles, samples were investigated by scanning electron microscopy (SEM) equipment available in the lab of Division of Surface- and Corrosion Science. Unfortunately no sign was found on the surface of the coarse particles, while on the finer particles the SEM images reveal proof of some kind of corrosion-related process, figure 5.16. This signs remind of a pit in the surface of the electrode tip that is covered with particles. Pitting corrosion is a very common phenomena observed for stainless steel bulk materials in this acidic solutions with high chloride content. However, the concept of pitting is a bit weird to transfer on particles if this size even though theoretically, the site for pit initiation is typically in the nanometer range. Fully developed pits could be of dimensions that are similar to the ultrafine particles which make the interpretation of the observed phenomena as a pit basically meaningless. It is then more likely that some kind of crevice corrosion phenomena in between the particles

caused an area that in some way worked as a local anode where the current was concentrated and the area thereby became preferable to corrosion processes to take place. Or perhaps a part or a section of a particle layer covering the electrode tip simply just fell off the electrode during the linear potential sweep measurement.

Below the pictures of ultrafine 316L stainless steel particles mounted on the electrode tip by SEM are reported, figures 5.15 and 5.16. They are related to before and after the polarization process in 0.7% hydrochloric acid.

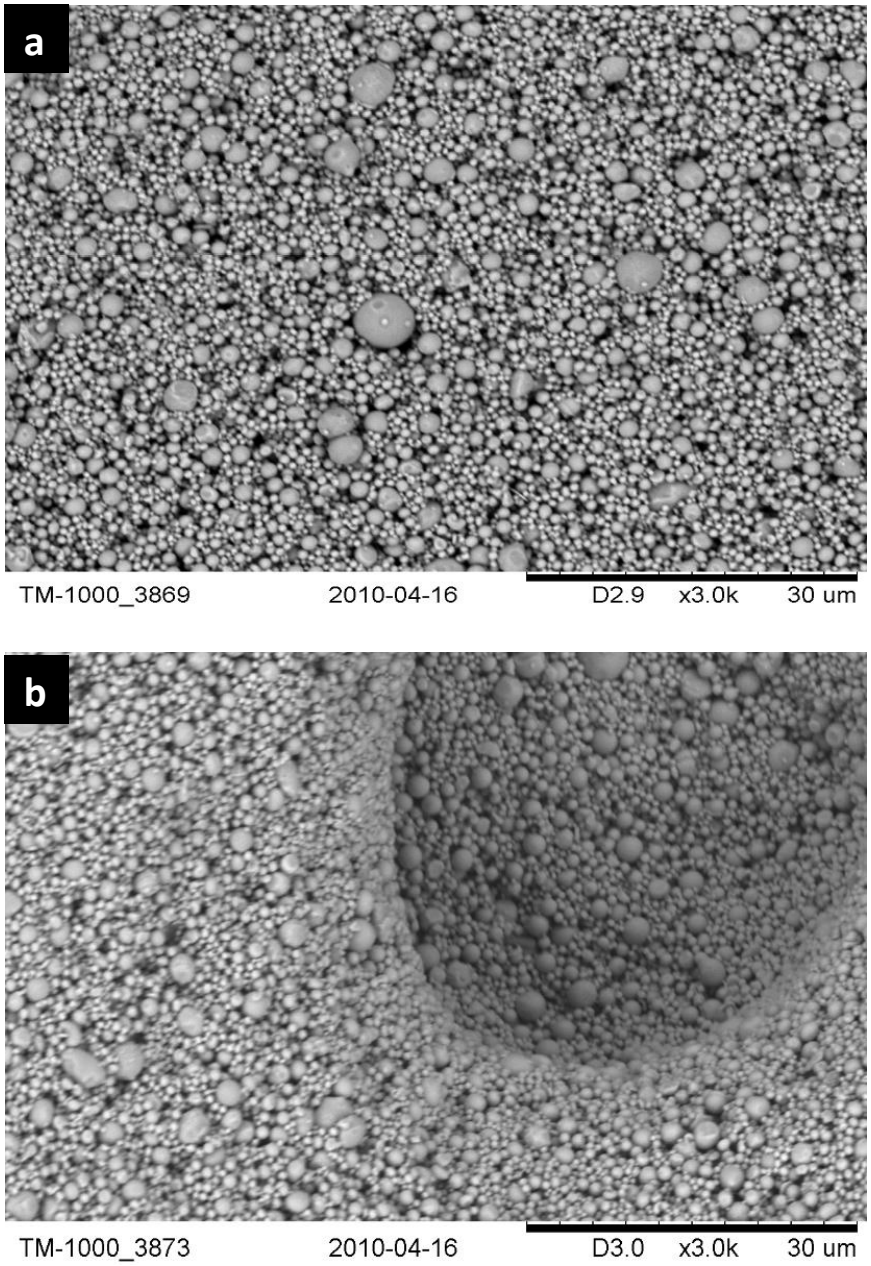

Fig.5.16: SEM image of the electrode tip covered by ultrafine 316L stainless steel particles before (a) and after (b) polarization in 0.7% HCl (magnification: x3.0k). these images show that due to the corrosion activity entire area of the deposition either dissolved or fall from the electrode leaving behind a hole.

To conclude, the results form parallel electrochemical and metal release investigations prove that it is necessary to decrease the pH until values around 0.9 in order to observe corrosion for the 316L stainless steel in particulate form since these particles have an uncanny passivity resulting in high resistance to corrosion, compared to bulk stainless steel material.

A summary of the results from electrochemical studies and metal release investigations is compiled in table 5.3 below. Typical open circuit potentials and current ranges are given for the coarse and fine particles in 0.7% HCl. Release rates calculated from data from metal analysis are represented in terms of released amount of metal (μg) per surface area unit of the particles mounted on the electrode tip (cm^2) and the time of exposure in the solution (including 30 min for obtaining a stable OCP and thereafter the time duration of the potential sweep).

Table 5.4: Summary of the results obtained for fine and coarse 316 L stainless steel particles and the separated austenitic and ferritic particles in 0.7% hydrochloric.

	Coarse 316 L particles <45 μm	*Fine 316 L particles <5 μm*
OCP range (mV) Max; min	23 ± 4	-202 ± 12
Max current (A) (typical)	0.000362	0.000101
Fe release μg/cm² particles/h	29.1315 ± 6.7588	1.6727 ± 0.9952
Cr release μg/cm² particles/h	8.1982 ± 2.0178	0.4810 ± 0.0.0337
Ni release μg/cm² particles/h	0.0717 ± 0.0880	0.0493 ± 0.0080
Fe release μg/cm² electrode/h	509.8021 ± 118.2783	294.7292 ± 174.1545
Cr release μg/cm² electrode/h	143.4687 ± 35.3111	84.1667 ± 5.8925
Ni release μg/cm² electrode/h	1.2552 ± 0.5394	8.6319 ± 1.4044

5.1.5 Comparison of results in the different test media

Previously the results from linear potential sweep investigations in the different test media have been analyzed and discussed one by one with focus on the differences between the two particle sizes of 316L stainless steel powder. In the following, the observed trends in electrochemical performance of the test materials during testing in the different test media, will be compared and discussed altogether.

Linear potential sweep

The polarization curves that were recorded in the different test media (0.3% NaCl, ALF, GST and 0.7% HCl) during linear potential sweep are compiled altogether in figure 5.17 below.

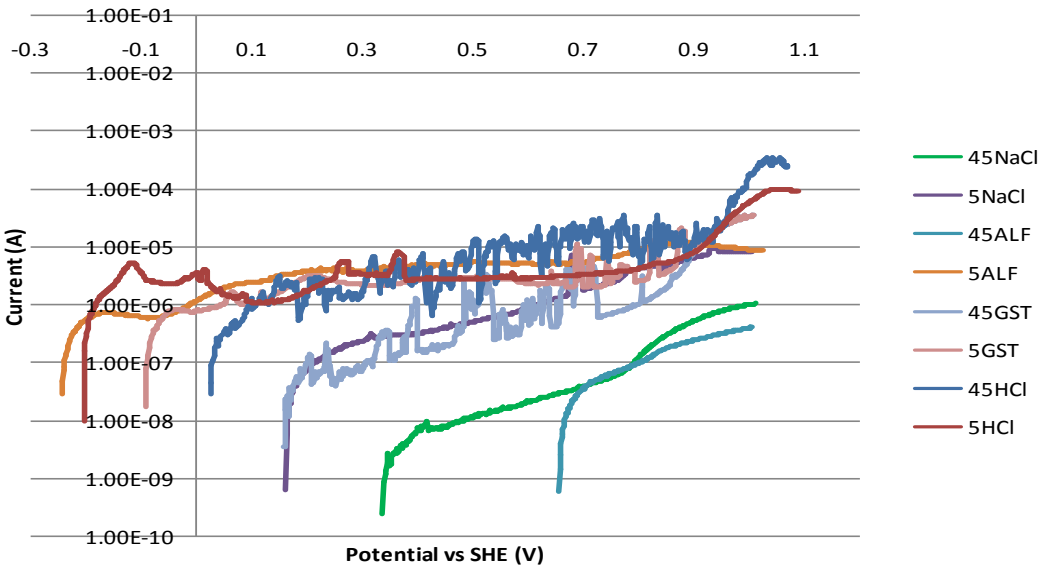

Fig.5.17: Polarization curves for stainless steel coarse (45) and fine (5) particles in all the different solutions; 0.3%NaCl, ALF, GST and 0.7%HCl. As it is possible to see lowering down the pH the current range moves to higher values, while the OCP value decreases.

From the current response of fine (< 5µm) and coarse (<45 µm) stainless steel particles in the acidic media GST and HCl, it seems as the polarization curves are translated towards higher current ranges when lowering down the pH. Moreover the length of the polarization increases due to the decrease of the OCP values in the two acidic test media (GST and HCl). It is interesting to observe that also the shape of the curves changes with pH, a behavior that is likely to be due to an increase in the corrosion activity of the stainless steel particles. In 0.3% NaCl (pH 5.5) for instance, the initial polarization around values of the starting potential, show an initial high increase in current and thereafter the current steadily increases until the end potential for both the particle sizes. In GST (pH 1.5) the trend is quite different; the initial current response is quite similar to the observation in NaCl, but around the potential of 0.85V, current show a sudden raise, both for the coarse and fine sized particles. This trend is observed for both the most acidic

test media GST and HCl and it is likely that the polarization of particles is getting into the transpassive region.

Furthermore, there is a fluctuation in the curve for the acidic test media with many instantaneous peaks on the curve. These peaks may represent pitting events, meaning that on the surface of the electrode a pit was eventually formed and repassivated. The definition of pitting is maybe not compatible with the particulate form of the sample, though it will be used in absence of a better term. Obviously the more aggressive the solution is, the more corrosion events are observed. In line with this, the number of peaks seen in the polarization curves increases and this "pitting" behavior gets more pronounced in the results passing from NaCl via ALF and GST, to the 0.7% HCl solution.

Open circuit potential

From the comparison of polarization curves for the different test solutions, it was possible to see how lowering of the pH changed the current response of the 316L stainless steel particles during linear potential sweep tests. An important parameter of the electrochemical behavior is the open circuit potential that is obtained before any potential manipulation is applied to the particle sample.

For the test media of low pH, the OCP values move to lower potential values compared to the behavior in test media of the higher pH and therefore the polarization curve starts at lower potentials and the length of the sweep gets longer since the end potential for these experiments was fix.

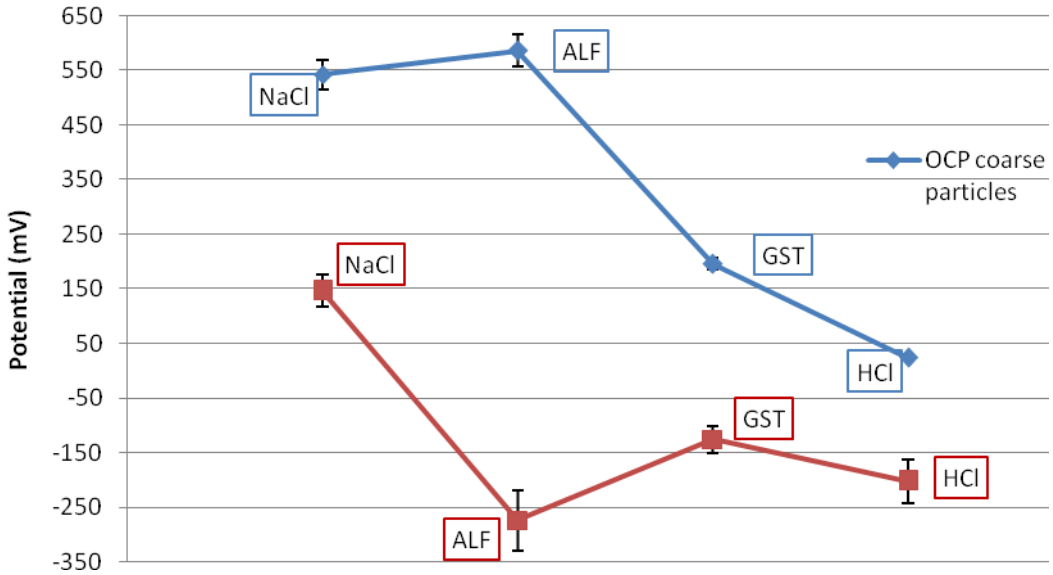

Fig.5.18: OCP values for the coarse (< 45µm) and fine (< 5µm) 316L particles observed in the different test solutions, 0.3% NaCl, ALF, GST and 0.7% HCl. From this graph it appears that reducing the pH the difference in passivity for the two sizes is reduced. Oddly the ALF stands out from this trend, probably because of its more complex composition.

Figure 5.18 show the OCP values in the different test media for the fine and coarse 316L stainless steel particles. These results suggest that the more aggressive the solution becomes the more the OCP value decreases. It is though interesting to observe that the OCP values in ALF (for both particle sizes) represent

an exception to this general trend. In fact the coarse particles show an OCP quite close to the first saline solution (0.3% NaCl), while for the OCP for ultrafine particles is much lower in ALF. It is even lover the OCP value obtained for the most aggressive solution. From this observation is consistent to assume that the behavior in ALF is strongly affected by the size of the particles under exam and other properties of the test media than pH. The results in ALF always shows a peculiar behavior, for instance the release of nickel is way higher than in other much more aggressive media.

Moreover the polarization curves for the two particle sizes presented an oddly different behavior, which was not observe in any other solution. These finding are probably due the much more complex composition of ALF, a solution designed to mimic the actual biological solution inside the lung cells at inflammation conditions.

Average and highest current

The current response of the particle samples during linear potential sweep in the different test media is the most important parameter to be analyzed. A more detailed description and comparison of the variations in current ranges for the particles in the different test media is reported in the following.

In general, also the current range increases passing from solutions of aggressive pH to those more neutral. Furthermore, an analysis concerning the trend in average and highest current for both the sizes of the particles in the different solutions was performed. As just mentioned, the current range increases with a reduction of the pH and as a consequence it is expected that both the average and highest currents are elevated in acidic test media for both particle sizes.

From the graphs of average current and highest current, figures 5.19 and 5.20, it can be observed that the current obtained for the coarse particles remain at lower values with the exception for 0.7% HCl. In the latter, very harsh and acidic electrolyte, the inverse relation is observed; both average and highest currents are higher for the coarse particles while the ultrafine particles seem more resistant and passive in the 0.7% HCl. These results indicate that the coarse particles maintain a higher passivity for moderately aggressive media throughout the sweep, while the fine sized particles tend to verge on the coarse ones when lowering down the pH.

Finally it is worth to mention that in ALF (pH 4.5), the coarse particles shows an average and highest current lower than the currents in the 0.3% NaCl solution (pH 5.5), indicating a lower reactivity despite the decrease in pH.

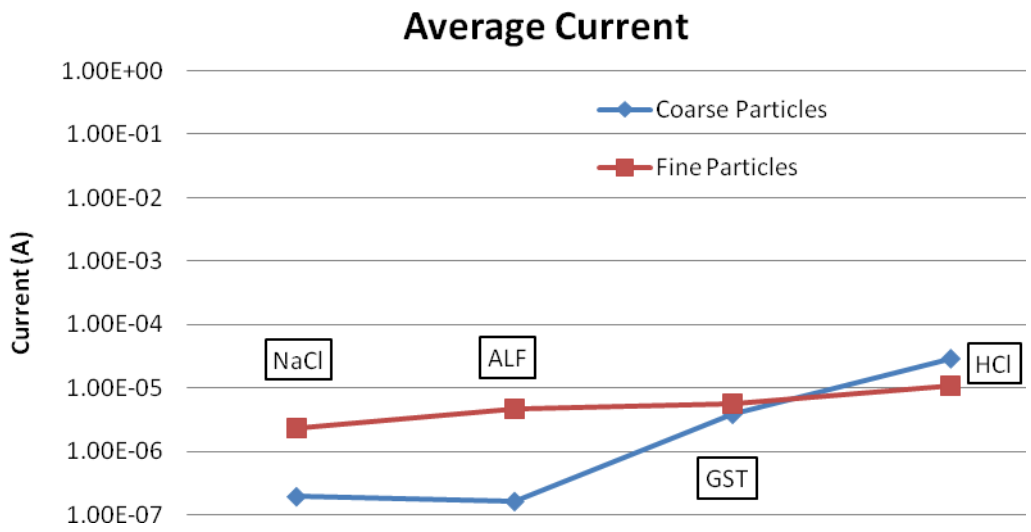

Fig.5.19: Comparison of the average currents for the coarse (< 45µm) and fine (< 5µm) 316L particles during linear potential sweep in the different test solutions, 0.3% NaCl, ALF, GST and 0.7% HCl. As seen for the OCPs the gap between 45 and 5 µm is reduced passing to more aggressive solution. Moreover for the most aggressive solution the situation is inverted, for the coarse particles in fact is measured a higher current than for the fine ones.

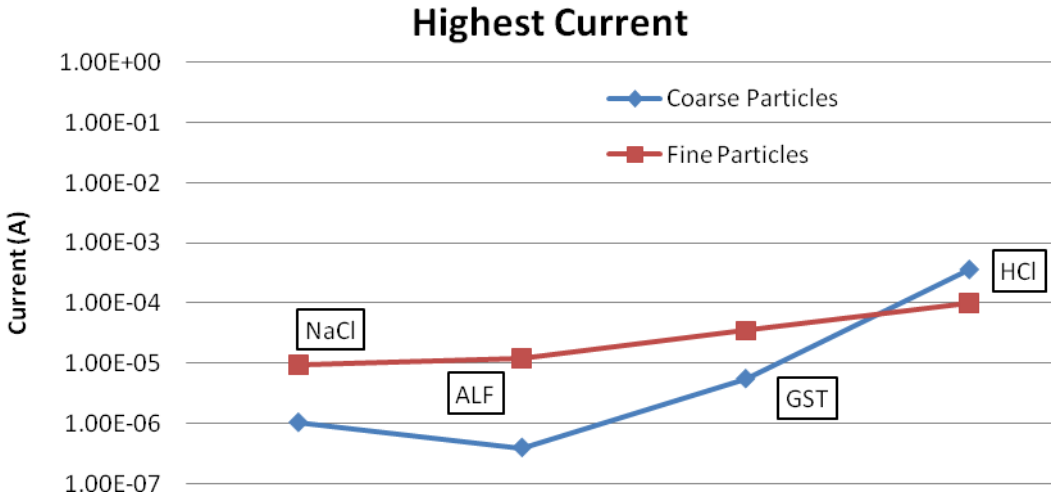

Fig.5.20: Comparison of the highest currents for the coarse (< 45µm) and fine (< 5µm) 316L particles during linear potential sweep in the different test solutions, 0.3% NaCl, ALF, GST and 0.7% HCl. As seen for the OCPs the gap between 45 and 5 µm is reduced passing to more aggressive solution. Moreover for the most aggressive solution the situation is inverted, for the coarse particles in fact is measured a higher current than for the fine ones.

Metal release

Finally also the release rates for each elements have been compared for the different solutions. In the previous paragraphs for the single solutions the main goal was defining the influence of the size and phase on the dissolution process, while in this section the aim will be observe and compare the release extent among the different solutions. In the following part are listed the total release rates for the different particles sizes. Moreover in the last part of the section are reported the single release rates for iron, chromium and nickel, in the order.

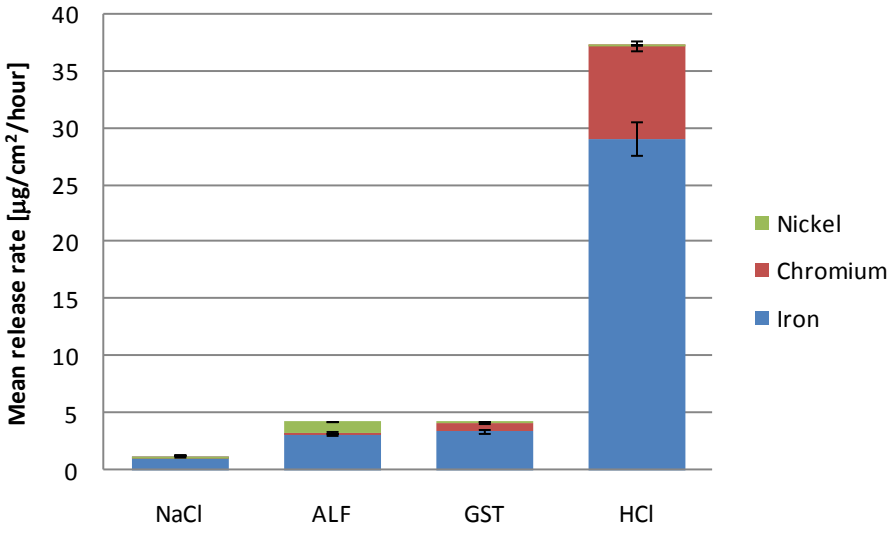

Fig. 5.20: Total release rate for 45 µm particles. The release increases remarkably for the last solution, while for NaCl, ALF and GST the release extent remains of the order. As expected the fraction of the iron release is much larger than the one for alloy elements.

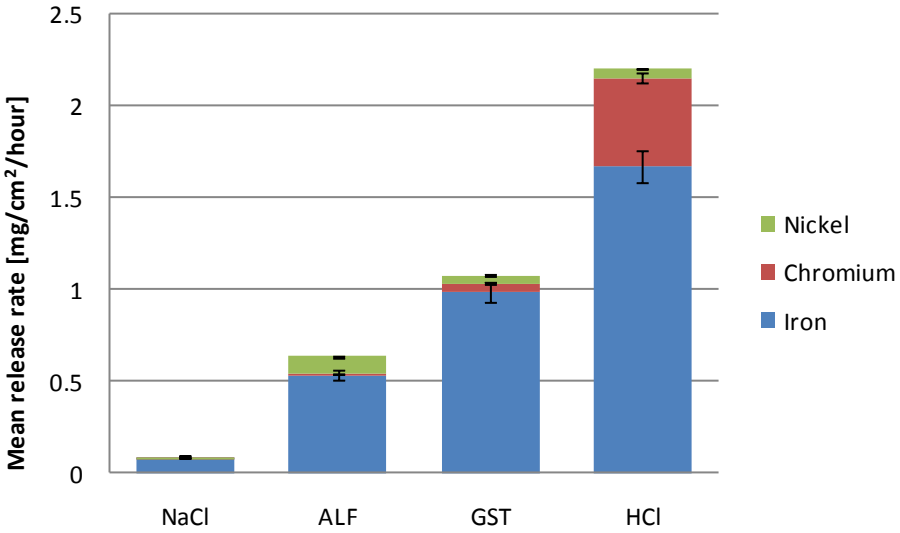

Fig. 5.21: Total release rate for 5 µm particles. The release appears to increase clearly decreasing the pH, and as expected the fraction of the iron release is much larger than the one for alloy elements.

Starting from the iron it is possible to observe an increase in the release extent passing to more aggressive solutions, this trend is especially remarkable for the coarse particles. In fact in the case of the 45 μm particles, while the difference between the ALF and GST is not large, regardless the drop in pH, on the other hand the release extent for the last solution justify the assumption of an actual breakdown of the passive layer (Fig 5.21). Also for chromium the release extent raises using more aggressive solutions. As shown in figure 5.22 the release extent increases remarkably for the last two solutions. Therefore it safe to assume that only in GST and 0.7% HCl the passive layer starts dissolving, while in the remaining solutions the oxide is almost intact.

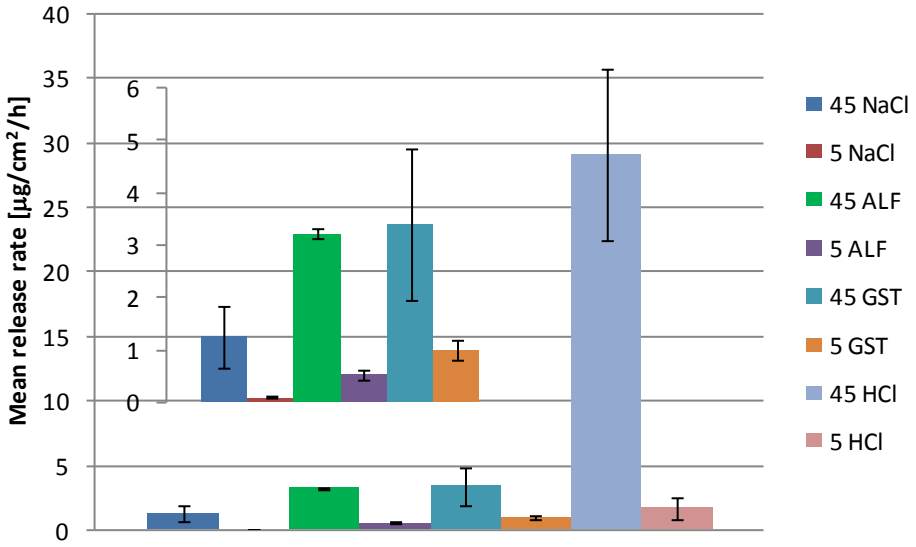

Fig 5.23: Iron release rate for the different solutions of both particles sizes. As expected the release extent increase lowering down the pH, especially for the last solution that shows a release rate much higher than the previous solutions. Probably the so high release for the HCl solution is due to an intense dissolution of the oxide layer.

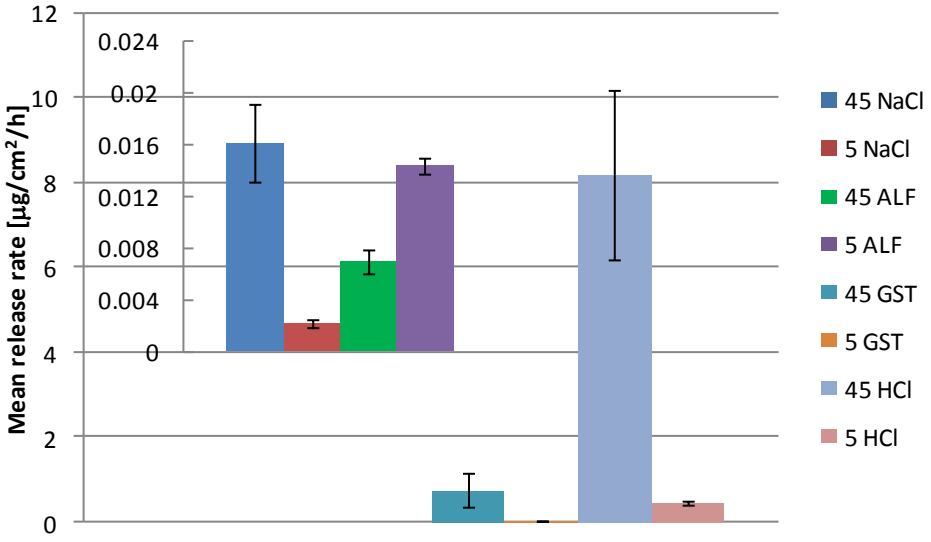

Fig 5.24: Chromium release rate for the different solutions of both particles sizes. As expected passing to more aggressive solution the particles release larger extent of alloy elements. Furthermore the higher release extent for the GST and HCl solutions is due to the incoming dissolution of the passive layer rich in Cr.

While for the previous elements the highest release extent was measured for the most aggressive solution (0.7% HCl), for nickel it has been observed a peak in release corresponding to ALF. The reason of this striking result might be found in the strong complexation ability of this solution, that, regardless the quite high pH, managed to react with the nickel enriched surface of the particles (K. Midander). Concerning the other solutions, the release of nickel never reaches the extent observed for chromium, indicating that the oxide layer for the last two solutions might be enriched in Ni at expenses of Cr.

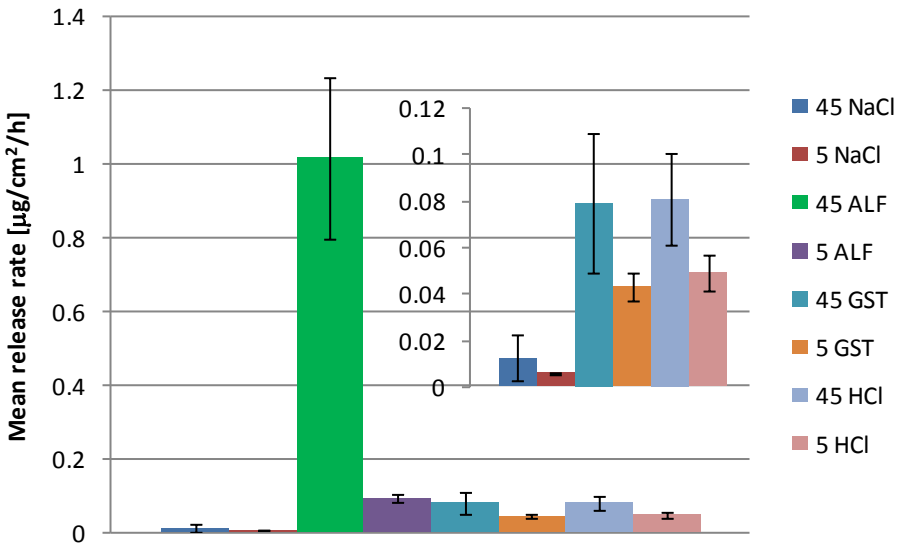

Fig. 5.25: Nickel release rate for the different solutions of both particles sizes. Regardless of the decrease in pH the largest release is observed for the quite mild ALF solution, due to its complexation ability. This characteristic allows the Ni enriched surface of the particles to react with the media to form chemical complex.

5.2. Potentiostatic investigations in artificial gastric fluid

Artificial gastric fluid, GST pH 1.5, was proven to be a quite aggressive solution for the stainless steel particles and it also simulates the conditions present in the gastrointestinal tract of a human body. For these reasons it was chosen as the electrolyte for a series of potentiostatic test. As was previously described in section 4.3.4 these tests consist in holding the potential (at 0.4, 0.6; 0.8 and 1V) for a fixed amount of time (30 minutes) and thereafter the solutions were analyzed for the content of iron, chromium and nickel. The following two graphs report the total released amount of metal from fine and coarse 316L stainless steel particles during potentiostatic tests as in GST. Results are expressed as µg of metal per surface area unit of the particles mounted on the electrode tip, and hour of the test, see figures 5.29 and 5.30.

The comparison of measured total metal release rates (iron+chromium+nickel) from stainless steel particles at potentiostatic tests is actually fair to do since in this case “apples and pears” are not compared with each other. In figure 5.29 the coarse 316L stainless steel particles were kept at the different fixed potentials during 30 minutes and the total metal release after the test show higher amounts of released metal from

the higher potentials. Both the iron and chromium release rate is increasing with the higher potentials while there is most release of nickel at 0.8V. This is in accord with the LSV curves in GST, in fact at 0.8 V corresponds a rapid increase in current and a strong activity, while at 1 V the curve reaches a plateau. Therefore the data related to the last two potentials indicates a partial dissolution of the surface layer, since the large release of alloy elements it is often associated to a weakening of the protective oxide. Although the decrease in release associated to the following potential suggests a repassivation-stabilization of the surface.

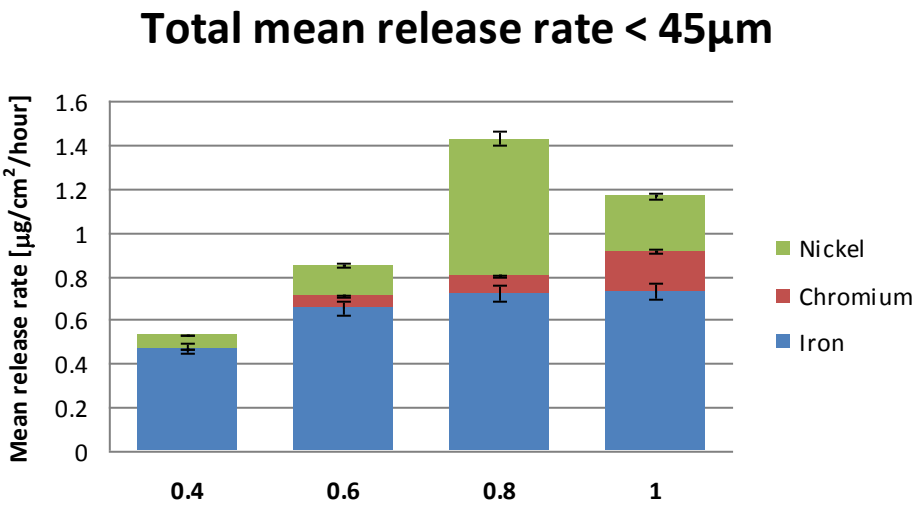

Fig.5.29: Total mean release rates of iron+chromium+nickel from coarse 316L stainless steel particles in GST under potentiostatic tests at 0.4, 0.6, 0.8 an 1V. From this graph it safe to assume that the potential influences the release process, especially of alloy elements.

Moreover comparing the total release for the PST tests and for the LSV tests in GST, it appears that the latter one is quite larger than the former. The reason for this difference could be found in the longer exposure time for the LSV polarization (almost four times longer) and in a stronger sensitivity of the particles toward sweeping rather than holding the potential.

The total release rates from ultrafine 316L stainless steel particles under potentiostatic tests show the particles to be relatively unaffected by the magnitude of the applied potential. In general, the total release rates are lower than those observed from the coarse particles at the same potentials. This is in line with results from linear sweep voltammetry studies in the same test media.

Furthermore the release extent for the PST test and LSV test in GST are quite similar, indicating that the for the finer particles holding or sweeping the potential or using different time of exposure does not affect the release process,. Furthermore it is interesting to observe that the release of alloy elements with respect to the iron is way inferior than in the case of the coarse particles. This result combined with the fact that the release is basically unaffected by the exposure time means that for the ultrafine particles the oxide layer is still intact and protective and richer in alloys elements than for the coarse particles.

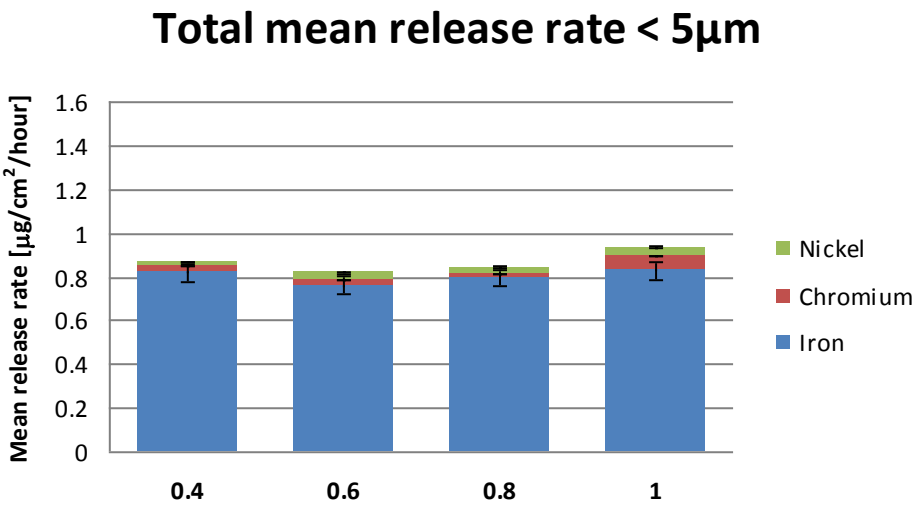

Fig.5.30: Total mean release rates of iron+chromium+nickel from ultrafine 316L stainless steel particles in GST under potentiostatic tests at 0.4, 0.6, 0.8 an 1V. From this graphs it possible to assume that the effect of the potential on the release process is not relevant.

The measured total release rates after potentiostatic investigation of both the coarse and ultrafine stainless steel particles are compiled together in figure 5.31 below.

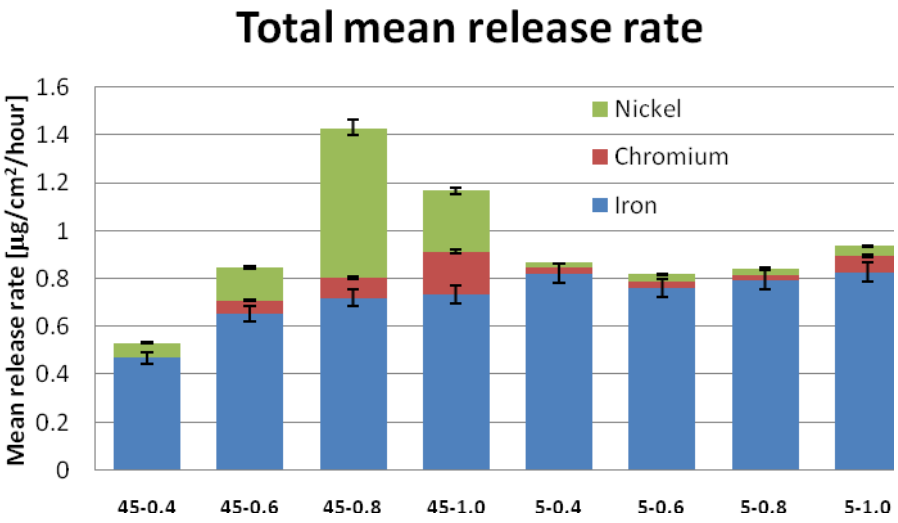

Fig.5.31: The total mean release rates (iron+chromium+nickel) for coarse and ultrafine 316L stainless steel particles in GST under potentiostatic tests compiled in the same graph for facilitated comparison.

The total release rate does not show the large differences between the coarse and fine particles observed for the LSV tests, instead the differences are rather small. The total release extent is affected by the size and potential in different ways depending from the element considered. For iron the inluence of the size is quite weak, in fact, except for the case of 0.4 V, the difference in release extent between the two sizes is small. On the other hand the size appears to affect the release process also in an indirect way, in fact the coarse and fine particles react differently to the variation of potential. This observation is especially true for

the alloying elements. For example in the case of chromium the release extent increases remarkably with the potential for the 45 μm, while for the 5 μm it remains stable. Therefore the difference between the particles size is not indipendent, but increaces with the potential. A similar situation is observed also for nickel, although the largest gap among coarse and fine particles is observed for the 0.6 V. A possible expalnation for this unsual and combined dependence from size and potential is an ongoing dissolution releated to a corrosion process for the coarse particles increasing the potential.

As stated in the previous section the mean release rate normalizated with repect to the particles surface area and time, since for PST tests the time is fixed there is no difference from coarse to fine sized particles, while the surface is stil an issue. Also in this section it has preferred to display the mean release rate, although in this case it is worth to report also the release normalized not to the effective area of the particles, but to the area of the electrode (πr^2 = 0.0002 m^2). As shown in the graph below normalizing the released amount for the electrode area changes radically the profile of the release rate. In fact now the release rate for the fine particles is much larger than for the coarse ones.

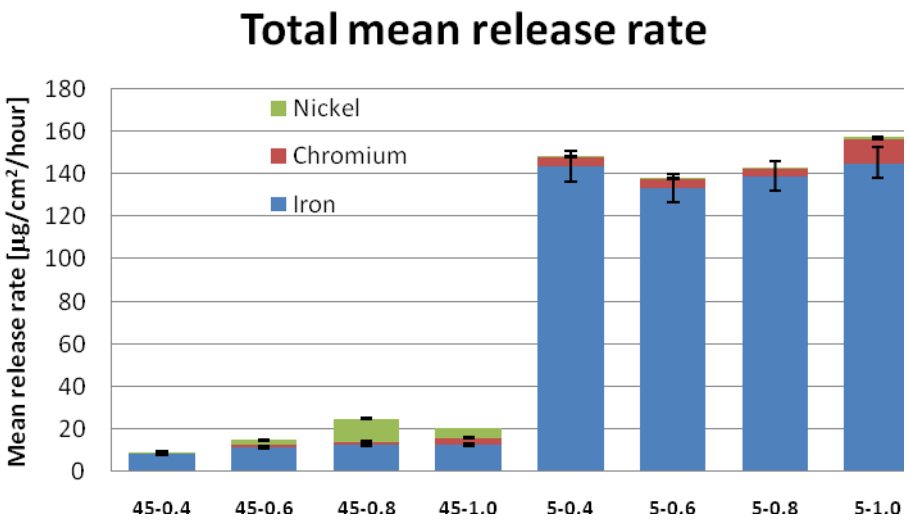

Fig.5.32: The total mean release rates (iron+chromium+nickel) normalized to the electrode area for coarse and ultrafine 316L stainless steel particles in GST under potentiostatic tests compiled in the same graph for facilitated comparison.

Table : Summary of the results obtained for fine and coarse 316 L stainless steel particles in GST with the potentiostatic tests.

	0.4_45 µm	*0.4_5 µm*	*0.6_45 µm*	*0.6_5 µm*	*0.8_45 µm*	*0.8_5 µm*	*1.0_45 µm*	*1.0_5 µm*
Fe release µg/cm² particles/h	0.4706 ± 0.2825	0.8219 ± 0.0229	0.6540 ± 0.5652	0.7619 ± 0.2640	0.7213 ± 0.5475	0.7943 0.2370	0.7333 ± 0.0544	0.8295 ± 0.1657
Cr release µg/cm² particles/h	-	0.0253 ± 0.0126	0.0555 ± 0.0490	0.0260 ± 0.0125	0.0821 ± 0.0102	0.0197 ± 0.0082	0.1796 ± 0.0465	0.0661 ± 0.0013
Ni release µg/cm² particles/h	0.0611 ± 0.0508	0.0210 ± 0.0056	0.1388 ± 0.1246	0.0312 ± 0.0192	0.6274 ± 0.4978	0.0312± 0.0205	0.2553 ± 0.1781	0.0413 ± 0.0207
Fe release µg/cm² electrode/h	8.2356 ± 4.9430	143.8333 ± 4.0069	11.4444 ± 9.8901	133.3333 ± 46.1976	12.6222 ± 9.5815	139 ± 41.4836	12.8333 ± 0.9522	145.1667 ± 28.9913
Cr release µg/cm² electrode/h	-	4.4358 ± 2.2074	0.9713 ± 0.8570	4.5433 ± 2.1873	1.4365 ± 0.1784	3.4533 ± 1.4401	3.1433 ± 0.8132	11.5733 ± 0.2357
Ni release µg/cm² electrode/h	1.0699 ± 0.6894	0.3675 ± 0.1783	2.4283 ± 1.1813	0.5467 ± 0.3352	10.9797 ± 6.7109	0.5457 ± 0.3585	4.4677 ± 2.1165	0.7232 ± 0.3618

5.3 Sonication

As explained in paragraph 4.3.6 the investigation of the effects of the ultrasonic treatment employs two different techniques: LSV and Zeta-potential measurements. The aim of this section is attempting to define how the ultrasonic waves interact and affect the particles, especially their surface properties. Hence this section is divided in two parts, the first is focus on investigate the effect of sonication on the polarization curves shape and parameters, such as OCP value, current range, highest and average current. While in the second is investigated in which manner the sonication affects the Zeta-potential value. The particles investigated in this section do not include the coarse ones (45 μm), but only the ultrafine (5 μm). The reason of this choice is because the procedure designed for this investigation failed to apply to the coarse sized particles.

Three replicas of non treated, sonicated by means of ultrasonic bath (time = 2 min) and by means of sonic probe (time = 2 min; output = 2; duty cycle = 10%) particles are tested using the LSV technique. The curves reported in figure 5.33 represent the typical behavior for the three replicas considered. The media used for the polarization is GST, since this electrolyte proved to be quite aggressive even for the stainless steel in particulate form, thus suitable to detect an eventual increase or decrease in passivity. Furthermore this solution simulates the environment present in the gastrointestinal tract of a human being.

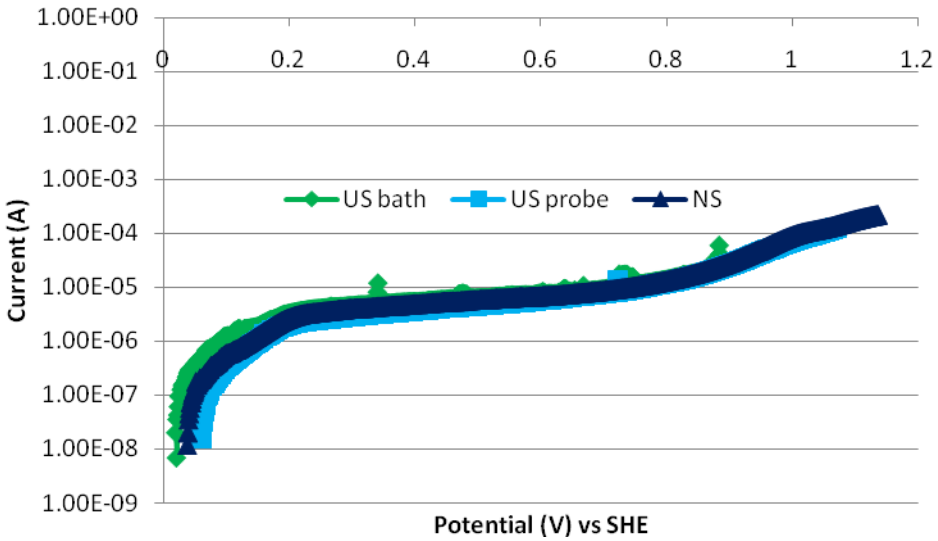

Fig.5.33: Polarization curves for stainless steel ultrafine (5) particles in GST solution. NS = non sonicated; US Bath = sonicated by means of ultrasonic bath for 2 min; US probe = sonicated by means of sonic probe for 2 min with output 2 and duty cycle 10%. The sonication treatment does not seem to affect the polarization curves.

These results confirm the previous findings for the ultrafine particles in GST, although the polarization curves do not show any differences not so ever. The OCP values are very close and the current range are almost superposed. Thus it is safe to assume that the treatment do not affect the passivity of the particles.

The possible reasons of this results might found in the large dimensions of the particles, in fact most of the research works on sonochemistry have been focus on nanometric particles. The stainless steel particles used in this research are far from the nanometric size, thus it is reasonable to question if their large dimensions might have hindered the effect of the ultrasonic waves. In order to dissipate these doubts the settings of the sonic probe have been modified seeking for a more intense treatment.

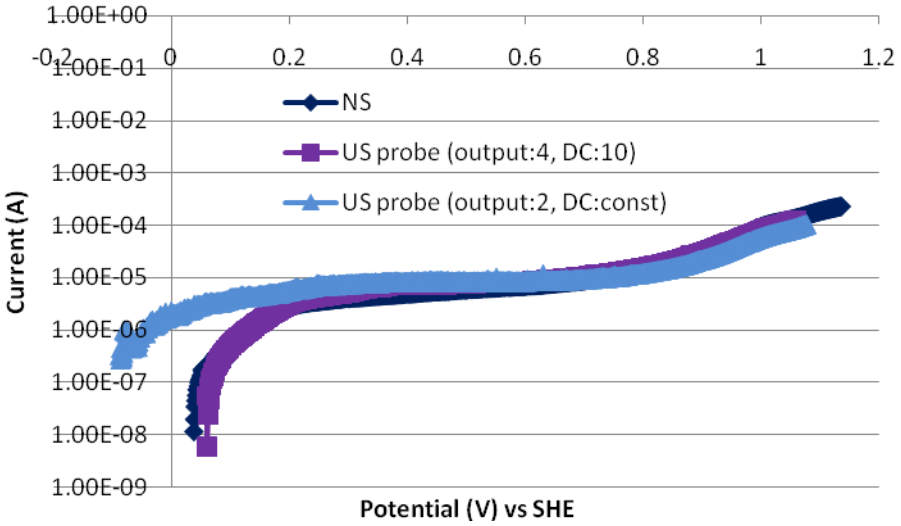

Fig.5.33: Polarization curves for stainless steel ultrafine (5) particles in GST solution. NS = non sonicated; US probe = sonicated by means of sonic probe for 2 min with output 2 and duty cycle constant or with output 4 and duty cycle 10%. The sonication treatment does not seem to affect the polarization curves.

Even increasing the intensity of the treatment the polarization curves do not present any particular differences. Only the particles sonicated with output 2 and duty cycle constant show a OCP lower than the other reaching the negative field, although the difference is too slight to be defined as an effect of the sonication and not a simple fluctuation of the OCP value. Furthermore the current ranges are still very close, meaning that the polarization process is not affected.

The sonication process seems to not influence the passivity properties of the stainless steel in particulate form not even increasing the intensity of the treatment. The reasons of this fact could be many, one could argue that the treatment was still too weak given the dimensions of the system or that maybe the particles are too big to be affected in the first place. On the other hand the treatment might have been to short in time to see any effect, in support of this theory the Ni powder experiment carried out by K.S. Suslik mentioned in the background section considered treatment period from 15 minutes to 120 minutes.

This work has been carried out in parallel with another project, that instead of investigate the influence on passivity considered the effect on the dissolution process. Since the procedure followed for the ultrasonic treatment and the particles used are the same it is possible to compare the two researches. During this project it was found that the sonication strongly affects dissolution of the particles, for every elements

tested the release difference among sonicated and as-received samples was quite large. Thus the ultrasonic waves affect the particles changing the surface composition and properties, although this is not visible in the polarization curves. A possible explanation for this discordance of results could be that the eventual effects of the sonication treatment vanishes during the OCP waiting time. In other words the high-energy interactions associated with the ultrasonic waves create a non-equilibrium state, that corresponds to the surface modified particles. Although when put in to the electrolyte this state degenerate back to the equilibrium (non sonicated state), thus by the time the OCP is settle and the polarization begins the particles are again in their unmodified state. If is this true the polarization would not detect any variation from the non sonicated particles. While the release tests would detect the effect of the ultrasonic treatment since to return to the original state the surface layer of the particles would have to dissolve.

After the polarization curves also the Zeta-potential values has been measured and examined. Since it is proven that the sonication affects the surface properties the Zeta-potential has been chosen as an useful parameter to quantify the surface modifications. Below are reported the analysis sheets obtained from the Zetasizer Malvern 5.20 used in this investigation.

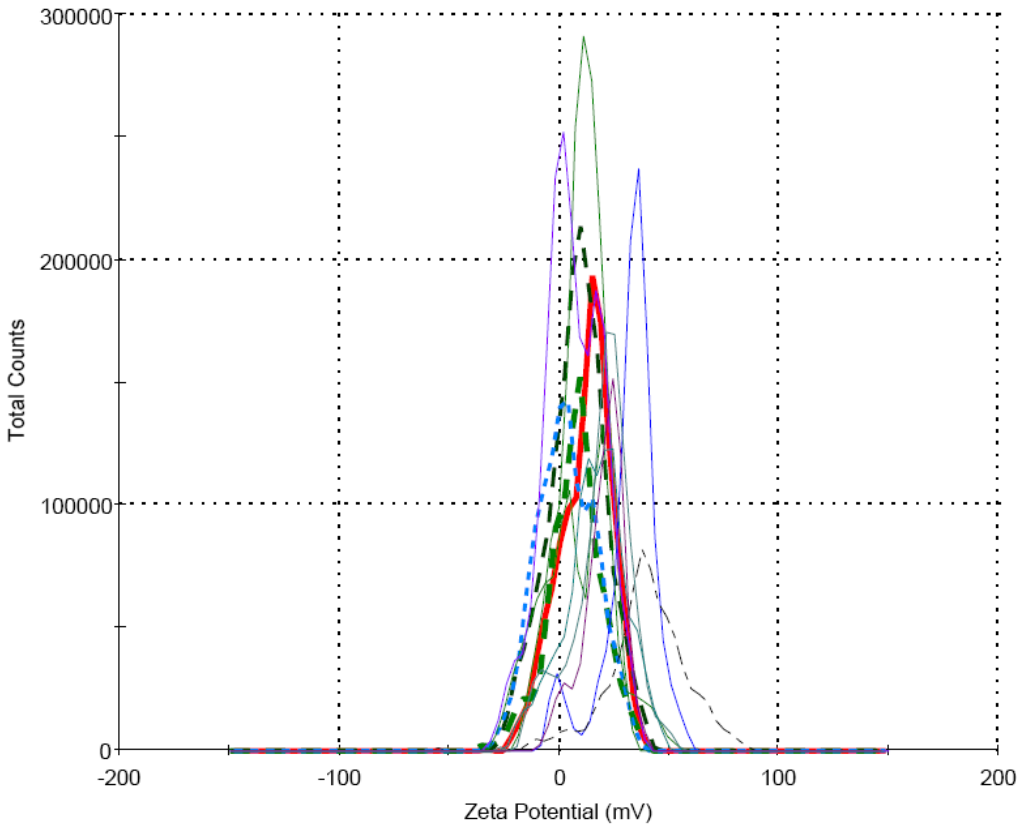

Fig. 5.34 : Zeta potential results for stainless steel in particulate form.

Unfortunately due to the large average size of the ultrafine particles these measurements are not reliable. The particles, in fact, settle to rapidly and hindered a correct measurement, thus the Zeta-potentials have a too large standard deviation that render the comparison impossible even for the sonicated case. Moreover in the table below are reported the summary of the OCPs range and typical highest currents measured for the different set up.

Table 5.5: Summary of the results obtained for fine and coarse 316 L stainless steel particles in GST.

	Non sonicated	*Sonicated probe (2;10%)*	*Sonicated bath*	*Sonicated probe (4;10%)*	*Sonicated probe (2;const.)*
OCP range (mV) Max; min	90 ± 50	13 ± 46	6 ± 46	33 ± 84	115 ± 22
Max current (A) (typical)	0.000184	0.000125	0.000126	0.000125	0.000104

6 Conclusions

The data generated from this study are part of a large on-going project at the Surface and Corrosion Science Division at the KTH. Although this Master Thesis project is focused on the passivity and reactivity of stainless steel 316 L in particulate form. The study provides both electrochemical measurements and release tests in order to assess the influence of size in the corrosion properties of alloyed materials. From the results obtained in the experimental part the following main conclusions can be drawn:

- It is impossible to deduce the release amount from the bulk composition.
- For Stainless steel in the particulate form has been observed a much higher passivity than in the bulk form. Both OCP value and current range shows a that the particles withstand conditions usually very aggressive for a bulk material;
- Obviously lowering down the pH also the particles show an increasing activity. Thou only in the 0.7% HCl test media (pH= 0.9) it has been possible to detect the transpassive potential ($E_{transpassive}$ = 0.9 V).
- The increase in ferrite fraction observed with the reduction of the size meant a decrease in the passivity properties, indicating that the two phases have different corrosion properties despite they show the same composition. Although it is still open the issue about the surface area difference, that might reduce the passivity difference.
- The separation procedure of austenite and ferrite has been successful, allowing to observe the different polarization behavior of the two phases.
- The ferrite has always been reported to show a in-between behavior of coarse and fine particles. Hence both size and phase are believed to affect the electrochemical properties, even thou the size plays a much more important role;
- For the less aggressive test media (3% NaCl and ALF) it has been reported a weaker passivity for the ultrafine particles with respect to the coarse ones, indicated by more elevated average, highest current and lower OCP value. Although decreasing the pH (GST and 0.7% HCl) the difference in the polarization behavior tends to reduce;
- The release amount is generally low for chromium and nickel, since the iron is dissolved selectively. It has been observed an increase in the dissolution for the different elements lowering down the pH, with the exception of ALF, in which the nickel showed a larger release due to the high complexation ability of this solution;
- The release rate for the linear sweep voltammetry is always larger for the 45 μm particles for each solutions and element. Although the release rate obtained from the potentiostatic test does not show the large differences between the coarse and fine particles observed for the LSV tests,

instead the differences are rather small. The total release extent is affected by the size and potential in different ways depending from the element considered. For iron the influence of the size is quite weak, in fact, except for the case of 0.4 V, the difference in release extent between the two sizes is small. On the other hand the size appears to affect the release process also in an indirect way, in fact the coarse and fine particles react differently to the variation of potential. This observation is especially true for the alloying elements. In fact in this case the difference between the particles size is not independent, but increases with the potential;

- There is no direct correlation between release process and polarization;
- The sonication process did not show any relevant variation in the passivity properties, nor regarding the polarization curves nor the Zeta-potential values;
- Even increasing the intensity of the ultrasonic treatment the polarization curves do not show any differences.

7 References

1. *A NON-RUSTING STEEL.; Sheffield Invention Especially Good for Table Cutlery.* **Savage, John M.** 1915, New York Times, p. XX7.

2. **International Stainless Steel Forum.** http://www.worldstainless.org/NR/rdonlyres/B2617D50-73AE-4FAB-BDCD-88ABD7891B97/4933/TheStainlessSteelFamily.pdf. *http://www.worldstainless.org.* [Online] International Stainless Steel Forum.

3. **Corporation, AK Steel.**
http://www.aksteel.com/pdf/markets_products/stainless/austenitic/316_316L_Data_Sheet.pdf. *http://www.aksteel.com.* [Online] AK Steel.

4. **WELD, MIG.** http://www.migweld.de/english/service/welding-stainless-steels/schaeffler-diagram-for-standard-analysis.html. *http://www.migweld.de.* [Online] MIG WELD.

5. **S. A. M. Refaey, F. Taha and A. M. Abd El-Malak.** Corrosion and Inhibition of 316L stainless steel in neutral medium by 2-Mercaptobenzimidazole. *International journal of electrochemical science.* 2006, Vol. 1.

6. **Ullmann, Yolanda.** Master of Science Thesis. Stockholm : KTH, 2009.

7. **Oudar, P. Marcus and J.** *Corrosion Mechanisma in Theory and Practice.* s.l. : Deker, 2008. 0-8247-9592-X.

8. **Sedriks, A. John.** *Corrosion of Stainless Steels.* s.l. : Wiley-Interscience, 1996. 0-471-00792-7.

9. **M. I. Romàn, A. Contreras and M. Molero.** Metallic composition and sources of airborne atmospheric particulates in the industrial belt of the city of Madrid. *Water, Air, & Soil Pollution: Focus.* 2002, Vol. 3.

10. **Obenholzner, J. H.** Articles from the plume of Popocatépetl volcano, Mexico — the FESEM/EDS approach. *Geological Society London Special Publications.* 2003, Vol. 213.

11. **Bhaskar, B. Vijay.** Ionic and heavy metal composition of respirable particulate in Madurai, India. *Environmental Monitoring and Assessment.* 2010, Vol. 164.

12. **Somers, Christopher M.** Reduction of Particulate Air Pollution Lowers the Risk of Heritable Mutations in Mice. *Science.* 2004, Vol. 304.

13. **Zhao, J.** Occupational toxicology of nickel and nickel compounds. *Journal of Environmental Pathology, Toxicology and Oncology.* 2009, Vol. 28.

14. **Chiba, A., Sakakura, S., Kobayashi, K., Kusayanagi, K.** Dissolution amounts of nickel, chromium and iron from SUS 304, 316 and 444 stainless steels in sodium chloride solutions. *Journal of Materials Science.* 1997, Vol. 32.

15. **Leygraf, C., Hultquist, G., Olefjord, I., Elfström.** Selective Dissolution and Surface Enrichment of Alloy Components of Passivated Fe18Cr and Fe18Cr3Mo Single Crystals. *Corrosion Science.* 1979, Vol. 19.

16. **Yolanda Hedberg, Klara Midander, and Inger Odnevall Wallinder.** *Particles, Sweat, and Tears: A Comparative Study on Bioaccessibility of Ferrochromium Alloy and Stainless Steel Particles, the Pure Metals and Their Metal Oxides, in Simulated Skin and Eye Contact.* 2010.

17. **Klara Midander, Alfredo de Frutos, Yolanda Hedberg, Grant Darrie,y and Inger Odnevall Wallinder.** *Bioaccessibility Studies of Ferro-Chromium Alloy Particles for a Simulated Inhalation Scenario: A Comparative Study With the Pure Metals and Stainless Steel.* 2009.

18. **Yolanda Hedberg, Johanna Gustafsson, Hanna L Karlsson, Lennart Möller.** Bioaccessibility, bioavailability and cytotoxicity invitro studies of commercially relevant iron- and chromium-based particles – an inhalation scenario. *Journal of Science.* 2010.

19. **K. Midander, J. Pan, I. Odnevall Wallinder and C. Leygraf.** Metal release from stainless steel particles in vitro—influence of particle size. *Journal of Environmental Monitoring.* 2006.

20. **A. Fattah-alhosseini, A. Saatchi, M.A. Golozar, K. Raeissi.** The transpassive dissolution mechanism of 316L stainless steel. *Electrochimica Acta.* 2009, Vol. 54.

21. **Iva Betova, Martin Bojinov, Petri Kinnunen, Pekka Pohjanne, Timo Saario.** Influence of the electrolyte composition and temperature on the transpassive dissolution of austenitic stainless steels in simulated bleaching solutions. *Electrochimica Acta.* 2002, Vol. 47.

22. **Iva Betova, Martin Bojinov, Timo Laitinen, Kari Makela.** The transpassive dissolution mechanism of highly alloyed stainless steels highly alloyed stainless steels. *Corrosion Science.* 2002, Vol. 44.

23. **M.A. Blesa, A.D. Weisz, P.J. Morando, J.A. Salfity.** The interaction of metal oxide surfaces with complexing agents dissolved in water. *Coordination Chemistry Reviews.* 2000, Vol. 196.

24. **Suslick, K. S.** Sonochemistry. *Science.* 1990, Vol. 247.

25. http://www.bioresearchonline.com/article.mvc/Automated-Protein-Characterization-With-The-M-0002. *bioresearchonline.com.* [Online]

26. **Datta, S.** *Electronic Transport in Mesoscopic Systems.* Cambridge : Cambridge University Press, 1995. ISBN 0 521 41604 3.

27. **Kuhn AT, Rae T.** Synthetic environments for the testing of metallic bioSynthetic environments for the testing of metallic biomaterials. *American Society for Testing and Materials.* 1988.

28. **Stopford W, Turner J, Cappellini D, Brock.** Bioaccessibility testing of cobalt compounds. *Journal Enviroment Monitoring.* 2003, Vol. 5.

29. *Private Comunication.*

8 Acknowledgements

At the end of this Master Thesis work I would like to thank some of the many people that helped me through this project and during the last year. Klara Midander, my supervisor, Yoland Hedberg, my co-supervisor, without them I would have not be able to finish this work, not even in a thousand years. Beside them I would like to thank everyone in the Division of Surface and Corrosion Science at KTH that share with me this experience, especially Lorena Osson. And would also thank my Italian supervisor Marco Ormellese that support me from the far away Italia. Moreover a huge thank goes to all my Erasmus friends that I met in this beautiful year. Thanks everyone!